6-2013

Analysis of Degenerative Cervical Spondylolisthesis and Corrective Orthopaedic Implants

Tyler Heck
Union College - Schenectady, NY

Analysis of Degenerative Cervical Spondylolisthesis and Corrective Orthopaedic Implants

By

Tyler Heck

* * * * * * * * *

Submitted in partial fulfillment
of the requirements for
Honors in the Department of Mechanical Engineering

UNION COLLEGE
June, 2013

ABSTRACT

HECK, TYLER Analysis of Degenerative Cervical Spondylolisthesis and Corrective Orthopaedic Implants. Department of Mechanical Engineering, June 2013.

ADVISOR: Professor Glenn Sanders

Back pain is often due to the degeneration of intervertebral discs, which can lead to a condition known as spondylolisthesis, whereby a vertebra slips out of position in the anteroposterior direction. There are numerous orthopaedic implants which are used by surgeons to correct this condition; however, there has been no conclusive research conducted in comparing the efficacies of these implants. In the cervical spine, this condition most commonly occurs over two levels. For the purposes of this study, an implant's efficacy depends on its ability to return the slipped vertebra back into natural position immediately after surgery. To test these implants and accurately compare their efficacies, a test fixture must be designed and constructed that can test both anterior and posterior implant systems and the surgical techniques used to apply them. Two fixtures were fabricated, assembled, and used to test a Zephyr anterior cervical plate based on the two common anterior surgical approaches: a standard three point bending method and a terminal three point bending method. A posterior fixture was fabricated and assembled but no testing was conducted with it due to a lack of availability of posterior implant systems (rod and pedicle screw). It was found that the standard three point bending method pulled the slipped vertebra completely back into position while the terminal three point bending method brought the slipped vertebra 0.80 mm from the corrected position; thus, the standard three point bending method was more effective for the Zephyr plate tested.

Table of Contents:

Introduction:

Back pain is very common in people the age of 40 and above, generally due to the degeneration of intervertebral discs. Approximately 80 percent of Americans have experienced some sort of back pain, while half of all working Americans describe having back pain every year [1]. This pain is most often a result of disc degeneration in the spine. Relative to the rest of the spine, the cervical spine is a sensitive area, as it allows for a larger range of motion than any other part of the spine; thus, pain in this area is not uncommon [2]. Around $90 billion is spent on back pain treatment every year in America, so it is necessary to develop the most effective procedures and products to treat serious back pain [3].

The overall objective of this project is to design a test mechanism which can simulate spondylolisthesis and the corrective surgery which treats this condition. No conclusive testing has been done to determine which types of surgical implants and techniques are superior in returning the lordosis of the cervical spine, so through this test fixture we wish to test these various surgical implants and methods/techniques and determine their efficacies. The degree of efficacy depends on the implant's ability to bring the slipped vertebra back into a position aligned with its superior and inferior vertebrae. The motive for defining efficacy as such is that the natural curvature of the spine coincides with comfort; with the ultimate goal behind any surgery being the reduction of pain and to enhance the wellbeing of a patient, the efficacy of one of these orthopaedic implants will be defined thusly [4]. There has been little research done on the efficacies of various implants ultimately meaning that this experiment will provide accurate comparisons between various surgical implants which could prove invaluable to

orthopaedic surgeons and major orthopaedic implant companies.

Moreover, it is not known how an implant's location and over which levels it is positioned affect the returning of lordosis. In other words, whether a terminal three-point bending, or "diving board," placement—whereby the slipped vertebra is fixed to the end of a two-level implant—or a standard three-point bending orientation—whereby the slipped vertebrae is fixed to the middle of a two-level implant—is more effective. We believe that a three-point bending approach to applying the implant will prove more effective in returning the lordosis of the cervical spine in both the short and long-term, because the implant is rooted at superior and inferior to the slipped vertebra, providing for a strong base to correct the affected vertebra's position. One rigid Zephyr anterior cervical plate will be used in both tests, as well as the same spondylolisthesis displacement conditions.

After giving a background on the anatomy of the spine from the vertebrae to the intervertebral discs, and discussing degenerative cervical spondylolisthesis and the orthopaedic implants used to correct the condition, the overall design of the three test fixtures designed—one for three-point bending anterior implant systems, one for "diving board" anterior implant systems, and one for posterior implant systems—will be explored. Then, the fixtures will be discussed and the specific purposes of the different parts of the three designs, and testing will be discussed that was performed to verify that the fixture will operate as expected. Furthermore, finite element analyses were done on each part to maintain that the various parts would not yield/deflect under loads that they will experience. Lastly, the preliminary testing and photogrammetry results will be discussed.

Background:

The Spine, Spondylolisthesis, and Corrective Orthopaedic Implants:

The spine is composed of three sections—cervical, thoracic, and lumbar—whereby the vertebrae vary in geometry according to location. The cervical section consists of the superior-most seven vertebrae, the thoracic sections consists of the middle twelve vertebrae, and the lumbar section consists of the five inferior-most vertebrae (see Fig. 1). From the superior to the inferior vertebra, the load supported increases while, consequently, the range of motion generally decreases due to a compromise between the two.

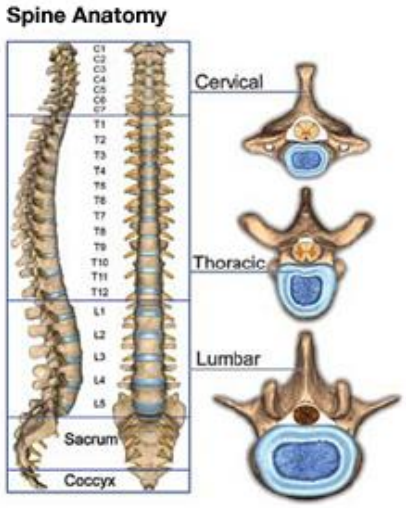

Fig. 1: Vertebral Column – The complete spine is shown on the left, divided into three sections: cervical, thoracic, and lumbar. A top view layout of a vertebra from each section is shown on the right side [5].

Spondylolisthesis is a common condition which can occur in any of these vertebral sections, whereby a vertebra has slipped out of position, most commonly in the antero-posterior direction. This is most commonly due to disc degeneration, as the disc is no longer able to provide the support necessary to keep a given vertebra in place [2]. The slippage of a given vertebra in the cervical spine makes the natural inward—or lordotic—

curve of the neck more extreme. This can result in the pinching of the spinal cord and other nerves, and if the spondylolisthesis and the accompanying pain are severe enough, the condition may require surgical treatment. Degenerative cervical spondylolisthesis is most common in C3/4 and C4/5 [6]. In these situations, either a standard three-point bending or terminal three-point bending approach to implant application will be taken; the former meaning that the slipped vertebra is attached to the middle of the implant, while the latter implies that the slipped vertebra is attached to an end of the implant, as seen in Fig. 2 [7]. If the intervertebral discs degenerate, this can also lead to facet hypertrophy, where the facet joints become larger in order to compensate for the lack of stability in the region; this leads to a less likely slippage in the posterior direction and supports the more likely occurrence of anterior slippage [8].

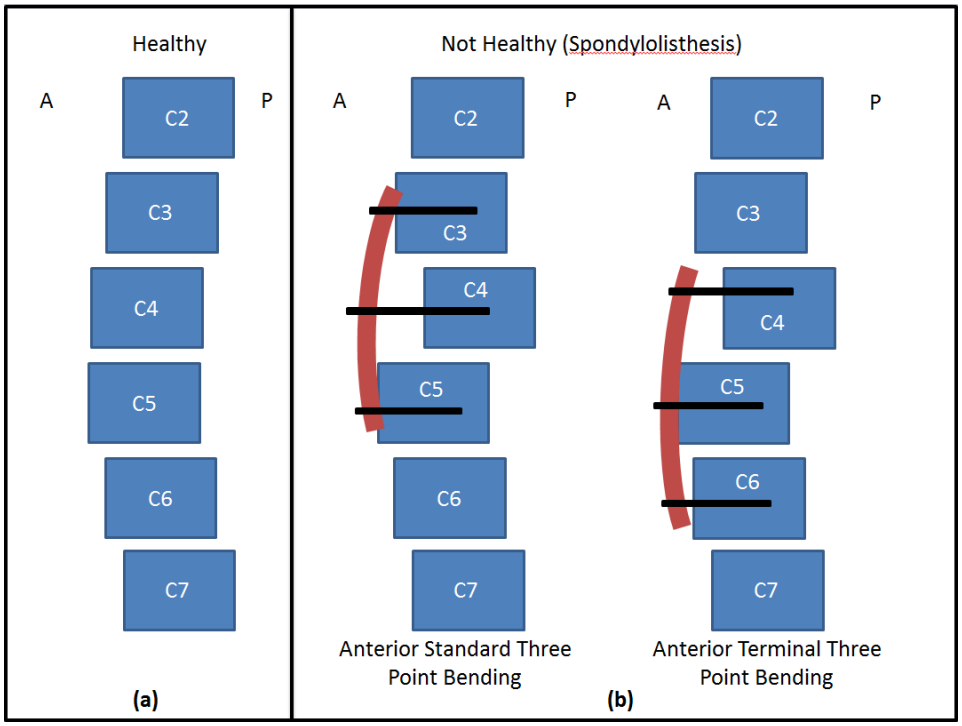

Fig. 2: Common Surgical Techniques – Part (a) shows the side view of a healthy cervical spine while part (b) shows a side view of cervical spines affected by spondylolisthesis, whereby C4 has been pushed back in the posterior direction, and the two common approaches to correcting it: standard and terminal three point bending.

A primary treatment method of cervical spondylolisthesis is anterior cervical discectomy and fusion (ACDF), whereby the intervertebral disc is removed from the anterior side of the spine and replaced with a bone graft, which will serve to fuse the adjacent vertebrae together [3, 9]. This surgery is performed from the anterior so as to avoid working around the neck muscles, spinal cord, and nerves on the posterior side. An interbody cage can be used to promote bone growth in the intervertebral disc space while simultaneously providing support. Interbody cages can also be supplemented with a bone plate which is attached to the number of vertebrae which are affected by the spondylolisthesis for increased stability in the region.

Other cervical spondylolisthesis surgery involves decompression and fusion, whereby the spinal canal is widened by removing either anterior or posterior elements to correct the impingement of the vertebra on the spinal cord. An interbody cage can then be implemented in the intervertebral disc space, as was done with the ACDF. Further stabilization can come from an anterior surgical plate. For both the ACDF and the decompression and fusion, a posterior system such as a rod and pedicle screw system can also be implemented. This system consists of two rods positioned parallel to each other and the spine. These rods are attached to screws that are inserted into the pedicles of all the vertebrae which are adjacent to the slipped vertebra [2]. This involves the removal of posterior elements—generally the lamina and spinous process—so that the screws can be inserted into the pedicles [2].

In addition, a new surgical implant (Anterior Cervical Interbody Fusion, ACIF) has been developed and has recently become quite popular. Essentially, it is a small, grooved cage which is inserted into the disc space between the superior and/or inferior

vertebra and the vertebra which has slipped out of position [10]. Two screws are then inserted into both the superior vertebra and inferior vertebra (relative to the intervertebral disc space) at approximately a 40° angle [10]. This has become popular because of its low profile and ease-of-use. This type of implant requires the removal of the discs so that the cage can be implanted, deeming a discectomy necessary. These cages provide support and stability by tensioning the ligaments connecting the adjacent vertebrae [11]. However, the implementation of a cage requires the removal of anterior ligaments; thus, these cages provide little stability in extension [11]. These low profile cages are becoming more popular in multi-level systems, as using only an anterior plate for more than three levels is not the most effective system [11]. Overall, it is unclear whether this smaller implant is sufficient in repairing the lordosis in the cervical spine on its own.

Ultimately, the surgery can either be done anteriorly or posteriorly and the surgical approach determines the mechanical system to be used to correct the spondylolisthesis. Ease of inserting the surgical implant and the effectiveness of the surgical implant need to be taken into account when correcting spondylolisthesis, and based on a surgeon's personal preference, different corrective surgery will be taken. The type of surgery is also dependent on the severity of the spondylolisthesis. The Meyerding Grading System is used to determine the relative severity of the vertebral slippage. The percentage of the vertebra which has slipped in the AP direction—toward the posterior side in the case of the cervical spine—off of the inferior vertebra determines the severity grade, as seen in Table I [11]. In the cervical spine, slippage of approximately 4.2 mm or greater can require surgical treatment, but with greater vertebral slippage increases the likelihood for surgery. Meyerding grades of 3 and 4 generally necessitate surgical

treatment [11]. In addition, a vertebral displacement of 2.7 mm or greater is considered clinically unstable and generally requires some sort of treatment, whether that be rehabilitation or surgery [12].

Table I: Meyerding Severity Grading System – This table displays approximate displacement ranges due to spondylolisthesis of cervical vertebrae (based on average end plate depth of all cervical vertebrae) [11]

Meyerding Severity Grade	Percentage of Slippage	Approximate Displacement Range (mm)
1	0-25	0-4.2
2	26-50	4.2-8.4
3	51-75	8.4-12.5
4	76-99	12.5-16.5
5	>100	>16.5

Furthermore, the intervertebral discs of the cervical spine, which range from approximately 4 mm to 6 mm, are significantly smaller than that of the lumbar vertebrae—by approximately 4 mm to 6 mm on average [13]. This larger thickness in the lumbar intervertebral discs is due to the significant amount of body weight which must be supported by the vertebrae in this segment of the spine, as they are well below the human body's center of mass. The intervertebral discs in the thoracic spine have approximately the same disc height as the cervical spine on average [13]. The cervical spine also lacks the added support which the thoracic and lumbar spine benefit from via the rib cage which serves to better distribute the weight of the body in the spine [2].

Biomechanics of the Cervical Spine:

The cervical spine is a more sensitive area of the spine which allows for a larger range of motion than either the thoracic or lumbar spine. The center of mass of the human

body is below the cervical vertebrae, and as a result, the cervical spine only has to bear the weight of the head. See Fig. 3 for the range of motion data of the spine.

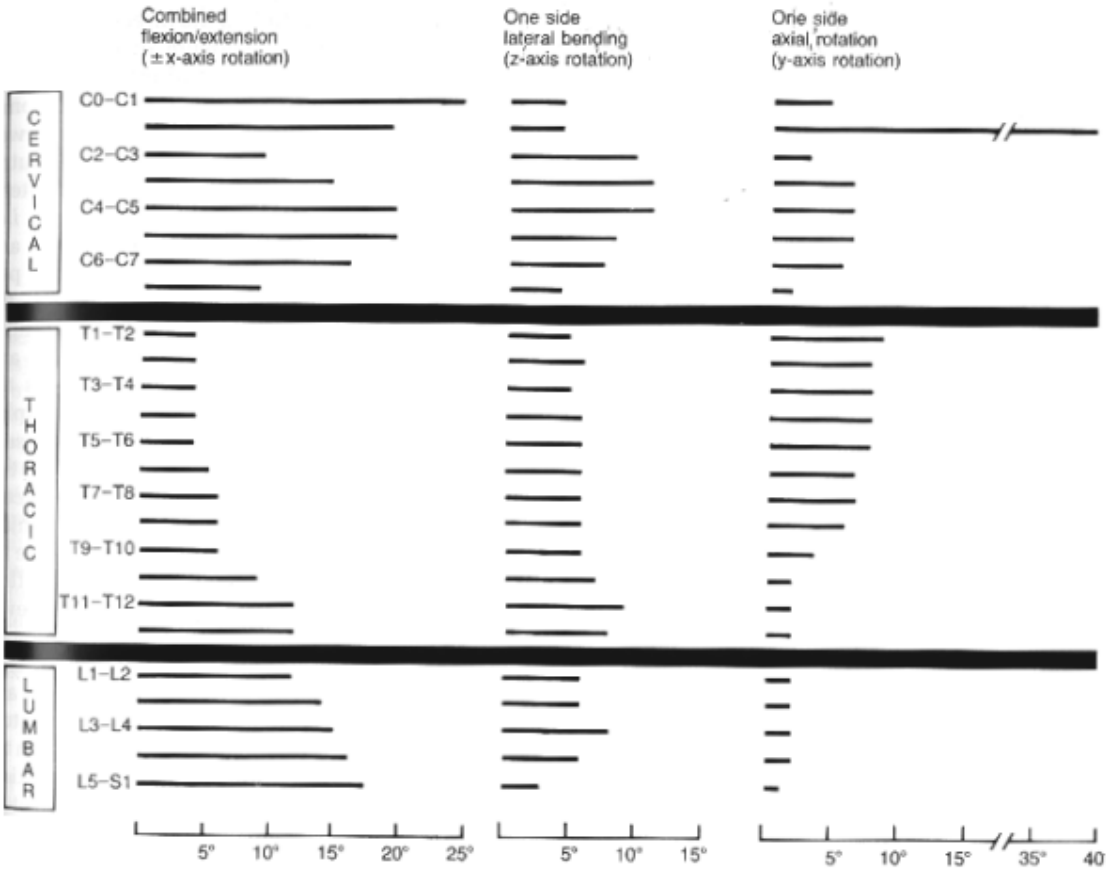

Fig. 3: Range of Motion of Spine – The range of motion is listed in degrees with the type of movement—flexion/extension, lateral bending, and axial rotation—listed at the top of the figure [14].

This requires a less bulky nature of the cervical vertebrae, and in comparison with the thoracic and lumbar vertebrae, the cervical vertebrae are significantly smaller—both in vertebral body height and width—with much larger spinal canal areas (see Fig. 1). This increased size in the spinal canal allows for greater movement and less impingement on the spinal cord during movement. See Table II for general cervical vertebral dimensions.

Table II: Cervical Vertebral Dimensions – Listed are the linear dimensions for C2-C7, where EP stands for End-Plate, VBHp stands for Vertebral Body Height, D stands for depth, W stands for width, u stands for upper (superior), and l and stand for lower (inferior) [15].

	Cervical Vertebral Level					
Linear Dimension (mm)	C2	C3	C4	C5	C6	C7
EPDu	-	15.0	15.3	15.2	16.4	18.1
EPWu	-	15.8	17.2	17.5	18.5	21.8
EPDl	15.6	15.6	15.9	17.9	18.5	16.8
EPWl	17.5	17.2	17.0	19.4	22.0	23.4
VBHp	-	11.6	11.4	11.4	10.9	12.8

This greater movement can also be attributed to the orientation of the facet joints in the cervical spine. With the exception of the C1 (atlas) and C2 (axis) vertebrae which have more unique shapes to connect the spine with the skull, the cervical vertebrae have facet joints which are angled at approximately 45° in the antero-posterior (AP) direction. This allows for distribution of the weight of the head to both the facet joints and the end-plates—and consequently, the vertebral bodies. More resistance is encountered in the antero-posterior direction than in the postero-anterior direction (PA), but more overall there is a larger range of motion compared to other sections of the spine. This is in comparison with the thoracic and lumbar spine, where the facet joints are perpendicular to the AP axis and parallel with the longitudinal axis (or vertical direction). Thus, the lumbar vertebrae distribute most of their load on the vertebral bodies, while also limiting the movement in the AP direction as the facet joints serve as more of a boundary for movement in the PA direction [16]. Due to the larger loads which must be supported by the lumbar vertebrae, it is necessary to limit the movement allowed in these vertebrae without compromising the stability in this spinal region. The different regions of the spine have different ranges of motion due to the load they bear; there must be a proper

balance between movement and stability. In the cervical spine, the removal of the posterior elements—which include the facet joints—affects the compressive response as these are load-bearing elements [16].

Moreover, the movement allowed for a given vertebra is generally a coupled motion, meaning that the vertebra—or vertebrae—will not just move along a single axis, but rather, along multiple axes [17]. However, for shear displacements in either the AP or PA direction, or for displacements due to compression, there are not significant coupled motions [16]. This is significant when dealing with spondylolisthesis, as it means that replacing the natural lordosis in the cervical spine will not alter the orientation of the vertebrae in directions other than along the AP or PA directions. The intricacies of each of the spinal segments are unique to the loading in the region, which, in turn, determines the range of motion which can be allowed while maintaining stability.

Also, while under load, a functional spinal unit (FSU)—which consists of two adjacent vertebrae—or a multi-level spinal unit (MSU)—which consists of more than two connecting vertebrae—the vertebrae exhibit a unique behavior. With smaller loads, a FSU will undergo a quick and significant displacement. This is known as the neutral zone, which allows the spine to make large movements with minimal muscle use [18,2]. As the load on the spine is increased, the spine stiffens and enters the elastic zone; for larger loads, smaller displacements result in this region [18,2]. When a maximum load has been applied, or the largest possible motion has been achieved, the range of motion for a FSU has been found; it is simply the displacement achieved for that maximum load [18].

Intervertebral Discs and Degeneration:

The intervertebral discs consist of an outer layer called the annulus fibrosis and an inner section called the nucleus pulposus (see Fig. 4). The annulus fibrosis is a resilient, but elastic structure of fibrous layers oriented at different angles per layer [13]. This outer structure serves to house the nucleus pulposus, which is a gel-like center consisting of mainly water and fiber [13]. The result of this combination of fibrous material and water in the disc is viscoelastic behavior. Essentially, this means that if the discs are loaded and then unloaded continuously, faster loading speeds will yield different load-displacement curves [13]. Viscoelasticity is a time-dependent property, where the discs will behave stiffer with higher loading rates [13].

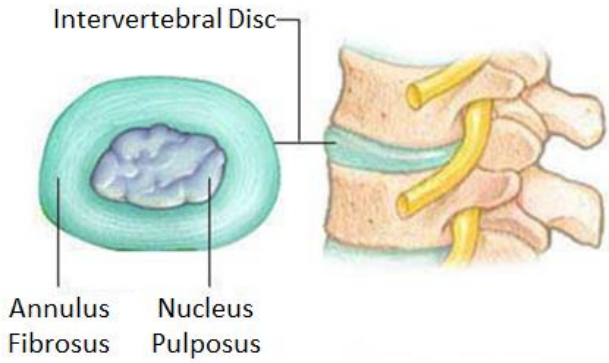

Fig. 4: Cross-Section of an Intervertebral Disc [19]

Creep is associated with viscoelasticity, which is the tendency of a material to slowly deform over time under the influence of a force or stress. Over time, intervertebral discs continue to deform under a constant load. Higher loads tend to result in faster creep rates and larger deformations. Moreover, the rate of creep is directly proportional to the degree of degeneration in a given disc; as seen in Fig. 5, with greater disc degeneration results, faster rates of creep [13].

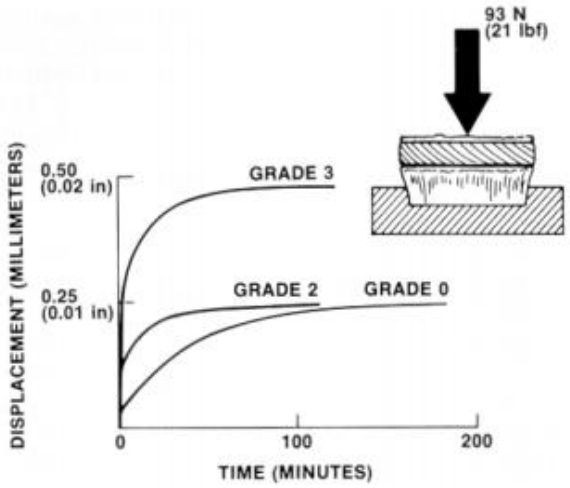

Fig. 5: Creep with Respect to Disc Degeneration – The plot depicts the relationship of vertebral compression vs. time, with the various curves corresponding to different degrees of disc degeneration [13].

Also, viscoelastic materials exhibit hysteresis, which is a phenomenon whereby energy is lost in a material with continual load and unload cycles [14]. This is a mode of protection for the body, as the discs serve to protect the rest of the body from the continual shock of repetitive loading and unloading by means of energy dissipation [14]. Younger people have larger hysteresis than in middle-aged or older people due to the lesser wear that has been put on their discs.

These discs degenerate over time from overuse, improper posture, genetics, etc. Along with this degeneration comes a decrease in viscoelastic behavior. As the discs are loaded and unloaded over time, the water content in the discs continually decreases [2]. With this, the ability of the disc to exhibit hysteresis is impaired, while the rate of creep also increases when a load is applied. Also, the disc's ability to restore energy that is lost due to hysteresis is impaired. These properties associated with the viscoelastic nature of the intervertebral discs are necessary in understanding the behavior of the discs and their resulting behavior when degenerated. As a result of the lesser viscoelasticity of the discs

from degeneration, they are not able to cushion and stabilize the vertebrae as well; thus, this opens the possibility for harmful injuries to occur, such as spondylolisthesis.

However, there are no direct correlations between the degree of disc degeneration and the overall behavior of the disc [16]. Lateral and axial bending exhibited no relationship between disc degeneration and degree of movement [16]. However, intervertebral discs with degeneration grades of 3 and 4 exhibited a 50 percent decrease in compression stiffness and a 300 percent increase in shear stiffness (in the AP direction) [16]. As cited in the study of Moroney et al., a preload force of 49 N was applied in all of their tests, as this is a good approximation of the weight of the head [16]. Moreover, Moroney et al. used a test fixture which was able to apply loads to the intervertebral discs at the mid-plane of the disc being tested in a cervical FSU, yielding the most accurate stiffnesses of the discs. This improved upon the testing done in Panjabi et al., where loads were applied to the middle of the superior vertebrae in a FSU which resulted in larger stiffnesses due to the presence of moments from the location of the applied force [16]. Thus, the results of Moroney et al. are more accurate and the compression and shear stiffnesses for disc segments—which are functional spinal units whose posterior elements are removed (lamina and posterior muscles and ligaments)—are displayed in Table III.

Table III: Disc Stiffnesses by Disc Degeneration in Disc Segments – The stiffnesses below are categorized by the degree of disc degeneration, where 1 is barely degenerated and 4 is severely degenerated. Anterior shear is the stiffness in the postero-anterior direction while posterior shear is the stiffness in the antero-posterior direction [16].

Disc Degeneration Grade	Compression (N/mm)	Anterior Shear (N/mm)	Posterior Shear (N/mm)
All	492	62	50
1	737	31	18
2	603	39	40
3	320	99	72
4	328	76	53

In addition, Moroney et al. presents results of testing of intact spinal segments—or cadaver spinal units which still have all posterior elements—and these stiffnesses are shown in Table IV. All in all, they are comparable to the disc segment stiffnesses, but are slightly larger for the compression and anterior shear stiffnesses.

Table IV: Stiffnesses in Intact Segments – The average stiffnesses are given for compression, anterior shear, and posterior shear, where the number in parentheses is the standard deviation. Also, the range of stiffnesses are given for all specimens tested [16].

	Compression (N/mm)	Anterior Shear (N/mm)	Posterior Shear (N/mm)
Stiffness	1318 (1170)	131 (157)	49 (24)
Range	116-3924	29-631	15-96

Fixture Specifications and Model Validation:

General Design and Constraints:

In order to do this, three vertebrae (MSU) modeled using cylindrical Delrin pieces will be mounted in a test fixture. The motive for creating a fixture modeling a two-level spinal unit is that correcting spondylolisthesis over two levels is much more common

than a single level condition. It was desired to create a test fixture which could be reusable to test countless implant systems and surgical techniques which would be applied to it, and to be able to perform the tests on these implants without having to replace costly multi-level spinal units for each test (e.g., with sawbones multi-level spinal units or cadavers). With this constraint, the most practical approach to creating a two-level spinal unit fixture in spondylolisthesis would be to have the shear resistive force which would be encountered in moving the slipped vertebra back into position come from an external system; in other words, the shear resistive force would not be coming from a material in the intervertebral disc space, facet joints, etc (see Fig. 6 for general models). As the displacement of spondylolisthesis is generally within the range of 3-5 mm, this is the range which the fixtures will be able to achieve.

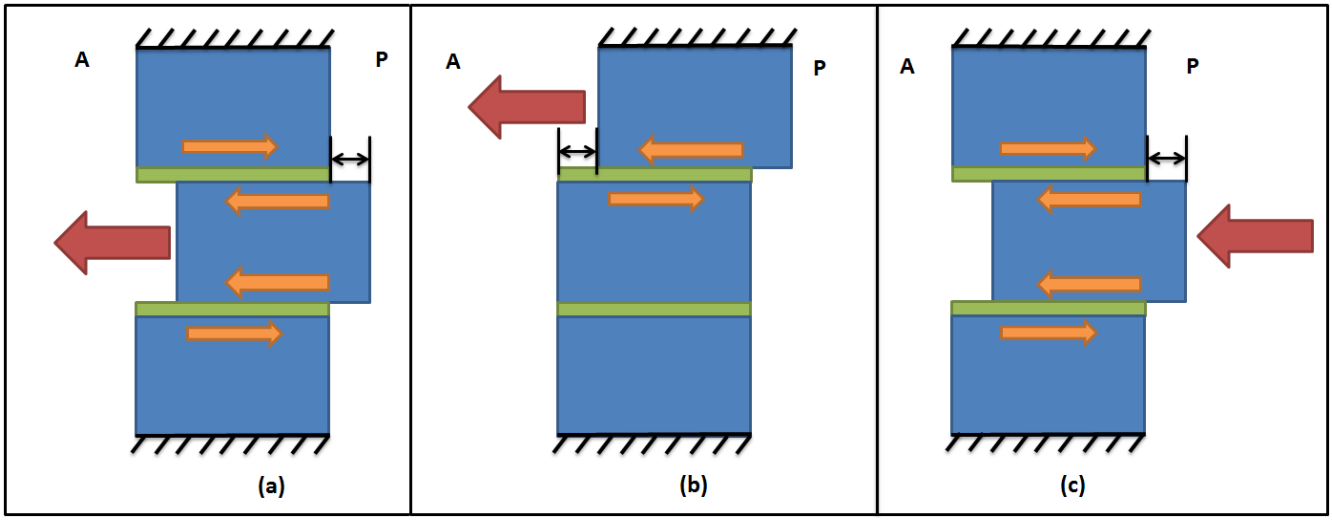

Fig. 6: Side View of Two-Level Spondylolisthesis Model – The blue rectangles represent the vertebrae and the green rectangles represent the intervertebral discs. The side labeled A represents the anterior side while the side labeled P represents the posterior side. Part (a) depicts the case for which an anterior implant system would be applied using standard three point bending where the red arrow represents the restoring force of the implant system, part (b) depicts the case for which a anterior implant system would be applied using terminal three point bending with the red arrow representing the restoring force of the implant system, and part (c) depicts the case for which a posterior implant system would be applied using standard three point bending with the red arrow representing the restoring force of the implant system. The orange arrows illustrate the shear forces being experienced from moving the slipped vertebra back into its natural position.

With this notion that an external system would provide the shear resistive force, this meant that the intervertebral disc space between each vertebra needed to be filled with a frictionless material. As it turns out, the finished surface of Delrin plastic is very frictionless and no additional material was needed. In addition, since the part of the shear resistive force which would result from the geometry of the vertebra would be taken into account in this external system, it was not necessary to have geometrically accurate vertebrae in the test fixture. As a result, the Delrin vertebrae could be modeled as simplified vertebral bodies.

It was recognized that this external system should not be bulky, as the cervical vertebrae are small as it is. As a result, a weighted system was deemed impractical. Instead, a system where a material would be compressed/tensed and provide the proper resistance was determined to be the most practical idea. After designing around springs to model this resistance, a system with the necessary compressive/tensile stiffness was found to be too large and not easily adjustable, and polyurethane rubber rod segments were found to be practical (for the feasibility issues, see Appendix A: Spring System Analysis). Ultimately, it was determined that compressing a material, instead of placing it in tension, would lead to a smaller and simpler system.

With the shear resistance coming from an external system whereby polyurethane rod segments are compressed (one rod segment per level), it was then necessary to create a design which could allow for the application of both anterior and posterior implant systems, including both anterior surgical situations. To create a fixture which could accommodate these three situations, it was necessary to create three different fixtures in order to maintain that the polyurethane rod segments were in compression in both cases;

maintaining that the rod segments are in compression in both cases allows for accurate comparison between the anterior and posterior systems being tested. At the same time, it was necessary that these two designs be as similar as possible to guarantee interchangeability. Also, it was important to maintain that the weights of the two systems would be relatively equal, so that the preload from the fixture's weight on the Delrin vertebrae would be similar. The two anterior fixture designs and the posterior fixture design are displayed in Fig. 7 (for more details on designs, see Appendix B: Technical Drawings).

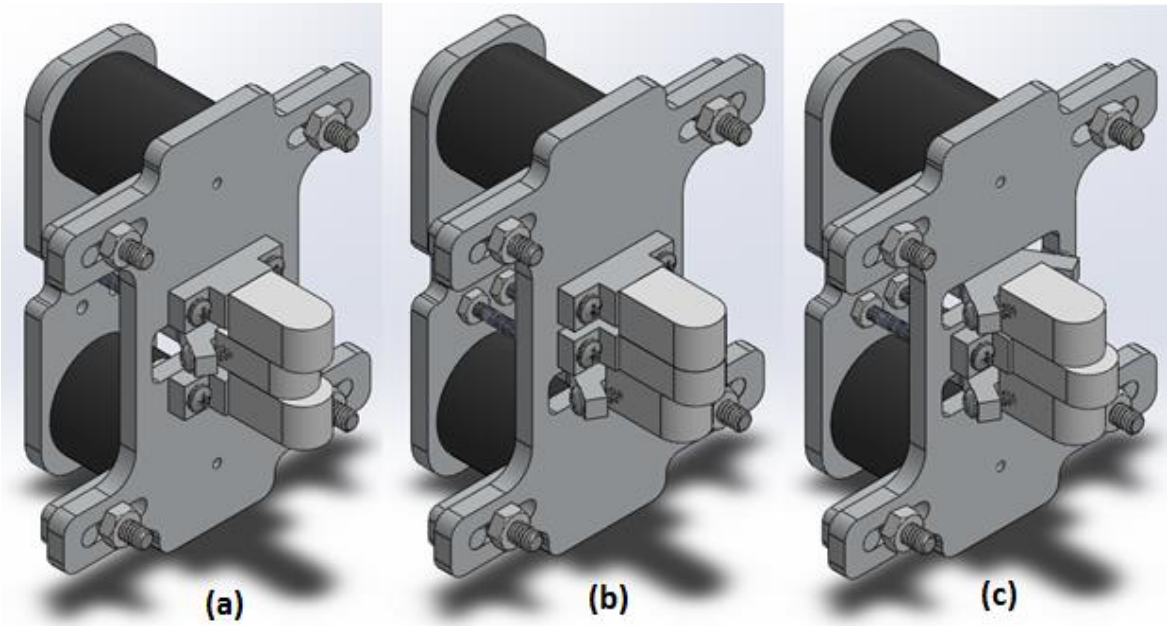

Fig. 7: Isometric Views of the Spondylolisthesis Test Fixtures: Part (a) is the anterior standard three point bending fixture, part (b) is the anterior terminal three point bending fixture, and part (c) is the posterior standard three point bending fixture. Note: in the actual model, washers will be implemented where nuts are used and there are no holes in the front plates (they were just there for ease of Solidworks assembly).

Design Specifics:

1. Delrin Vertebrae and Teflon Disc Design:

To simplify the designs in Solidworks, the Delrin vertebrae were all made the same size, although the fixtures will be able to account for slightly different vertebrae heights/widths; the vertebral body dimensions (displayed in Table II) do not vary so significantly that a large range of heights/widths need to be accounted for. As seen in Fig. 4, the Delrin vertebrae were created as rectangular prisms with one semi-circular edge. To create these simplified vertebrae, the superior and inferior endplate areas were averaged, yielding an average endplate area that could be used for both the superior and inferior sides of the Delrin vertebrae. As Delrin is readily available in cylindrical rods at a reasonable cost—unlike Delrin sheets—and a cervical vertebra can roughly be approximated as a cylinder, the vertebral cross-section was assumed to be circular. The average endplate area was used to calculate a vertebral body diameter, yielding the width of the Delrin vertebrae seen in Fig. 8 (see Appendix C: Delrin Vertebrae Size Calculations). The Delrin vertebrae were then extended as a rectangular prism in one direction (maintaining that the side which an implant system would be applied to was circular), so that any wood screws connecting a Delrin vertebra to the front plate or connection plate would not interfere with the surgical screws connecting the implant to a given vertebra. The vertebrae were extended 0.5 inches beyond the diameter from the semi-circular side (see Fig. 5), as 0.5 inches will provide enough catch to prevent any screw pullout during testing. Holes of diameter 0.125” were pre-drilled for the No. 8 wood screws.

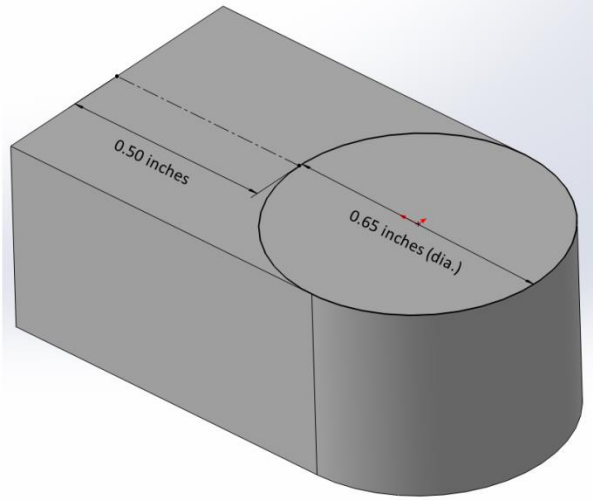

Fig. 8: Isometric View of Delrin Vertebra – The Delrin vertebra extends ½ inches beyond the circle labeled with a 0.65 inch diameter.

2. Back Plate Design:

In both the anterior and posterior fixture designs, the back plate is the same and is made of 6061 Aluminum Alloy. It is 5.384 inches in height, 1.772 inches in width, and 0.25 inches in thickness. There are six countersunk unthreaded holes to accommodate for the No. 8 flat head Phillips machine screws used in the anterior and posterior test fixtures. The back plate is large enough so that a polyurethane rod segment of 1.5 inches in diameter can be accommodated. Moreover, additional holes will be added to this plate so that the fixture for the anterior implant systems can be mounted to a table to mimic the supine position during surgery. Fig. 9 depicts the layout of the unthreaded holes and which are used for a given fixture.

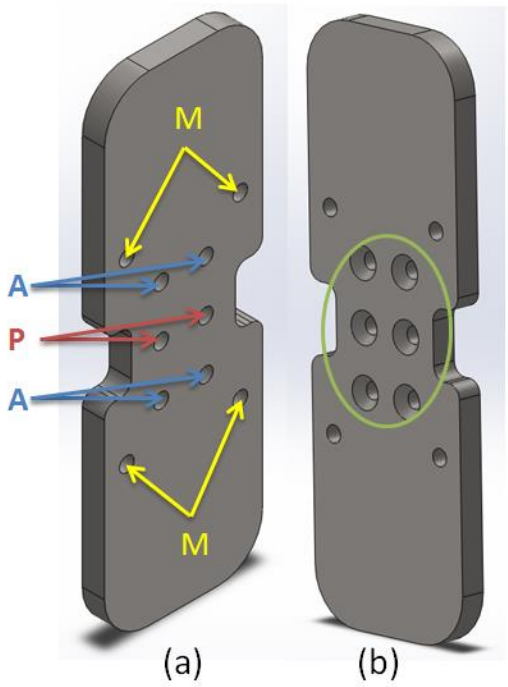

Fig. 9: Layout of Holes in Back Plate – Part (a) is an isometric view of the back plate, where the yellow arrows labeled with "M" refer to the mounting holes (used for the anterior fixture only), the blue arrows labeled with "A" refer to the holes used in the anterior fixture, and the red arrows labeled with "P" refer to the holes used in the posterior fixture. Part (b) is a back side isometric view of the back plate, where the green circle points out the countersunk holes. The mounting holes were not used in the actual design, but mounting was done similarly with vice/clamps during actual testing.

3. Front Plate Design:

In both the anterior and posterior fixtures, the front plate is very similar and made of 6061 Aluminum Alloy. The main difference between the two is that while the anterior front plate has two slits to allow for the connection between the back plate and the superior and inferior Delrin vertebrae, while the posterior front plate has one slit to allow for the connection between the back plate and the middle (slipped) Delrin vertebra. Both front plates have four slots which accounts for the addition of material on the sides of the top and bottom of the plate; these slots house the tightening plate-bolt assembly which is used to stabilize the varying-diameter polyurethane rod segments in the vertical mid-plane of the front plate. Essentially, the tightening plate-bolt assembly is needed to

maintain that the polyurethane rod segments will apply their resistive forces the same distance from the horizontal mid-plane of the front plate. Both the anterior and posterior front plates are 5.384 inches in height (same as the back plate), while the largest width of both front plates (the width at the slots) is 4.724 inches. The widths at the horizontal mid-plane of the anterior and posterior front plates are 2.272 inches and 2.5 inches, respectively. Moreover, both front plates have a 0.5 inch extension off of the plate at the location of the vertebra(e) connection to the front plate. The volumes of the anterior and posterior front plates are 54800 mm^3 and 62500 mm^3, but the volumes are small enough that their preload effect should be minimal. Figs. 10 and 11 display the anterior and posterior front plate designs.

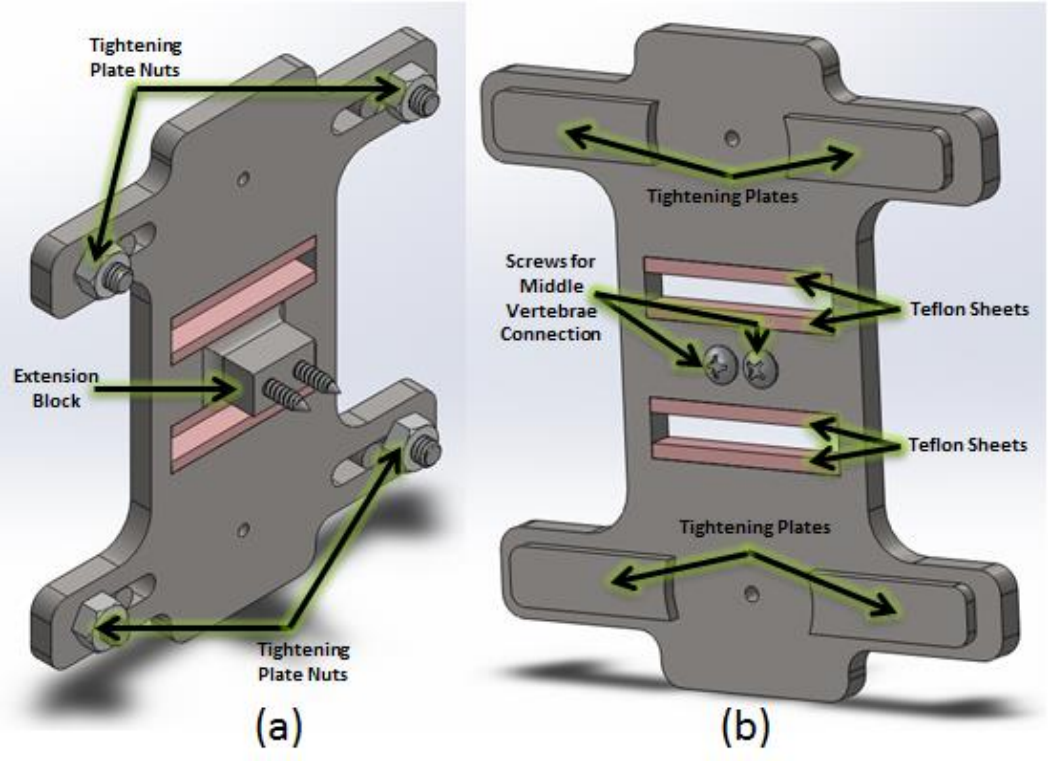

Fig. 10: Anterior Fixture Front Plate – Part (a) is an isometric view of the front plate, with labels for the tightening plate nuts and extension block, while part (b) is a back side isometric view of the front plate, with labels for the tightening plates, screws for middle vertebrae connection, and teflon sheets. Note: it was found that Teflon sheets were unnecessary.

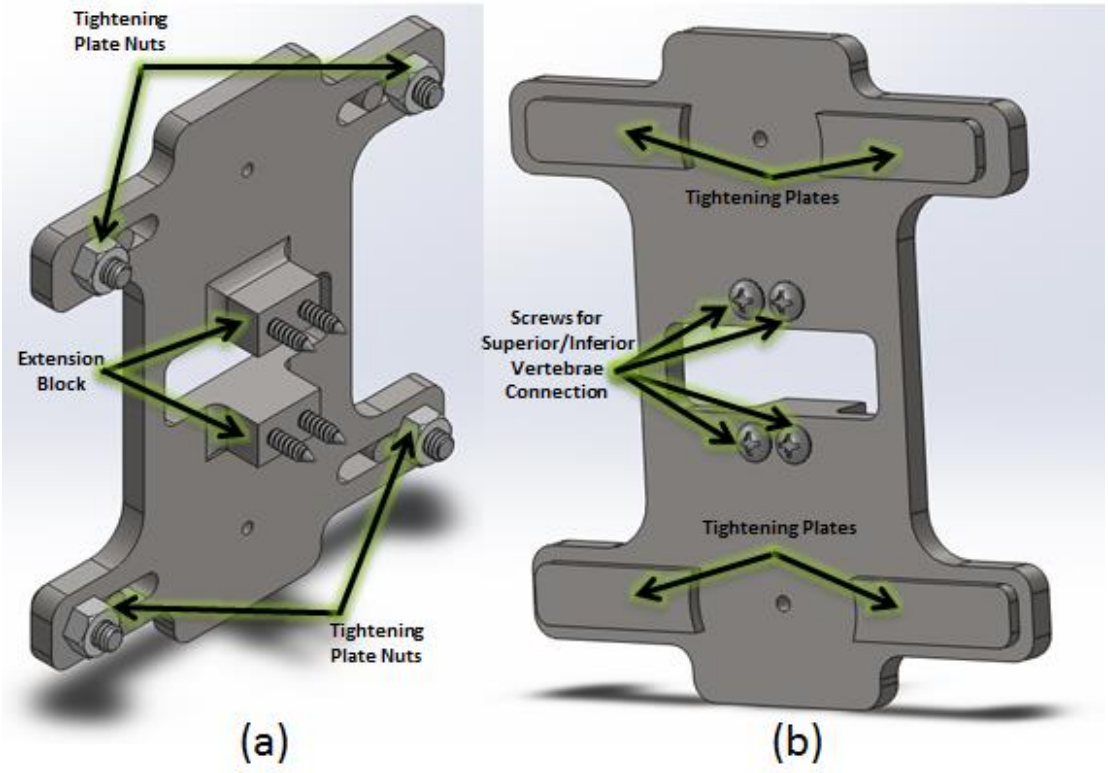

Fig. 11: Posterior Fixture Front Plate – Part (a) is an isometric view of the front plate, with labels for the tightening plate nuts and extension block, while part (b) is a back side isometric view of the front plate, with labels for the tightening plates, screws for middle vertebrae connection, and teflon sheets. Note: teflon sheets are not included, and it was found they were unnecessary.

4. Attachment from Back Plate to Delrin Vertebrae (Connection Plate):

In the anterior fixture, the superior and inferior vertebrae are connected to the back plate, while in the posterior fixture, the middle vertebra is connected to the back plate. This connection between the back plate and a given vertebra was designed to be adjustable, as anterior and posterior fixtures must be able to accommodate different length polyurethane rod segments. For each vertebra which needed to be connected to the back plate, two flat Phillips head No. 8 machine screws were inserted through the horizontally-paired unthreaded holes of the back plate to be screwed into the two threaded holes of the connection plate. A No. 8 washer is used on the opposite side of the back plate from which the machine screw was inserted so as to fasten the screw to the

back plate. Different length No. 8-32 machine screws ranging from 1 inch to 1.5 inches can be used to allow for a range of 20 mm to 40 mm length polyurethane rod segments. It was assumed that ¼ inch of each screw needed to be the minimum length threaded into the connection plate for sufficient attachment. The connection plate is ¼ inch thick and made from Cast Alloy Steel. Its general design and location of threaded holes is displayed in Fig. 12.

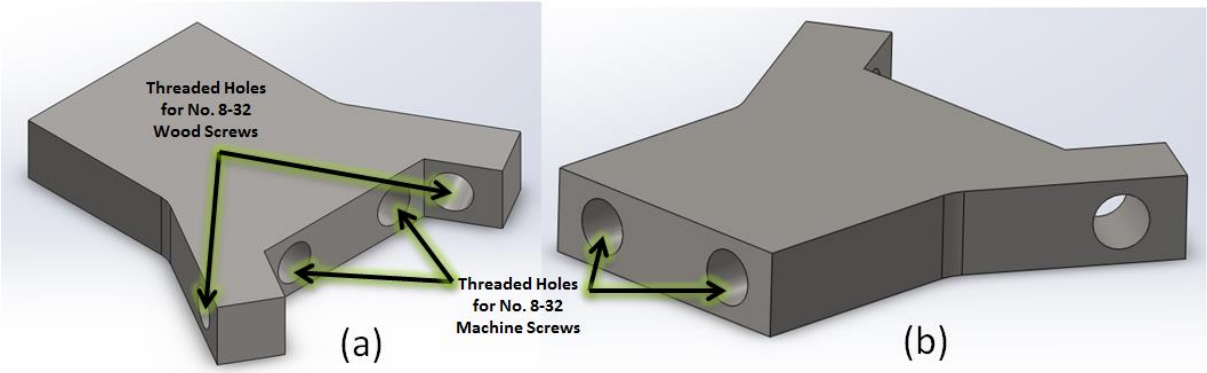

Fig. 12: Connection Plate – Part (a) is an isometric view of the connection plate and part (b) is a back side isometric view of the connection plate, both of which have labels for the machine screws which will go through each hole.

The general connection between the back plate and a given Delrin vertebra is the same for both the anterior and posterior fixtures. The implementation of the connection plate system into the anterior and posterior fixtures is seen in Figs. 13 and 14.

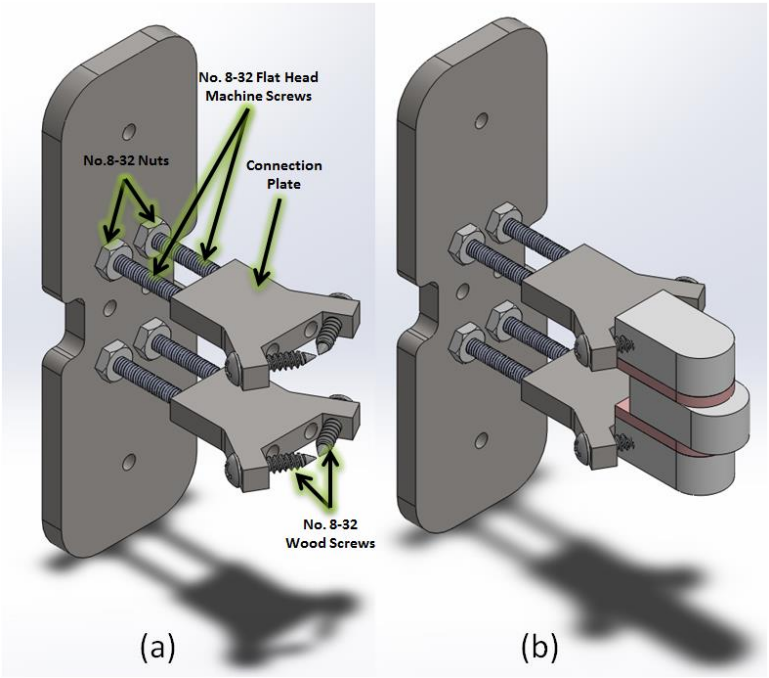

Fig. 13: Anterior Fixture Back Plate to Delrin Vertebrae Connection – Part (a) depicts the back plate to Delrin vertebrae connection without the Delrin vertebrae (so that the screw connection to the Delrin vertebrae can be visualized), while part (b) is the same view but with the Delrin vertebrae shown. Note: Teflon sheets were found to be unnecessary and the top and bottom Delrin vertebrae were made thick to account for the 1/8" gap.

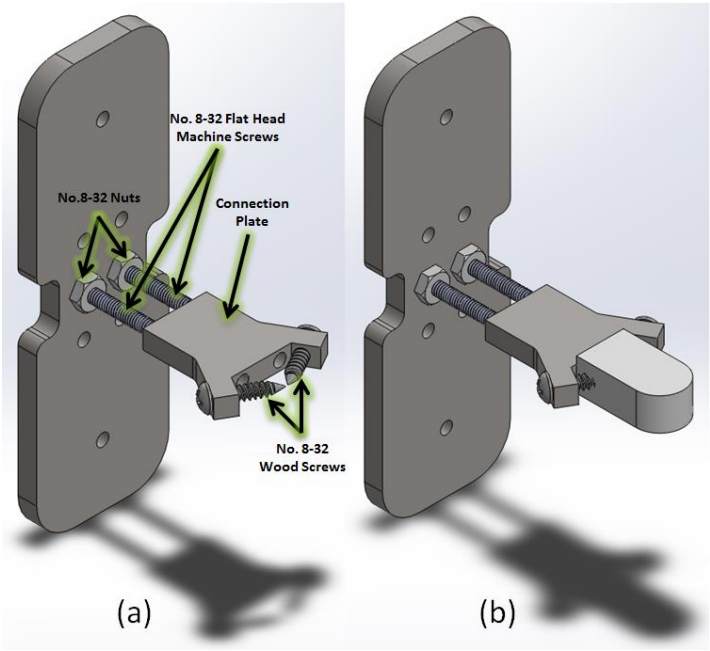

Fig. 14: Posterior Fixture Back Plate to Delrin Vertebrae Connection – Part (a) depicts the back plate to Delrin vertebrae connection without the Delrin vertebrae (so that the screw connection to the Delrin vertebrae can be visualized), while part (b) is the same view but with the Delrin vertebrae shown.

Finite Element Analysis:

1. Back Plate:

Although it is uncertain yet exactly how the anterior and posterior fixtures will be mounted, preliminary ideas have been explored and tested using FEA. These preliminary ideas are only for the initial testing which will take place as if the two-level spinal unit were in surgery. As the anterior fixture would be in the supine position, the back plate would be fixed to a table, so an analysis was done for both this case, as well as for the case of the posterior fixture whereby different forces and fixtures are implemented (see Fig. 15).

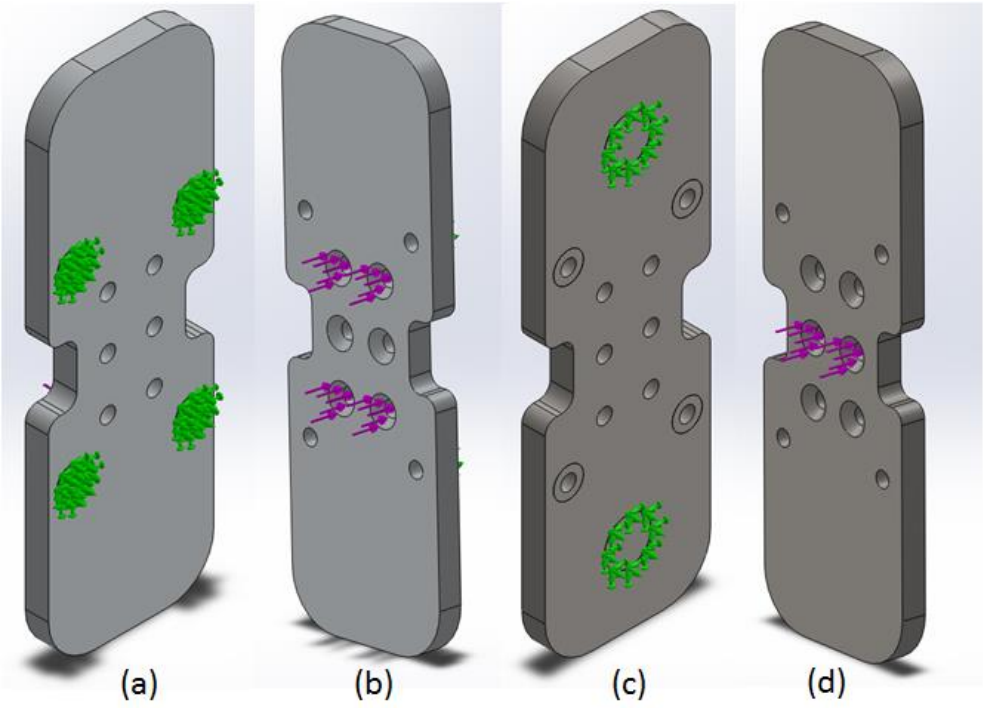

Fig. 15: Back Plate Loading/Fixture Conditions – Parts (a) and (b) are front and back side isometric views, respectively, for the anterior fixture, while parts (b) and (c) are front and back side isometric views, respectively, for the posterior fixture.

For the anterior fixture study, the plate was fixed at the mounting holes (where the head of the screws would be in contact with the plate) as seen in Fig. 15a. and a conservative total force of 1000 N (chosen as a conservative load, twice as large as

should ever be experienced) was applied to four countersunk holes Fig. 15b. The Von Mises stress distribution over the back plate is shown in Fig. 16. The maximum Von Mises stress occurred at the location of the bottom right fixture with a magnitude of 36.5 MPa, which is less than the yield stress of 6061 aluminum alloy of 55.1 MPa. The plate is geometrically symmetrical about the vertical and horizontal axes, so the same maximum Von Mises stress should be achieved at each of the mounting locations that were fixed. It was found that no significant bending would occur to the plate (for FEA results, see Appendix D: Additional Finite Element Analysis).

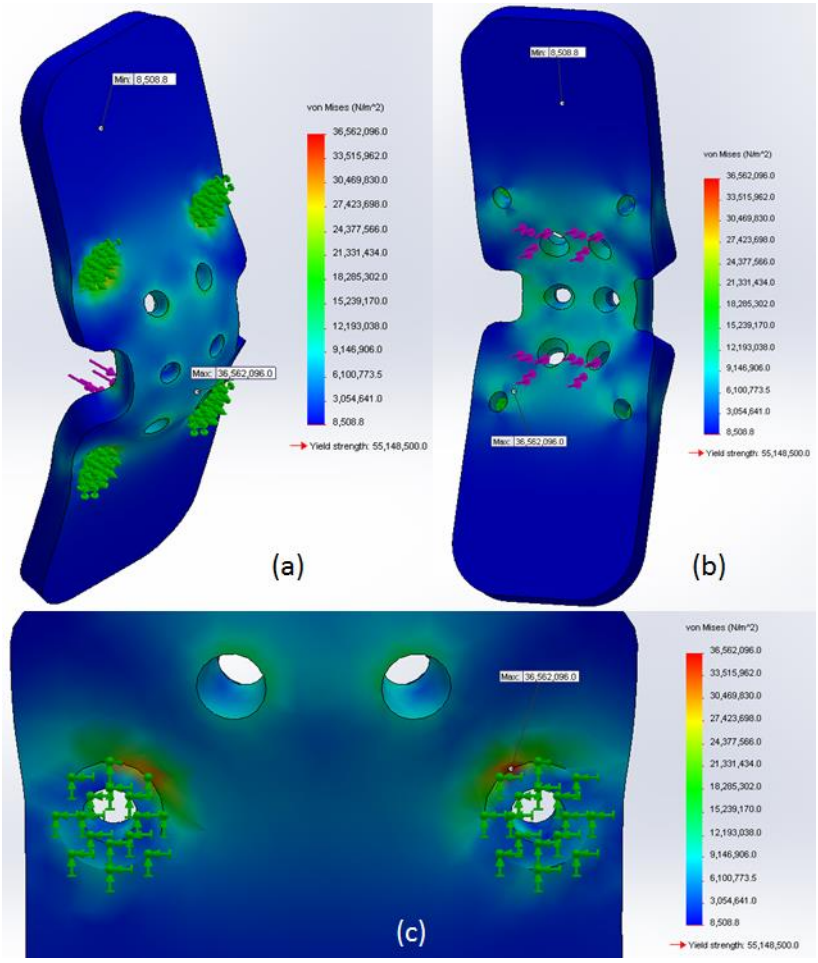

Fig. 16: Anterior Fixture Back Plate Von Mises Stress Results – Results from the FEA are displayed with part (a) showing a front side isometric view, part (b) showing a back side view, and part (c) showing a close up of the front side where the maximum Von Mises Stress was achieved. Note: the deformation scale for this analysis is 1329.21.

For the posterior fixture study, the back plate was fixed at the location of where the polyurethane rod segments would be in contact with it, as seem in Fig. 15c. A conservative area of contact was assumed as a circle of ½ inch diameter, as the smallest diameter polyurethane rod segment which would be used in testing is 5/8 inch. Compared to the anterior fixture back plate FEA, a less conservative total force of 500 N was applied to two countersunk holes seen in Fig. 15d, as a 1000 N force led to yielding. The Von Mises stress distribution over the back plate is shown in Fig. 17. A maximum Von Mises stress was achieved at the inner side of the right countersunk hole where half of the force was applied; the magnitude of the stress was 53.4 MPa, which is slightly less than the yield stress of 6061 aluminum alloy of 55.1 MPa. As this was a conservative analysis, yielding should not occur during actual testing. The plate is geometrically symmetrical about the vertical and horizontal axes, so the same maximum Von Mises stress would be achieved at each of the inner sides of those holes. It was found that no significant bending would occur to the plate (for more FEA results, see Appendix D: Additional Finite Element Analysis).

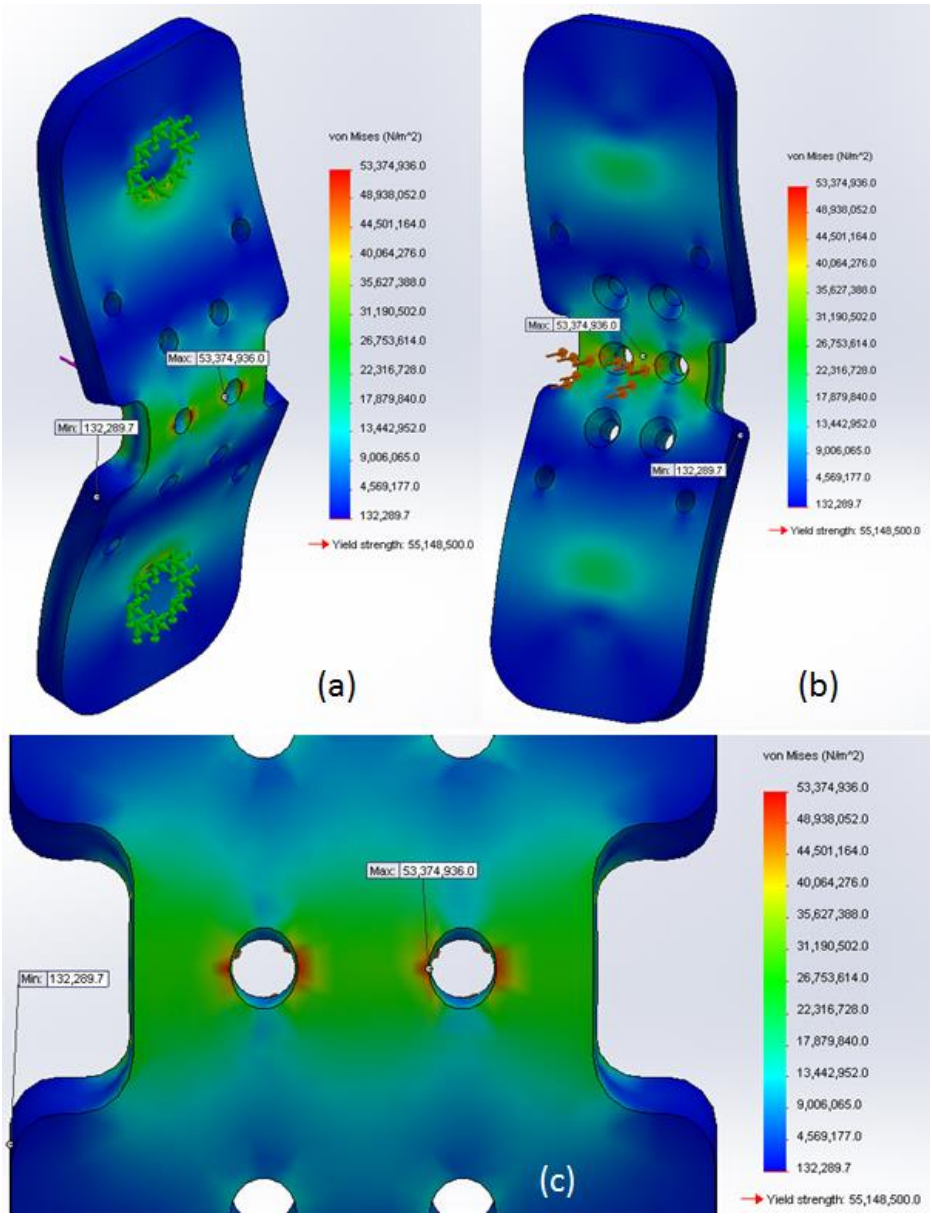

Fig. 17: Posterior Fixture Back Plate Von Mises Stress Results – Results from the FEA are depicted with part (a) showing a front side isometric view, part (b) showing a back side view, and part (c) showing a close up of the front side where the maximum Von Mises Stress was achieved. Note: the deformation scale for this analysis is 302.992.

2. Front Plate:

    a. Anterior Fixture:

The force from the middle (slipped) vertebra being pushed back into alignment with the superior and inferior vertebrae would be applied to the extension block

distributed about the area of the face of the Delrin vertebra that is contact with the block (see Fig. 18a). The front plate was restrained at the location where the polyurethane rod segments come into contact with the front plate, as seen in Fig. 18b. A conservative area of polyurethane rod segment contact was used, assuming a circular contact surface of ½ inch, which is a smaller diameter that would actually be used in testing.

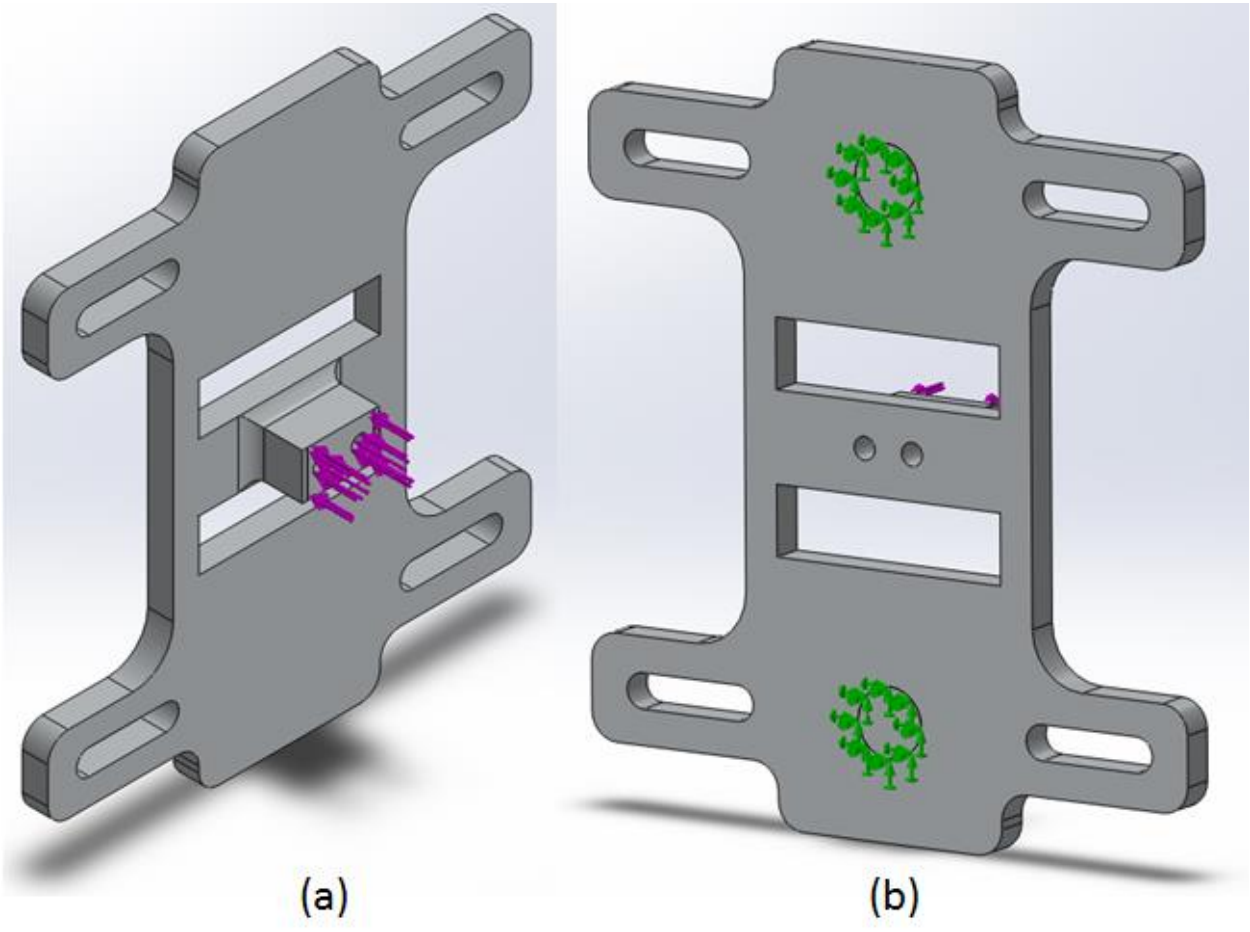

Fig. 18: Anterior Fixture Front Plate Loading/ Fixture Conditions – Part (a) shows a front isometric view with the applied force while part (b) shows a back isometric view with the surace which was fixed.

The magnitude of the force applied to the extension block was 500 N (as 1000 N led to yielding), which is still a conservative magnitude and that is larger than any force which would be applied to the plate. The Von Mises stress distribution over the anterior fixture front plate is shown in Fig. 19. The maximum Von Mises stress was achieved at

the location of the top right corner of the bottom rectangular opening; the magnitude of the stress was 37.4 MPa which is less than the yield stress of 6061 aluminum alloy of 55.1 MPa. The plate is geometrically symmetrical about the vertical and horizontal axes, so the same maximum Von Mises stress would be achieved at each of the corners closest to the horizontal mid-plane. It was found that no significant bending would occur to the plate (for more FEA results, see Appendix D: Additional Finite Element Analysis).

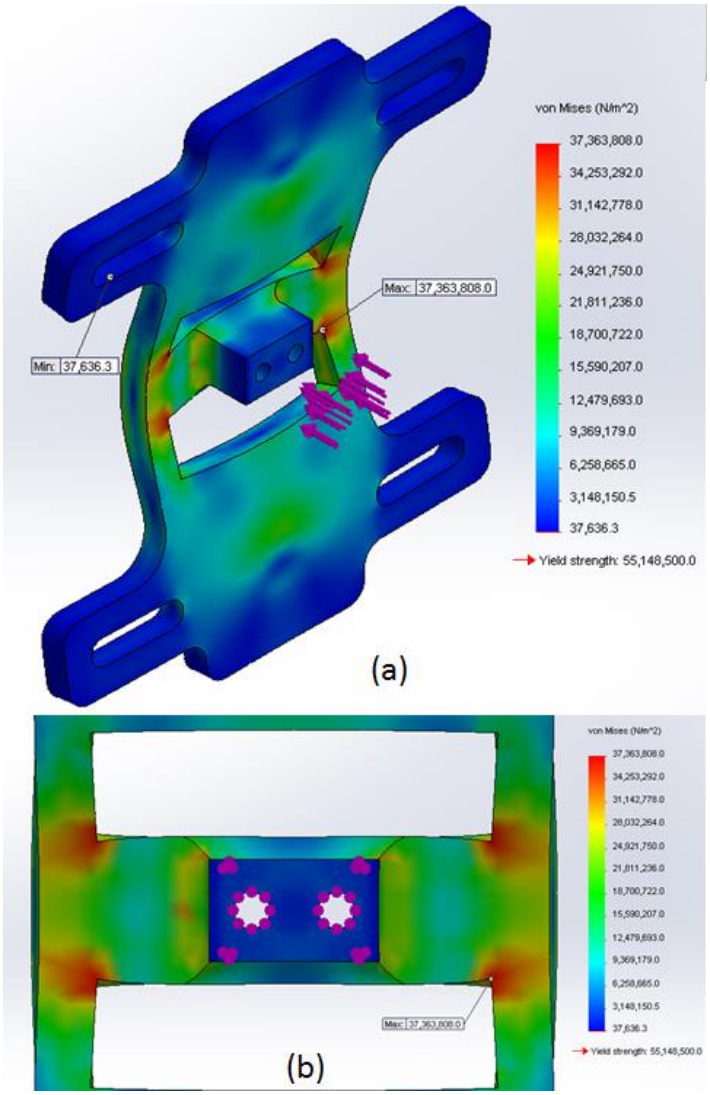

Fig. 19: Anterior Fixture Front Plate Von Mises Stress Results – Results from the FEA are displayed with part (a) showing a front isometric view and part (b) showing a close-up of the front side of the plate to better see where the maximum stress is occuring. Note: the deformation scale for this analysis is 187.157.

b. Posterior Fixture:

The force from the middle (slipped) vertebra being pulled back into alignment with the superior and inferior Delrin vertebrae results in a response force of the superior and inferior Delrin vertebra pushing on the upper and lower extension blocks of the front plate. The force on each extension block is distributed about the area of the face of the Delrin vertebrae which are in contact with the extension blocks, as seen in Fig. 20a. The front plate was restrained at the location where the polyurethane rod segments come into contact with the front plate, as seen in Fig. 20b. A conservative area of polyurethane rod segment contact was used, assuming a circular contact surface of ½ inch, which is a smaller diameter that would actually be used in testing.

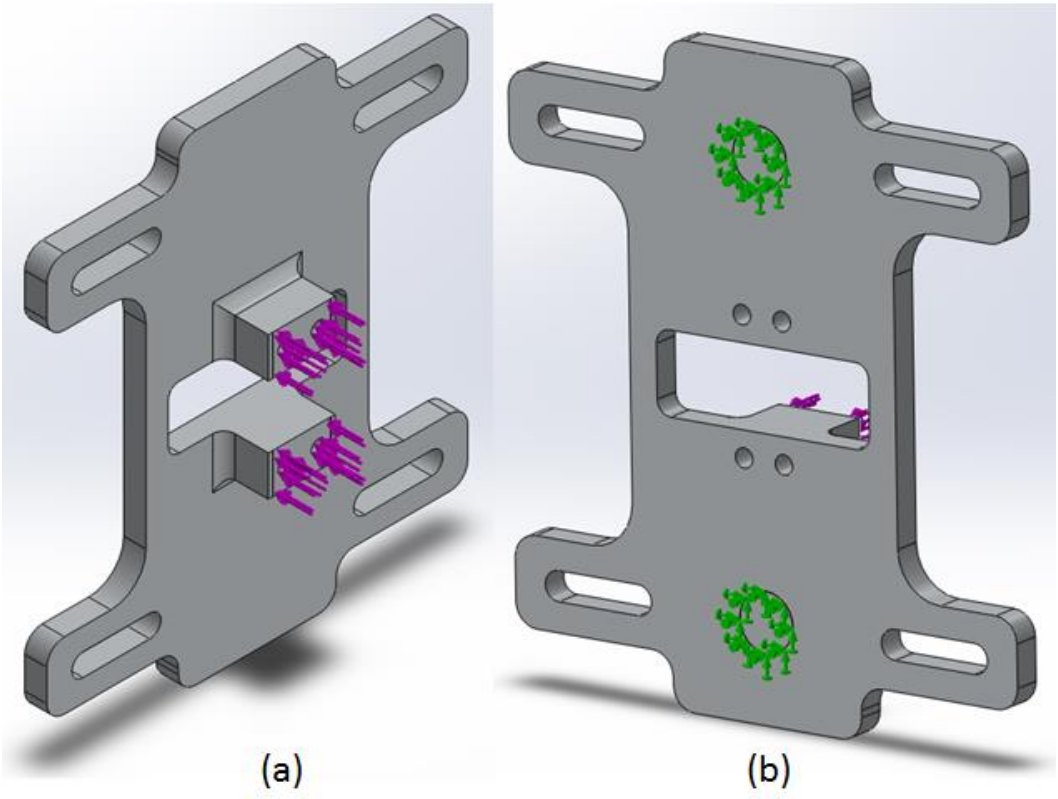

Fig. 20: Posterior Fixture Front Plate Loading/Fixture Conditions - Part (a) shows a front isometric view with the applied force while part (b) shows a back isometric view with the surace which was fixed.

The magnitude of the total force applied to both extension blocks was 500 N (as 1000 N led to yielding), which is still a conservative force as it is larger than any force that should be applied to the plate. The Von Mises stress distribution over the plate is displayed in Fig. 21. The maximum Von Mises stress was achieved at the location directly below the top circular area fixture (see Fig. 21c), with a magnitude of 42.3 MPa, which is less than the yield stress of 6061 aluminum alloy of 55.1 MPa. The plate is geometrically symmetrical about the vertical and horizontal axes, so the same maximum Von Mises stress would be achieved at each of the fixture locations. Also, it was found that no significant bending would occur to the plate (for more FEA results, see Appendix D: Additional Finite Element Analysis).

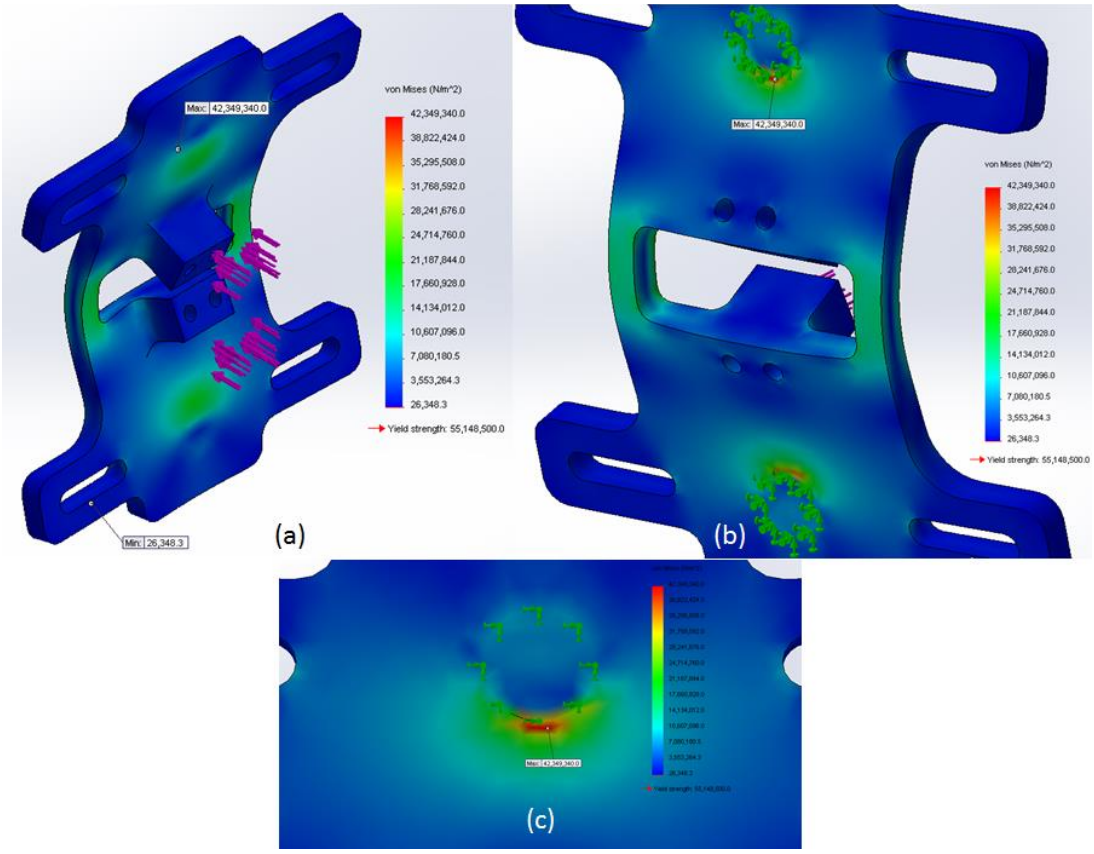

Fig. 21: Posterior Fixture Front Plate Von Mises Stress Results – Results from the FEA are displayed with part (a) showing a front isometric view, part (b) showing a back isometric view, and part (c) showing a close-up of the location where the maximum Von Mises stress occurred. Note: the deformation scale for this analysis is 358.267.

3. Connection Plate:

In both the anterior and posterior fixtures, the connection plate will essentially be pulled on through the front angled holes; the Delrin vertebra attached to a given connection plate will be attached via two wood screws through the angled holes, and that Delrin vertebra will experience a pulling force. The purple arrows in Fig. 22 show the direction of that pulling force being exerted on the connection plate. The connection plate will be restrained by the two machine screws which will be fastened a minimum of ¼ inch into the parallel, fully threaded holes extending the length of the connection plate. Thus, to maintain a conservative analysis, the connection plate was restrained ¼ inch into the two parallel threaded holes.

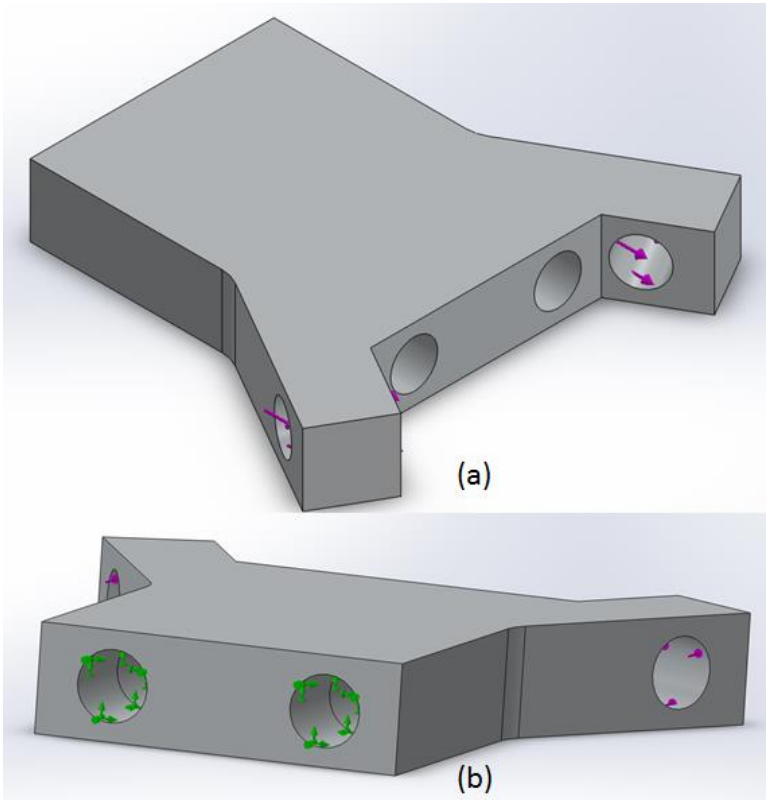

Fig. 22: Connection Plate Loading/Fixture Conditions – Part (a) shows a front isometric view where the applied forces can be seen, while part (b) shows a back side view where it can be seen that the connection plate is restrained inside the (threaded) holes which extend the length of the plate.

The total magnitude of the force applied to the two angled holes is 1000 N, which is much larger than any force which should be experienced by the connection plate. It was found that having the connection plate made of 6061 aluminum alloy would not be sufficient under forces that it would likely experience (~500 N) as yielding would occur. The Von Mises stress distribution over the connection plate is displayed in Fig. 23. The maximum Von Mises stress of 162.7 MPa was experienced at the opening of the left hole that runs the length of the plate, and was less than the yield stress of cast alloy steel of 241.3 MPa. The plate is geometrically symmetrical about the vertical and horizontal axes, so the same maximum Von Mises stress would be achieved at each of those holes, both at the top and bottom of the opening. In addition it was found that no significant bending would occur to the plate (for more FEA results, see Appendix D: Additional Finite Element Analysis).

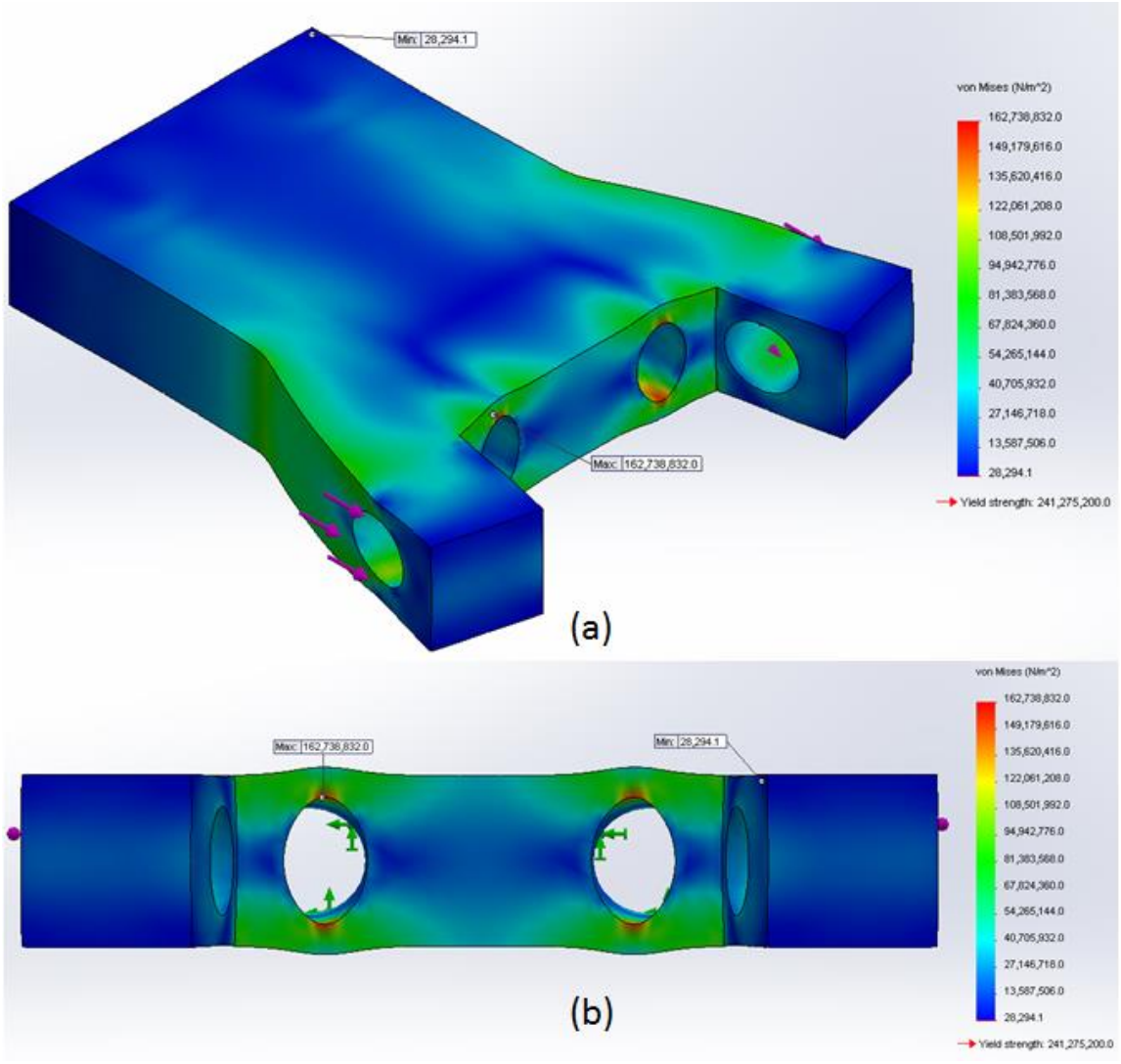

Fig. 23: Connection Plate Von Mises Stresses Results – Results from the FEA are illustrated with part (a) showing a front isometric view and part (b) showing a front view to better display the area of maximum Von Mises stress. Note: the deformation scale for this analysis is 295.018.

4. Delrin Vertebra:

    a. Fixed on Back:

The Delrin vertebrae connected to either the anterior or posterior front plate will always be in compression due to how the fixtures are set up. When an implant system applied to a Delrin vertebra in this situation, a compressive force from the implant system on the semi-circular front face is generated, as seen in Fig. 24a. Also, these Delrin

vertebrae will be in contact with an extension block and will be fastened with two 1 ¼ inch No.8-32 wood screws, 0.5 inch of which will be screwed into the Delrin vertebrae. As a result, the Delrin vertebra for this case was fixed about the approximate area of these two 0.5 inch holes (as seen in Fig. 24b).

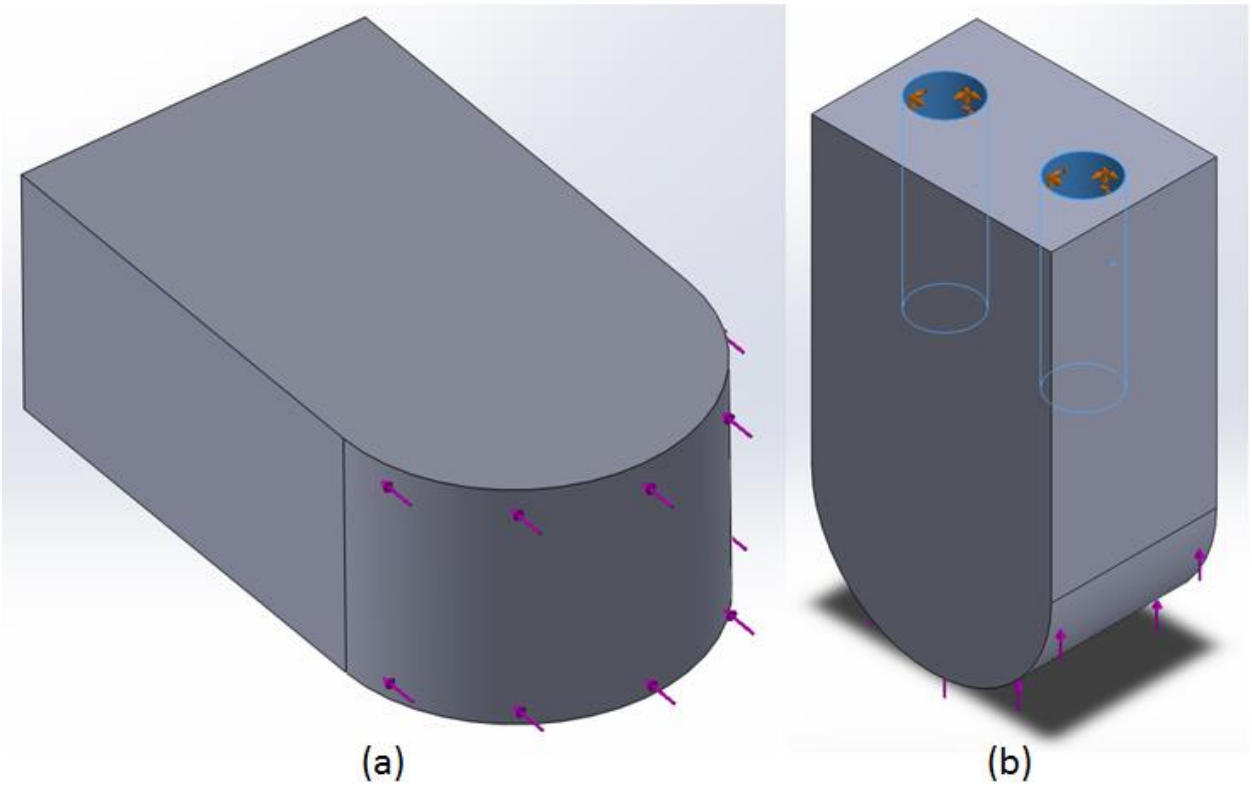

Fig. 24: Delrin Vertebra Fixed on Back Loading/Fixture Conditions – Part (a) shows the force being exerted on the semi-circular front face of the Delrin vertebra and part (b) shows the 0.5 inch deep holes which are fixed.

The magnitude of the force applied was 1000 N, which is conservative as no force this large will ever be applied to any of the Delrin vertebra. The Von Mises stress distribution over the Delrin vertebra which is fixed on the back is shown in Fig. 25. The maximum Von Mises stress occurs at the top of circumference 0.5 inch into the hole (at the end of the hole), with a magnitude of 6.89 MPa, which is significantly less that the yield stress of 63.0 MPa for Delrin 2700 NC010, Low Viscosity Acetal Copolymer (the Delrin available in Solidworks). As the Delrin vertebra is symmetrical from a top view,

this maximum Von Mises stress would be experienced at the top and bottom of the circumferences at the end of the holes. In addition, this fixed surface will be different during actual testing as the fixed surface will be threaded (a No.8-32 wood screw will be used). Also, it was found that no significant bending would occur to the plate (for more FEA results, see Appendix E: Additional Finite Element Analysis).

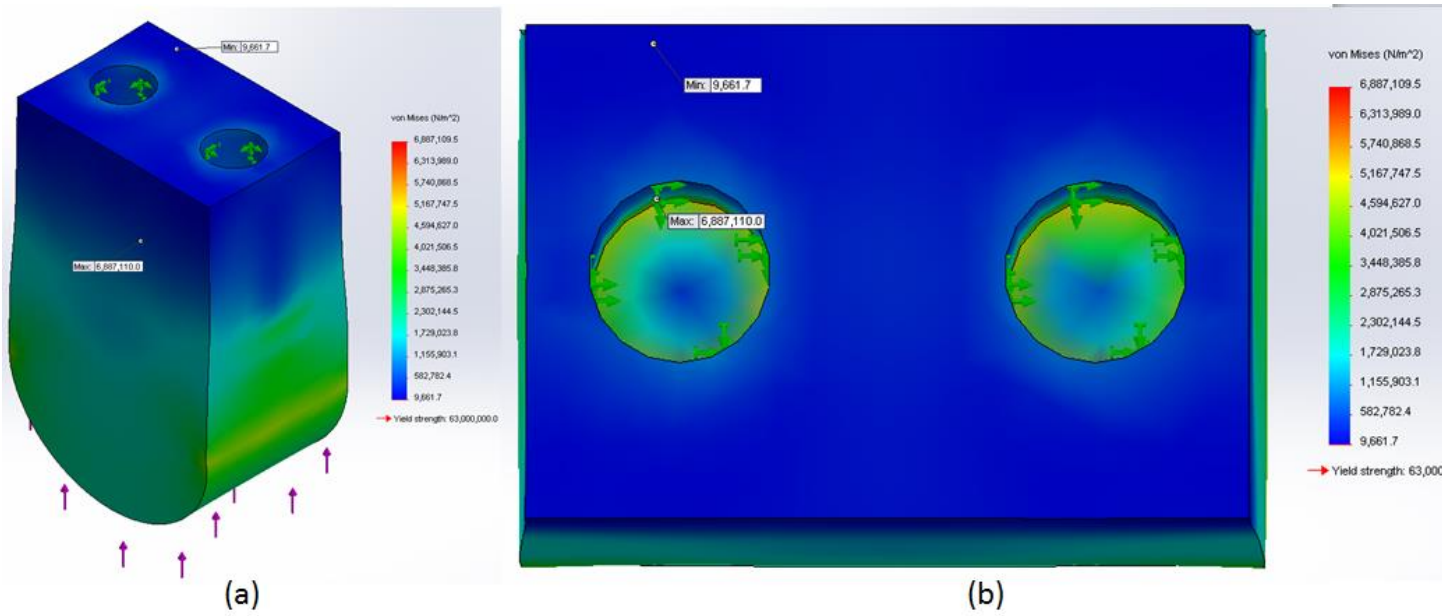

Fig. 25: Delrin Vertebra Fixed on Back Von Mises Stress Results – Results from the FEA are displayed with part (a) showing a front isometric view and part (b) showing a top view with the maximum Von Mises stress and the surrounding stress distribution. Note: the deformation scale for this analysis is 187.586.

b. Fixed on Sides (Angled Holes):

The Delrin vertebrae attached to a connection plate will always be in tension due to how the fixtures are set up. When an implant system is applied to a Delrin vertebra in this situation, a pulling force from the implant system on the semi-circular front face is generated, as seen in Fig. 26a. Also, these Delrin vertebrae will be fastened with two ¾ inch No.8-32 wood screws, of which less than 0.5 inch will be screwed into the Delrin

vertebrae. As a result, the Delrin vertebra for this case was fixed using the surface area of the two diagonal holes (see in Fig. 26b).

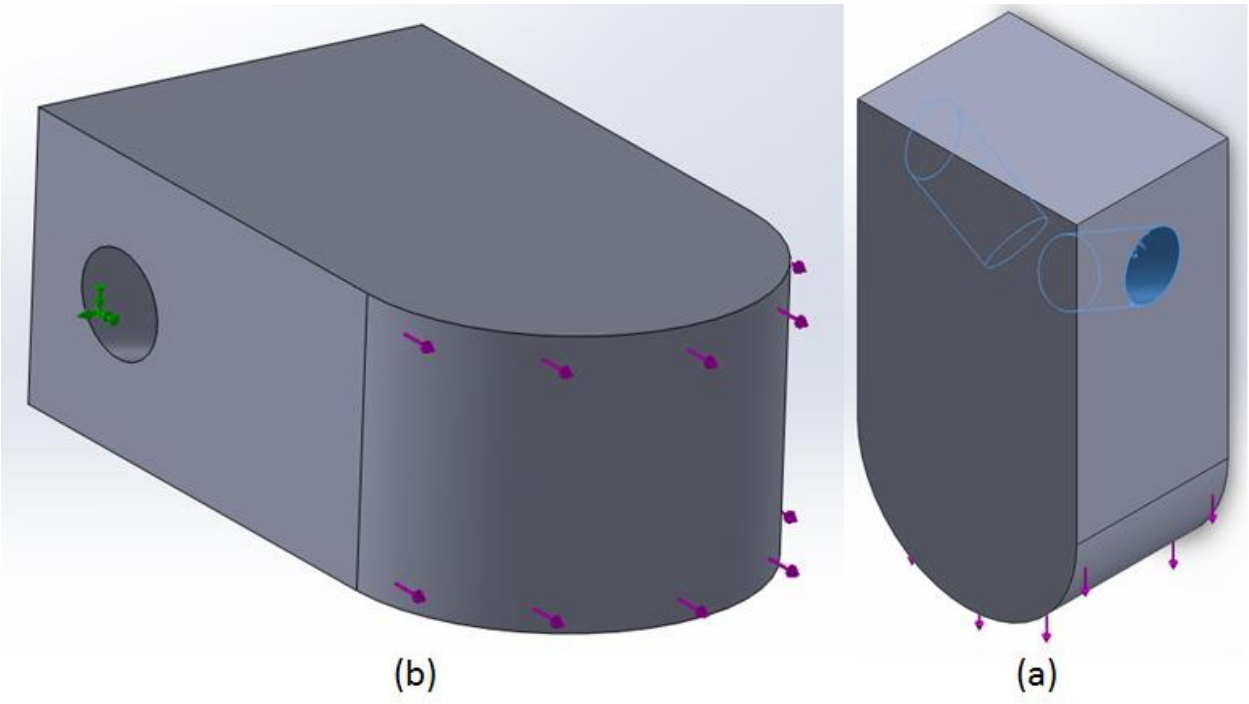

Fig. 26: Delrin Vertebra Fixed on Sides Loading/Fixture Condition - Part (a) shows the force being exerted on the semi-circular front face of the Delrin vertebra and part (b) shows the angled holes which are fixed.

The magnitude of the force applied was 1000 N, which is conservative as no force this large will ever be applied to any of the Delrin vertebra. The Von Mises stress distribution over the Delrin vertebra which is fixed on the sides is shown in Fig. 27. The maximum Von Mises stress occurs at the circumference at the end of the left angled hole, with a magnitude of 13.3 MPa, which is much less that the yield stress of 63.0 MPa for Delrin 2700 NC010, Low Viscosity Acetal Copolymer (the Delrin available in Solidworks). As the Delrin vertebra is symmetrical from a top view, this maximum Von Mises stress would be experienced at circumferences at the end of each of the holes. Also, this fixed surface will be different during actual testing as the fixed surface will be threaded (a No.8-32 wood screw will be used). In addition, it was found that no

significant bending would occur to the plate (for more FEA results, see Appendix D: Additional Finite Element Analysis).

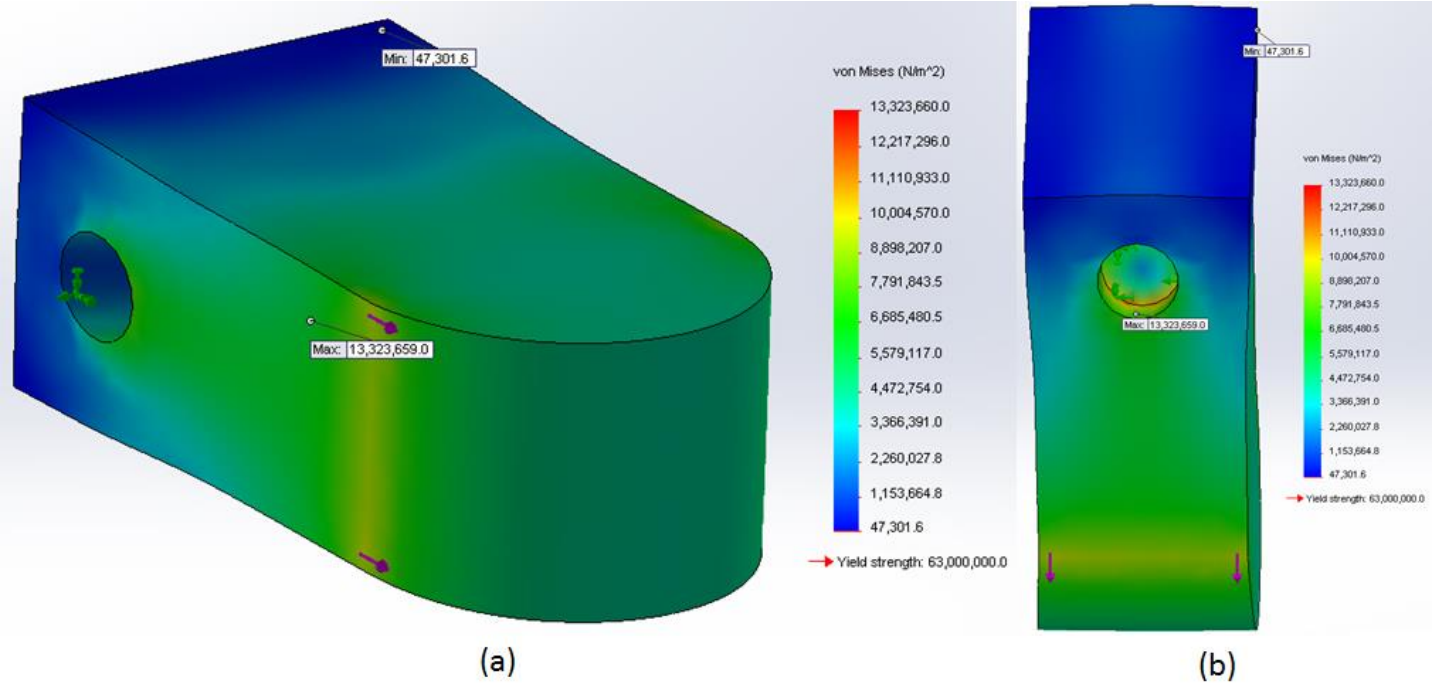

Fig. 27: Delrin Vertebra Fixed on Sides Von Mises Stress Results – Results from the FEA are illustrated with part (a) showing a front isometric view and part (b) showing a top view with the maximum Von Mises stress and the surrounding stress distribution. Note: the deformation scale for this analysis is 82.4928.

Note: no additional FEA was performed for the terminal three point bending front plate as it was verified during actual testing that no bending or deflection occurred in either the standard three point bending tests or the posterior fixture, and this front platen had one less hole than the posterior front plate (deeming it stiffer).

Polyurethane Rod Segment Selection, Testing, and Results:

Three 6 inch polyurethane rods were obtained, two of which were 60A (medium-hard rubber) hardness, and the other of which was 40A (soft-medium) hardness. Rubbers are measured in terms of their hardness using the Shore A scale on a scale of 0 to 100. Of

the two 60A hardness rods, one was 5/8 inch in diameter, while the other was 3/4 inch in diameter. The 40A hardness rod was 1.5 inches in diameter. Rubbers are not characterized with Young's Modulus, so based on a range of Moduli given for polyurethane rubber of 1-10 MPa, the 40A and 60A hardness polyurethane rods and their respective diameters were chosen; the 40A hardness polyurethane rod was obtained with a much larger diameter than that of the two 60A hardness polyurethane rods due to its softer nature [20].

Based on calculations assuming a range of 1-10 MPa for Young's Modulus, it was found that a range of 20 mm to 40 mm should provide the desired displacement of 3-5 mm based on a compressive load within the range of 250 N to 450 N (for these calculations, see Appendix E: Preliminary Rubber Rod Calculations). As a result, these 6 inch rods were measured to segments of 20 mm (short), 30 mm (medium), and 40 mm (tall) using a Vernier caliper and cut using a sawmill. However, this resulted in end surfaces of the rod segments that were not flat. Using custom-made chucks for the diameters of the three rods, the segments were loaded and more precisely flattened in the lathe. There were slight blemishes—possibly due to burning/melting—around the circumferences of the three segments made from the 40A hardness polyurethane rod due to their softer nature. The three segments for both the 60A hardness polyurethane rods were without blemishes. Three measurements were recorded for the heights and diameters of each of the rod segments and are listed in Table V (see Appendix F: Polyurethane Rod Segment Testing).

Table V: Average Diameters and Heights of Polyurethane Rod Segments – To identify the rod segments, they were divided based on their diameter first, and then their length. Thus, A refers to the thickest rod, B refers to the middle thickness rod, and C refers to the least thick rod, while 1 refers to the longest segment, 2 refers to the middle length segment, and 3 refers to the shortest segment.

General Rod Segment Label	Sample ID	Average Diameter (mm)	Average Diameter (in)	Average Height (mm)	Average Height (in)
A (~1.5 in diameter)	A1 (tall)	37.9	1.49	38.9	1.53
	A2 (medium)	37.7	1.48	28.6	1.13
	A3 (short)	37.6	1.48	18.5	0.73
B (~0.75 in diameter)	B1 (tall)	19.3	0.76	38.9	1.53
	B2 (medium)	19.4	0.76	28.5	1.12
	B3 (short)	19.4	0.76	17.2	0.68
C (~0.625 in diameter)	C1 (tall)	15.8	0.62	38.3	1.51
	C2 (medium)	15.9	0.63	27.9	1.10
	C3 (short)	15.9	0.62	18.3	0.72

The polyurethane rod segments were tested in a 50 lb (222 N) load cell (SN: 342) in a 20-kip load frame (BUT101-02). A compression cage fixture with fixed platens was used in the load cell, with 4 ½ ” x 4 ½” x ½” platform plates, platens of 2” diameter x ¾” height, 8 guide posts of 8 ½” in height with linear bearings 3/16” in diameter. The rod segments were loaded at a rate (cross-heard) of 1 mm/min (or ~0.04 in/min) with the test to be terminated after 5 mm of cross-head. In addition, the 50 lb load cell used was not to exceed 200 N (or ~45 lb). As a result, there were two restraints—displacement and load—which could not be exceeded, with the displacement restriction established so as to not permanently deform the segments, while the load cell was not able to handle loads greater than 200 N. The desire of this testing was to characterize the load-displacement

behavior of the segments; it is assumed thus far that for such small displacements, the rod segments have roughly linear load-displacement behavior.

After calibration, the segments were loaded with a small preload ranging from 1 N to 2 N. The maximum cross-head (displacement) achieved at the maximum load are listed in Table VI, along with the specific preloads from each test. The rod segments which predict a load of approximately 250 N to 450 N to be displaced 5 mm are within the desired range.

Table VI: Results from Polyurethane Rod Segment Testing – Listed for each segment are the preload applied to it, max load, max cross-head, and the prediction for the load to displace a given segment 5 mm (assuming a linear load-displacement relationship).

General Rod Segment Label	Sample ID	Preload (N)	Max Load (N)	Max Cross-Head (mm)	Load Prediction for 5 mm Displacement	Rod Segment Stiffness (N/mm)
A (~1.5 in diameter)	A1 (tall)	1.0	195.0	4.48	217.6	43.5
	A2 (medium)	1.0	195.0	3.36	290.2	58.0
	A3 (short)	1.0	195.0	2.43	401.2	80.2
B (~0.75 in diameter)	B1 (tall)	1.0	197.3	5.00	197.3	39.5
	B2 (medium)	2.0	195.0	3.93	248.1	49.6
	B3 (short)	1.5	195.0	2.34	416.7	83.3
C (~0.625 in diameter)	C1 (tall)	1.0	145.0	5.00	145.0	29.0
	C2 (medium)	1.0	195.0	4.66	209.2	41.8
	C3 (short)	1.0	195.0	3.16	308.5	61.7

Based on the disc stiffnesses in Table III and IV, the shear stiffness experienced in antero-posterior shear are 30 N/mm for no disc, 40-50 N/mm for moderately degenerated discs, and 60-90 N/mm for severely degenerated discs. The force-

displacement relationships for the polyurethane rod segments are not perfectly linear, but after about a ½ mm of displacement they start behaving linearly, as seen in Fig. 28.

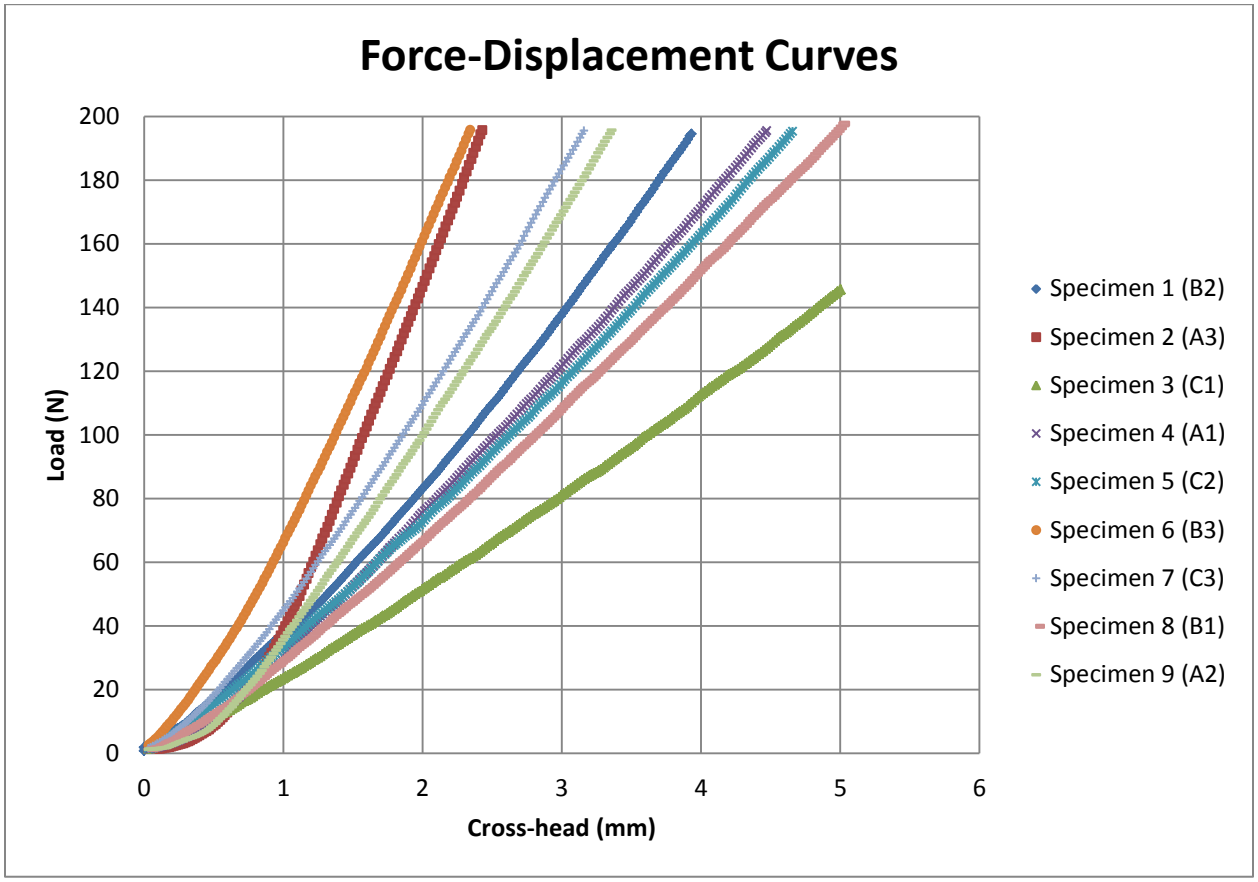

Fig. 28: Force-Displacement Curves – The relationship between the force appled and the resulted displacement for the polyurethane rod segment testing is displayed.

Fixture Testing:

General Assembly and Fixture Preparation:

1. Delrin Vertebrae Connection

Overall, the three fixtures are interchangeable, with the front plate in each assembly being the single part which changes. Based on the front plate used, one or two extension blocks will be used and must be secured using ¾" No. 8-32 machine screws and nuts (via the two through-holes on the ¼" thick portion of the block). If the extension

block is located in the middle of the front plate, a Delrin vertebra of thickness 14. 575 mm (0.574 in) with parallel holes must be used. Two 1.25” No. 8 wood screws were used to secure this Delrin vertebra to the front plate. If the extension block is located at either the superior or inferior end of the front plate, a Delrin vertebra of thickness 11.4 mm (0.450 in) must be used. Once again, two 1.25” No. 8 wood screws were used to secure this Delrin vertebra to the front plate. It is necessary to use two wood screws to guarantee that the Delrin vertebra is secured to the front plate, but it is difficult to maintain that the vertebra is level when screwing in both wood screws. Even if the vertebra is positioned level relative to the extension block, as the screws catch deeper into the Delrin, the vertebra will become fastened at a slight angle (as the screws catch slightly different in each of the pre-drilled holes). As a result, it is necessary to orient the Delrin vertebra so that it is at a slight angle opposite to the angle that it tends to orient itself towards; thus, the angle is offset and the Delrin will more easily orient itself levelly (see Fig. 29). It is necessary to twist a couple turns on each screw and then do the same to the other screw, and then continue to alternate until the Delrin vertebra is secured.

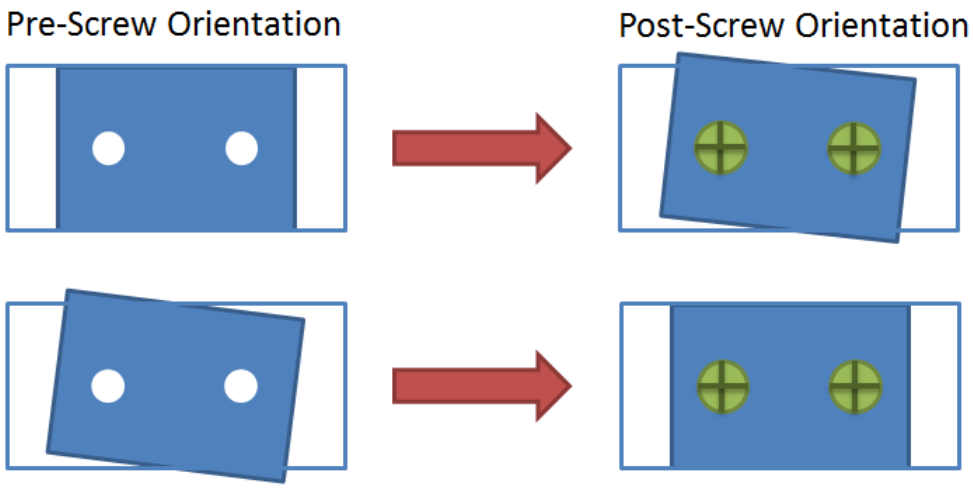

Fig. 29: Pre- and Post-Screw Orientation for Front Plate Delrin – Before tightening in screw into Delrin vertebra, the Delrin should be angled slightly to one side to maintain that the vertebra is tightened in levelly.

In the case of the front plate of the terminal three point bending case, after the first Delrin vertebra has been attached, it is easier to maintain that the adjacent Delrin vertebra will be secured in a proper orientation. The No. 8 wood screws can be turned in enough to just fix the Delrin vertebra in the correct position. Then the two vertebrae can be tightened in a table vice with slits of wood on the outer edges of the Delrin vertebrae not in contact with each other (as seen in Fig. 30) to protect those edges from the roughened surface of the vice grips. The No. 8 wood screws can then be screwed in until completely tightened, screwing in a couple turns per screw in alternation.

Fig. 30: Fastening of Delrin to Front Plate – For the anterior terminal three point bending fixture, after the first Delrin vertebra has been fastened to the front plate, the second one can more easily be secured. After positioning the left unfastened vertebra correctly, it is wedged between two slits of wood and tightened in a vice. The proper orientation will then be maintained during fastening.

The Delrin vertebra(e) which are connected to the back plate for a given fixture are done so via the connector plate. The connector plate is connected to the back plate via two No. 8-32 machine screws and nuts, where a range of lengths from 1” to 1 1/2” of the bolts can be used to accommodate for different length polyurethane rod segment pieces and the spondylolisthesis displacement for a given test. If the Delrin vertebra connected to the back plate is the middle vertebra in the fixture, it must be of thickness 14.575 mm

(0.574 in) with angled side holes, while if it is the superior or inferior Delrin vertebra of the fixture, it must be of thickness 11.4 mm (0.450 in) with angled side holes. Two ¾" No. 8 wood screws are used to connect the connector plate to the Delrin vertebra. As there is a space between the top and bottom of the connector plate and the top and bottom of a given Delrin vertebra, connection was easier than for the parallel hole Delrin vertebrae. The Delrin vertebra (of either thickness) was taken and the screws fed in far enough into the pre-drilled holes such that the Delrin vertebra was correctly positioned. Then, thin slits of wood cut to a thickness of the overlap of Delrin on each of the connector plate sides were wedged on each side of the connector plate and the whole combination was tightened in a table vice (see Fig. 31). The No. 8 wood screws were then screwed into the Delrin vertebra a couple turns each at a time in alternation until completely fastened. By wedging the Delrin vertebra and connector plate with the two slits of wood, it maintained that the Delrin vertebra would maintain a level orientation relative to the connector plate.

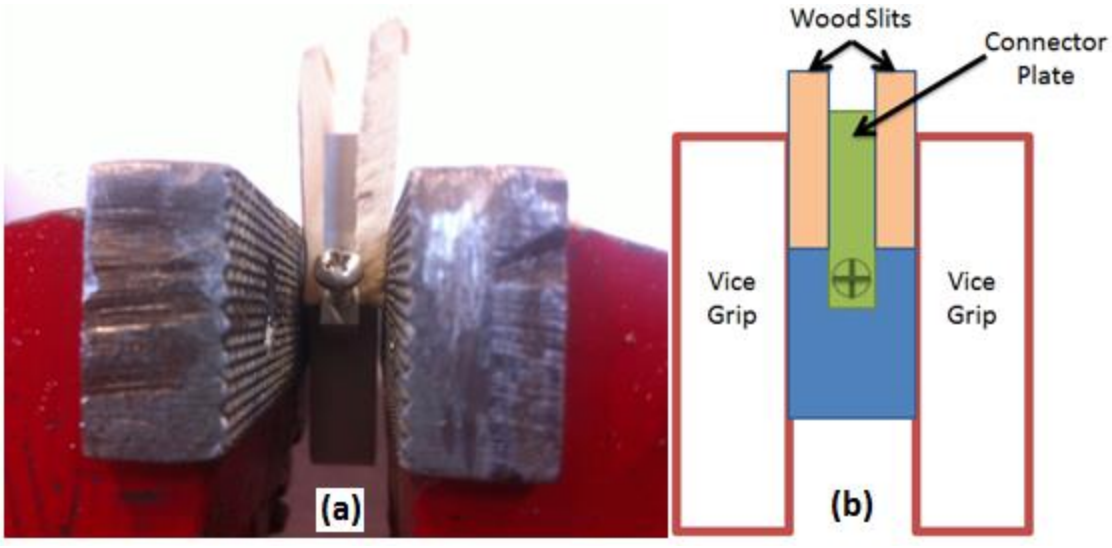

Fig. 31: Fastening of Delrin Vertebra to Connector Plate – Part (a) shows the connector plate/Delrin vertebra combination tightened in a vice, while part (b) shows a schematic of the set-up.

2. Connector Plate Attachment

After a Delrin vertebra has been secured to the connector plate, the connector plate must then be connected to the back plate. This is done by putting No. 8-32 machine screws varying in length from 1” to 1 ½” through the countersunk holes in the back plate with a washer and hex nut, and then threading the machine screws into the two threaded connector plate holes. It is important to note, however, that in the case of the anterior terminal three point bending and posterior fixtures because the superior and/or inferior Delrin vertebra(e) in these fixtures are too large to fit through the slits in their respective front plates. Thus, when screwing in the No. 8-32 machine screws to the connector plate, the connector plate must already be placed on the side of the front plate where the Delrin vertebrae connected to front plate are. In the case of the anterior three point bending fixture, the connector plate can be attached to the back plate without having trouble getting the Delrin vertebra connected to it through the front plate slit.

In addition, it is worth noting that it can be difficult to maintain that the No. 8-32 machine screws being screwed into the connector plate are screwed in an equal distance. As a result, the orientation of the connector plate must be observed to make certain that the connector plate/Delrin vertebra are level and will allow the fixture to function as it should. As the nuts threaded on the No. 8-32 machine screws are tightened down, and space between the flat head and the countersunk hole can be seen, that machine screw must be tightened down further to maintain that the connector plate is oriented/secured properly.

3. Securing of Polyurethane Rod Segments and Fixture Alignment

The polyurethane rubber rod segments can be secured to the front plate via the tightening plates. It is not recommended to tighten the segments down so that they will become deformed; thus, the tightening plates serve more as place holders, maintaining that the segments are centered relative to the front plate and have little wiggle room. Testing was only conducted on polyurethane rod segments of diameter 1 ½", which were easier to center as they have much larger surface area on each face in contact with a plate. There would be more wiggle room for smaller diameter segments, as the curve on the tightening plate contact surface is of radius ¾"; the fixtures were designed allowing for a maximum rod segment diameter of 1 ½". An adhesive may be necessary to secure rod segments of smaller diameters to maintain that they are centered.

Nonetheless, with the Delrin vertebrae in alignment use a fine-tipped marker/pen to trace around the perimeter of the polyurethane rod segment in contact with the back and front plates so that the correct/original location of the polyurethane rod segments is established and the position can be corrected if the rod segments accidentally move during mock surgery. Moreover, the initial positions of the polyurethane rod segments may not be perfectly centered on the back plate due to the connector plate or the Delrin vertebra connected to it being slightly off kilt. A slight off-centering of the rod segments on the back plate is permissible as long as the Delrin vertebrae are well-aligned to allow for implant application.

4. Delrin Vertebrae Preparation: Belt-Sanding and Pre-Drilling Implant Holes

Prior to testing, the curved face of the Delrin vertebrae in a given fixture were sanded down using the belt-sander, so as to match the contour of Delrin vertebrae to the implant being used (see Fig. 32). Delrin vertebrae connected to a given front plate should be sanded down equally so that they are as close to the same length as possible. This is most important in the case of the anterior standard three point bending fixture, as the spondylolisthesis displacement must be the same when measured relative to either the superior or inferior vertebra. In addition, since the fixture is assuming that the "correct curve" of the cervical spine is just maintaining that the Delrin vertebrae are in a straight line, sanding down the Delrin vertebrae connected to the front plate in the anterior terminal three point bending fixture could give it an unfair advantage or disadvantage; sanding down the middle vertebra more than the inferior one could make it more difficult for the implant to pull back the slipped vertebra, or in the opposite situation, it may be easier for the implant to pull back the slipped vertebra.

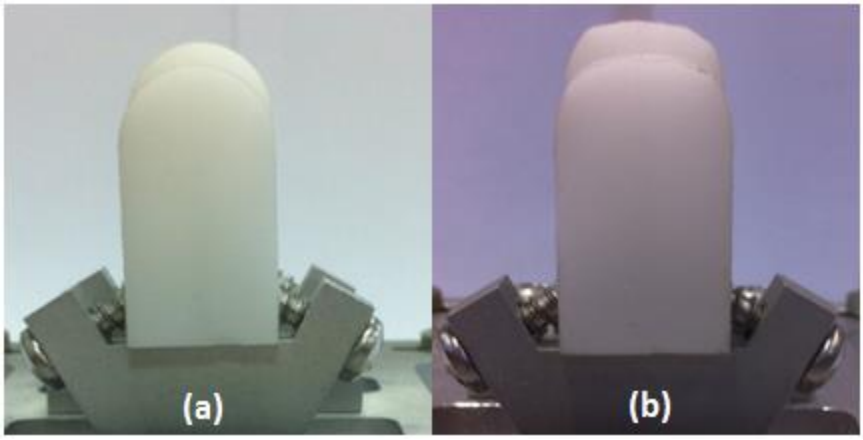

Fig. 32: Before and After Belt Sanding – Part (a) shows the Delrin vertebrae before belt sanding while part (b) shows the Delrin vertbrae after belt sanding.

After the belt-sanding of the vertebrae has been complete, holes must be pre-drilled where screws will be placed to secure the implant for a given fixture. To do this,

the fixture must be set-up as it would be during testing, with the polyurethane rod segments in place and the Delrin vertebrae lined up. The implant was then aligned longitudinally along the three vertebrae, with the center hole of the implant centered on the middle vertebra. A pencil was used to mark the locations of the holes on the Delrin vertebra. Using a portable vice, the back plate of the fixture being tested was fixed and 5/8" holes were pre-drilled at the pencil marks using a 0.095" diameter drill bit on the drill press (see Fig. 33). For the case of the anterior standard three point bending fixture, the connector plate attached to the back plate can be backed out of the slit it goes through in the front plate, and so the front and back plates can be fixed in the portable vice separately to more easily pre-drill the holes; the slight instability from the polyurethane rod segments can be avoided.

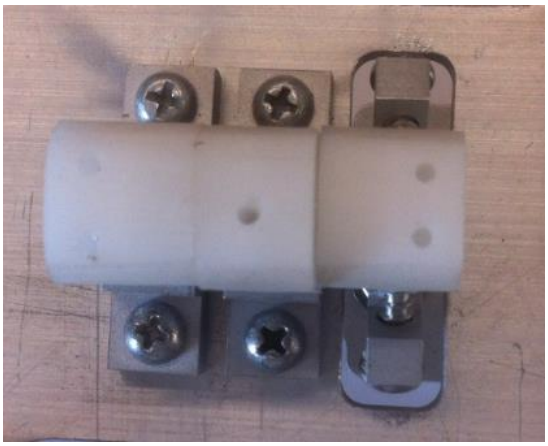

Fig. 33: Pre-Drilled Implant Holes – The alignment of the pre-drilled holes where the screws will be fastened to secure the implant are shown.

Preliminary Testing Methods:

Before testing, the diameter and length of each of the polyurethane rod segments need to be measured (take the average of three measurements for the length and diameter of each segment). Next, the back plate of the fixture being tested was fixed in a table vice, with the top face of the plate sitting flush with the top of the vice (see Fig. 34). After the

fixture is fixed in place in the table vice, the heights between the front and back plate near the polyurethane rod segments were measured (take the average of three height measurements for each side at each of the ends). Fig. 34 shows the orientation for recording and referencing the sides at each end of the fixture, whereby left and right are relative to a superior to inferior view.

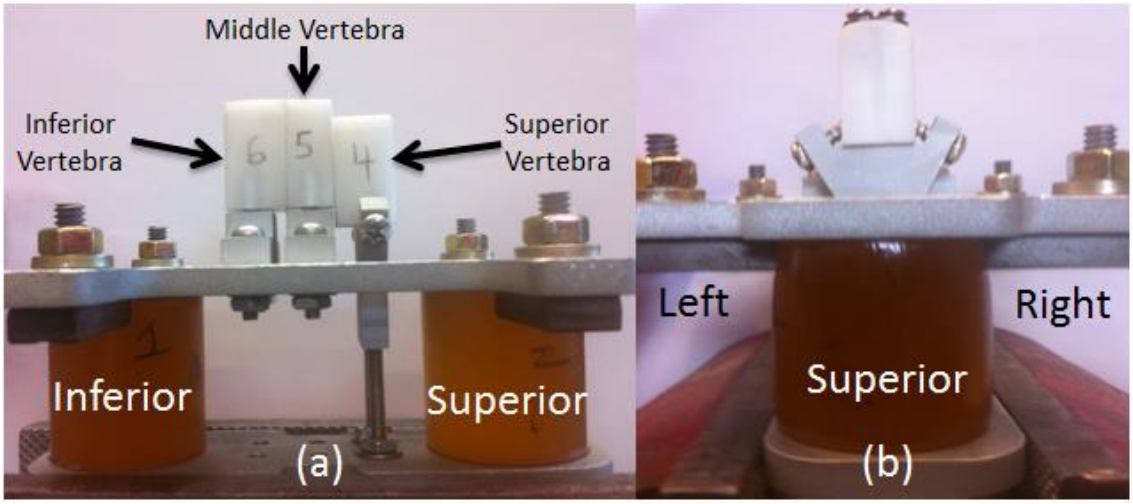

Fig. 34: Reference and Orientation of Fixtures– Part (a) labels the Delrin vertebrae relative to their location in the fixture while part (b) establishes the definition of left and right as looking from the superior end at the inferior end.

The spondylolisthesis displacement was then recorded taking the average of three measurements from various locations on the edge of un-slipped Delrin vertebra to the slipped vertebra (for the anterior standard three point bending fixture, the spondylolisthesis displacement must be measured relative to each of the un-slipped Delrin vertebrae on either side of the slipped Delrin vertebra).

After these pre-test measurements, the implant should be placed longitudinally along the Delrin vertebrae to make certain that the fixture is aligned correctly (the holes of the implant need to align with the pre-drilled holes in the Delrin vertebrae). No. 6 Phillips oval head sheet metal screws of length 5/8” were used during the mock surgery, as they were similar in diameter and length to actual anterior cervical surgical screws.

With the implant aligned, each of the screws was fastened just far enough so that they were holding their position, starting with the superior or inferior Delrin vertebra attached to front plate.

In the case of the standard three point bending fixture, the first screw was fastened to one of the non-slipped vertebra. Then, the screw at the opposite corner of the implant was fastened. The next two screws were inserted in the same manner. Lastly, the final screw was inserted into the middle implant slot. It was first fastened until the head of the screw had just come into contact with the implant, at which point the fixture was checked to make certain that all components were in proper positioning. The middle screw was then fully fastened in.

In the case of the terminal three point bending fixture, the first screw was fastened in the inferior vertebra. Next, the middle screw was fastened to the middle vertebra, and then the last inferior vertebra screw was fastened. Lastly, the final two screws were inserted into the slipped vertebra. Each were tightened down just until the head of the screws came in contact with the implant, at which time the fixture was checked to maintain that all components were in proper orientation. Then, each screw was fastened in the rest of the way, fastening one screw completely before moving onto the next one.

With the implant completely tightened down, the heights between the front and back plate near the polyurethane rod segments were measured again (take the average of three measurements at each end). In addition, the diameter of the polyurethane rod segments at the middle of the rod segments lengthwise was measured (take the average of three measurements for each rod segment).

Preliminary Testing Results/Discussion:

Testing was only performed on the two anterior fixtures, as more research may need to be conducted regarding the specifics of posterior cervical surgeries (since they are much less common). In both cases, the A1 polyurethane rod segments were used which have a stiffness of 43.5 N/mm, similar to the antero-posterior shear stiffness which would be encountered for a moderately degenerated disc.

1. Anterior Standard Three Point Bending:

The pre-test diameter and length measurements of the polyurethane rod segments used (same as rod segment "A1" in Table VI) were taken and are summarized in Table VII. Overall there is not much deviation among measurements for either; the polyurethane rod segments are uniform in their diameter throughout their lengths and the flat faces of the rod segments are fairly level.

Table VII: Polyurethane Rod Segment Pre-Test Diameters and Lengths

Measurement Number	Polyurethane Rod Segment 1 (Inferior Side)		Polyurethane Rod Segment 2 (Superior Side)	
	Diameter (mm)	Length (mm)	Diameter (mm)	Length (mm)
1	37.74	37.80	37.83	37.43
2	37.79	37.90	37.79	37.40
3	37.60	37.74	37.90	37.73
Average	37.71	37.81	37.84	37.52

No. 8-32 1 ½" long machine screws were used to attach the connector plate to the back plate. The No. 8-32 machine screws were threaded in far enough to allow for a spondylolisthesis displacement of 3.78 mm (see Table VIII).

Table VIII: Spondylolisthesis Displacement Measurements – Measurements are made relative to the superior and inferior sides for the standard three point bending fixture.

Measurement Number	Spondylolisthesis Displacement (mm)	
	Relative to Superior Delrin Vertebra	Relative to Inferior Delrin Vertebra
1	4.69	4.84
2	4.78	4.76
3	4.83	4.78
Average	4.77	4.79
Overall Average	4.78	

A side view of the three vertebrae in Fig. 35 shows the spondylolisthesis displacement before surgery.

Fig. 35: Pre-Test Side View of Anterior Standard Three Point Bending Fixture Vertebrae

The height between the front and back plates were recorded and listed in Table IX. The measurements taken reveal that the front plate was, more or less, parallel to the back plate, as there was not much variation in plate to plate distances; the plate to plate distance between on the inferior side was slightly less than that of the plate to plate distance on the superior side.

Table IX: Pre-Test Front to Back Plate Distance Measurements

Measurement Number	Front to Back Plate Distance (mm)			
	Inferior (Polyurethane Rod Segment 1) Side		Superior (Polyurethane Rod Segment 2) Side	
	Right	Left	Right	Left
1	38.95	38.87	39.06	39.08
2	38.78	38.78	39.13	39.01
3	39.06	38.97	38.96	39.16
Average	38.93	38.87	39.05	39.08

It was observed that the connector plate/machine screw connection was a little loose as the threads in the connector plate holes must have stretched during previous testing. Also, the polyurethane rod segments needed to be aligned slightly off-center to maintain that the Delrin vertebrae were well-aligned.

During the mock surgery, it was noticed that the slipped Delrin vertebra (the middle vertebra) was pinched in on by the superior and inferior vertebrae slightly. After all of the sheet metal screws were fully fastened, it was found that the slipped vertebra was pulled all the way back up into position (and slightly above the level of the superior and inferior vertebra). The post-surgery height between the front and back plates were recorded and listed in Table X. The measurements taken reveal that the plate to plate distance on the superior side was slightly lower than that of the plate to plate distance on the inferior side. This could be due to one of the superior or inferior Delrin vertebra being sanded down more or less than the other. As Fig. 35 depicts, the superior Delrin vertebra (labeled “3”) was sanded down a little more than the inferior Delrin vertebra (labeled “5”), while it was found that plate to plate distance on the side of the inferior vertebra

compressed less. Moreover, it could also be attributed to the positioning of the implant along the Delrin vertebra.

Table X: Post-Test Front to Back Plate Distance Measurements

Measurement Number	Front to Back Plate Distance (mm)			
	Inferior (Polyurethane Rod Segment 1) Side		Superior (Polyurethane Rod Segment 2) Side	
	Right	Left	Right	Left
1	35.53	34.71	34.18	34.14
2	35.38	34.43	34.17	34.09
3	35.33	34.75	34.10	34.40
Average	35.41	34.63	34.15	34.21

The diameter of the polyurethane rod segments at the middle of the rod segments lengthwise was also measured (see Table XI).

Table XI: Post-Test Mid-Length Polyurethane Rod Segment Diameters

Measurement Number	Mid-Length Diameter (mm)	
	Polyurethane Rod Segment 1 (Inferior Side)	Polyurethane Rod Segment 2 (Superior Side)
1	39.42	40.19
2	39.34	40.53
3	39.38	40.45
Average	39.38	40.39

The fixture after mock surgery is displayed in Fig. 36. As part (a) of Fig. 36 shows, the slipped vertebra was returned a little over its correct position. Also, in both parts (a) and (b) of Fig. 36, it can be observed that screws in the superior and inferior Delrin vertebra are not tightened down as much as the screws in the slipped vertebra.

This can be attributed to the flex in the plate which may occur while it is being screwed in. It is an interesting phenomenon which is difficult to explain as the screws in the superior and inferior vertebrae were completely tightened down previous to the slipped vertebra being screwed in. These screws could be pulling out slightly in response to the slipped Delrin vertebra being screwed in fully. Part (b) of Fig. 36 also reveals that the left side (viewing from inferior to superior axis) screw is higher than that of the right side, meaning that there may have been more loosening on one side than the other due to the location of the pre-drilled holes, orientation of implant, or a slightly uneven contour on the sanded down Delrin surface. Part (c) of Fig. 36 shows, however, that the implant is centered longitudinally along the three vertebrae, but that the screw in the slipped vertebra is not perfectly centered in the implant's center slot (it is closer to the inferior side of the fixture).

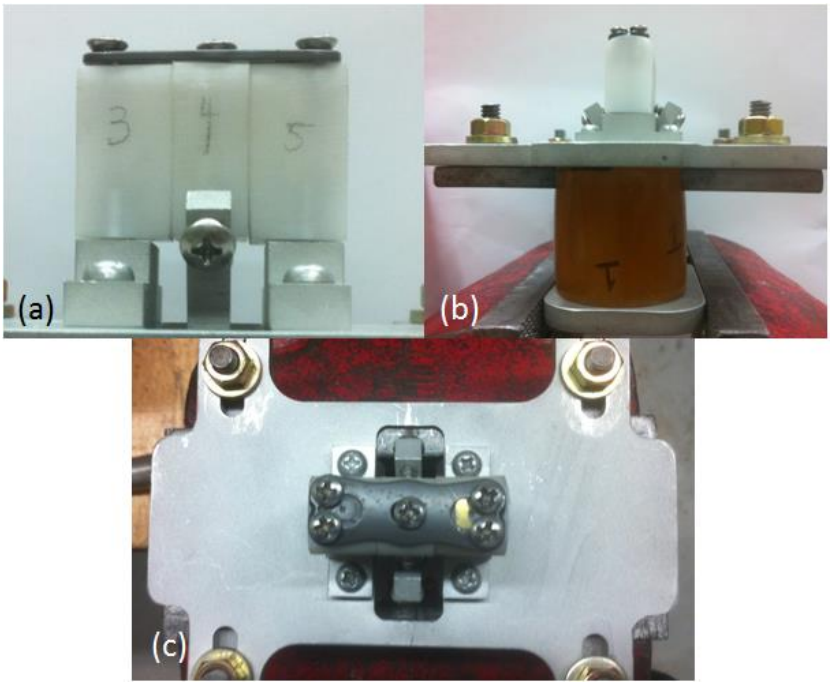

Fig. 36: Post-Test Pictures for Anterior Standard Three Point Bending Test – Part (a) shows a side view of the fixture with the numbers referring to the cervical vertebra they represent, part (b) shows a front view looking from superior to interior, while part (c) shows a top view of the fixture with implant in place.

2. Anterior Terminal Three Point Bending:

The pre-test diameter and length measurements of the polyurethane rod segments used (same as rod segment "A1" in Table VI) were taken and are summarized in Table XII. Overall there is not much deviation among measurements for either; the polyurethane rod segments are uniform in their diameter throughout their lengths and the flat faces of the rod segments are fairly level (they are the same rod segments used in the anterior standard three point bending test).

Table XII: Polyurethane Rod Segment Pre-Test Diameters and Lengths

Measurement Number	Polyurethane Rod Segment 1 (Inferior Side)		Polyurethane Rod Segment 2 (Superior Side)	
	Diameter (mm)	Length (mm)	Diameter (mm)	Length (mm)
1	37.74	38.84	37.83	38.87
2	37.79	38.86	37.79	39.02
3	37.60	39.04	37.90	38.92
Average	37.71	38.91	37.81	38.94

No. 8-32 1 ½" long machine screws were used to attach the connector plate to the back plate. The No. 8-32 machine screws were threaded in far enough to allow for a spondylolisthesis displacement of 3.01 mm (see Table XII).

Table XIII: Spondylolisthesis Displacement Measurements

Measurement Number	Spondylolisthesis Displacement (mm)
1	4.71
2	4.78
3	4.70
Average	4.73

A side view of the three vertebrae in Fig. 37 shows the spondylolisthesis displacement before surgery.

Fig. 37: Pre-Test Side View of Anterior Terminal Three Point Bending Fixture Vertebrae

The height between the front and back plates were recorded and listed in Table XIV. The measurements taken reveal that the front plate was, more or less, parallel to the back plate, as there was not much variation in plate to plate distances.

Table XIV: Pre-Test Front to Back Plate Distance Measurements

Measurement Number	Front to Back Plate Distance (mm)			
	Inferior (Polyurethane Rod Segment 1) Side		Superior (Polyurethane Rod Segment 2) Side	
	Right	Left	Right	Left
1	39.10	39.10	39.20	39.11
2	39.11	39.01	39.18	39.06
3	39.03	39.15	39.14	39.10
Average	39.08	39.09	39.17	39.09

It was observed that the connector plate/machine screw connection was a little loose as the threads in the connector plate holes must have stretched during previous

testing. Also, the polyurethane rod segments needed to be aligned slightly off-center to maintain that the Delrin vertebrae were well-aligned.

After all of the sheet metal screws were fully turned in, it was found that the slipped vertebra was pulled up to within 0.80 mm of the level of the middle and inferior vertebrae. The post-surgery height between the front and back plates were recorded and listed in Table XV. The measurements taken reveal that the plate to plate distance on the superior side (where the slipped vertebra was located) was approximately 3 mm lower than that of the inferior side. As the slipped Delrin vertebra is not connected to the center of the back plate, an uneven distribution of force is applied to the polyurethane rod segment on this side. This is a problem with the fixture design as both polyurethane rod segments are not being engaged evenly.

Table XV: Post-Test Front to Back Plate Distance Measurements

Measurement Number	Front to Back Plate Distance (mm)			
	Polyurethane Rod Segment 1Side		Polyurethane Rod Segment 2 Side	
	Right	Left	Right	Left
1	37.38	37.42	34.48	34.46
2	37.49	37.41	34.54	34.66
3	37.62	37.60	34.49	34.50
Average	37.50	37.48	34.50	34.54

The diameter of the polyurethane rod segments at the middle of the rod segments lengthwise was also measured (see Table XVI).

Table XVI: Post-Test Mid-Length Polyurethane Rod Segment Diameters

Measurement Number	Mid-Length Diameter (mm)	
	Polyurethane Rod Segment 1 (Inferior Side)	Polyurethane Rod Segment 2 (Superior Side)
1	38.78	40.59
2	38.91	40.57
3	38.82	40.60
Average	38.84	40.59

The fixture after mock surgery is displayed in Fig. 38. As part (a) of Fig. 38 shows, the slipped vertebra was not quite returned to its correct position. Also, in both parts (a) and (b) of Fig. 38, it can be observed that screws in the middle and inferior Delrin vertebra are not tightened down as much as the screws in the slipped vertebra. As was discussed in the other test, it is an interesting phenomenon which is difficult to explain as the screws in the superior and inferior vertebrae were completely tightened down previous to the slipped vertebra being screwed in. These screws could be pulling out slightly in response to the slipped Delrin vertebra being screwed in fully. Part (b) of Fig. 38 shows that the plate was tightened down levelly along its width. Part (c) of Fig. 38 shows, however, that the implant is centered longitudinally along the three vertebrae and that the screw in the slipped vertebra is centered in the implant's center slot.

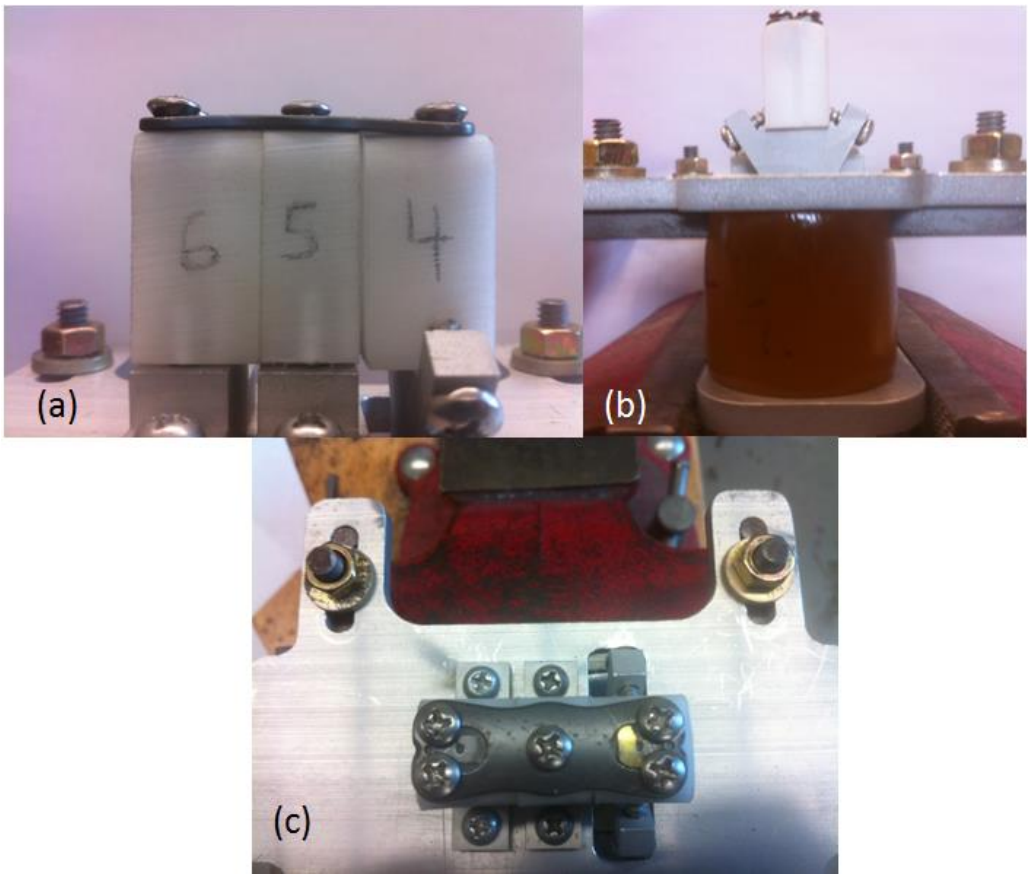

Fig. 38: Post-Test Pictures for Anterior Terminal Three Point Bending Test – Part (a) shows a side view of the fixture with the numbers referring to the cervical vertebra they represent, part (b) shows a front view looking from superior to interior, while part (c) shows a top view of the fixture with implant in place.

Comparative Discussion:

In comparing the results of the two anterior fixtures, both qualitatively from Figs. 36 and 38 above and quantitatively from the measurements taken, the standard three point bending surgical implantation method was more effective in returning the slipped Delrin vertebra back into position than the terminal three point bending orientation. Quantitatively speaking, the standard three point bending brought the slipped Delrin vertebra all the way back into position, while the terminal three point bending only brought the slipped vertebra to within 0.80 mm of its corrected position. As the same polyurethane rod segments were used in both tests, the comparison between the two

fixtures is accurate. Moreover, the standard three point bending test was performed before the terminal three point bending test, so if there was any permanent deformation or stiffness decrease in the polyurethane rod segments, it would have only helped—not hindered—the returning of the slipped Delrin vertebra back into position in the terminal test. As both of these surgical techniques are used, this is very useful information in recognizing that the standard three point bending method returns the slipped vertebra back into position more effectively in the case of using a rigid plate like the Zephyr plate used in testing.

However, assumptions were made which may limit the validity of the model used to test the implant. For example, it was assumed that the same resistance in the antero-posterior direction would be encountered for both surgical situations. For the case of the standard three point bending test, there would most certainly be two shear resistances to be accounted for in moving the slipped vertebra back into position, as there are two levels which must be accounted for. However, in the case of the terminal three point bending surgery, it is uncertain as to whether the same resistance in shear would be experienced or if it would be half as much—or some other ratio—as in the standard three point bending case; even though it is a two-level surgery, only one level's shear resistance would seemingly be encountered. Thus, comparing the two surgeries using polyurethane rod segments of the same stiffness may not be accurate.

In addition, the terminal three point bending fixture has one Delrin vertebra/connector plate attached to the back plate, but that attachment is not in the center of back plate, and is not matched with a symmetric back plate Delrin vertebra/connector plate attachment. As a result, when the implant was applied to the Delrin vertebra of the

fixture, the front plate was compressed more on the polyurethane rod segment on the (superior) side where the slipped Delrin vertebra was located. This makes sense, as the implant is pulling that slipped vertebra back into position, but the polyurethane rod segments are not being loaded equally which makes the validity of the fixture difficult to assess. After Dr. Darryl Dirisio, Ph.D. informed us of the common terminal three point bending surgical method, a front plate was designed and fabricated to fit with the fixture designs already created; thus, there may be some shortcomings in the terminal three point bending fixture, but it could be re-designed to better guarantee equal loading of the polyurethane rod segments.

Moreover, the stiffnesses of the polyurethane rod segments used in both of the tests were 43.5 N/mm, which are within the range of the antero-posterior stiffness for a moderately degenerated disc. As a result, the selection of stiffness was accurate when considering the healthiness of the intervertebral discs which are common in patients with these surgeries. However, surgeon's generally remove the discs and replace them with cage grafts to promote fusion between the vertebral bodies, which would deem that the only resistance would be from the remaining ligaments, the facet joints, etc. In this case, the antero-posterior shear stiffness is closer to 30 N/mm, which is not too much less than the stiffness of the polyurethane rod segments used in these tests.

Conclusion/Recommendations:

Degenerative cervical spondylolisthesis is a common cause of back pain, deeming it important to be able to characterize the efficacies of implant systems and surgical techniques used to correct this condition. The efficacy of a given implant system is

determined based on its ability to return the slipped vertebra back into its natural position to restore the cervical spine's natural lordosis (or in the test fixtures' case, to align the vertebrae linearly). The anterior standard and terminal three point bending methods were tested in this study using a Zephyr anterior cervical plate, and it was found that the standard three point bending method was the most effective in returning the slipped vertebra back into position; with two polyurethane rod segments of stiffness 43.5 N/mm, the standard three point bending returned the slipped vertebra completely, while the terminal three point bending returned the slipped vertebra to within 0.8 mm of the corrected position. The stiffnesses of the polyurethane rod segments used resemble that of moderately degenerated discs. The posterior fixture was not tested as there was a lack of understanding of the surgical methods associated with posterior implants, as well as a lack of a posterior implant to test.

For future work, it would be recommended to test other anterior cervical implants for the two surgical methods tested in this study. Moreover, testing with different polyurethane rod segments and spondylolisthesis displacements should be performed to see how results vary. Though the posterior fixture was not used, it could be as effective in testing the implants and surgical methods as the anterior fixtures given a little more knowledge of posterior cervical surgery (relating to rod and pedicle screw systems and how they are implemented) and the availability of a posterior implant system. The deflection of the implant systems tested could be analyzed using photogrammetry, which we were unfortunately unable to do before the conclusion of the term. The small thickness of the implant in combination with its contours provided calibration issues relating to the field and depth of view and prevented us from acquiring strain data using

the photogrammetry system in Professor Bucinell's lab. However, with more time, photogrammetry could be used to analyze an implant being tested on a given fixture and yield valuable results. Despite the problems with the photogrammetry system, useful qualitative and quantitative results were accrued and the fixtures designed helped to do some preliminary evaluation of the Zephyr anterior cervical implant and the standard and terminal three point bending surgical techniques.

Acknowledgements:

I would like to acknowledge Professor Sanders for all of his help over the course of this project. I would like to acknowledge Professor Bucinell for allowing us to use his lab and for helping us perform various mechanical and photogrammetry tests. Also, I would like to recognize Dr. Darryl DiRisio at Albany Medical Center allowed us to view a surgery and provided much information regarding surgical techniques. Lastly, I would like to acknowledge Paul Tompkins and the Machine Shop for their great help in fabricating the fixtures.

References:

[1] "Back Pain Facts and Statistics." *American Chiropractic Association*. N.p., 2012. Web. 10 Sept. 2012. <http://www.acatoday.org/level2_ css.cfm?T1ID=13&T2ID=68>.

[2] Sanders, Glenn P. "Independent Project Meeting: Week 1." NY, Schenectady. 10 Sept. 2012. Lecture.

[3] Brook, Martin I., Richard A. Deyo, Sohail K. Mirza, Judith A. Turner, Bryan A. Comstock, William Hollingworth, and Sean D. Sullivan. "Expenditures and Health Status among Adults with Back and Neck Problems." *Pubmed.gov*. National Center for Biotechnology Information, 11 June 2008. Web. 30 Oct. 2012. <http://www.ncbi.nlm.nih.gov/pubmed/18270354>.

[4] Harrison, Donald D., Deed E. Harrison, Tadeusz J. Janik, Rene Cailliet, Joseph R. Ferrantelli, Jason W. Haas, and Burt Holland. "Modeling of the Sagittal Cervical Spine as a Method to Discriminate Hypolordosis." *Spine* 29.22 (2004): 2485-492. Print.

[5] "Spinal Disorders." *MBJC: Muscle, Bone & Joint Center*. N.p., 2013. Web. 9 June 2013.

[6] Woiciechowsky, Christian, Ulrich-Wilhelm Thomale, and Stefan-Nikolaus Kroppenstedt. "Degenerative Spondylolisthesis of the Cervical Spine – Symptoms and Surgical Strategies Depending on Disease Progress." *European Spine Journal* 13 (2004): 680-84. Web. <http://www.kreuzschmerzen.org/fileadmin/redaktion/pdf/36-Degenerative_spondylolisthesis_of_ the_cervical_spine.pdf>.

[7] DiRisio, Dr. Darryl. "Anterior Cervical Discectomy and Fusion Surgery at Albany Medical Center" NY, Albany. 14 May 2013.

[8] Jiang, Sheng-Dan, Lei-Sheng Jiang, and Li-Yang Dai. "Degenerative Cervical Spondylolisthesis: A Systematic Review." *International Orthopaedics* 35 (2011): 869-75. Print.

[9] Lombardi, Joseph S., Leon L. Wiltse, James Reynolds, Eric H. Widell, and Curtis Spencer, III. "Treatment of Degenerative Spondylolisthesis." *Spine* 10.9 (1985): 821-27. Print.

[10] Zhou, Jian, Xilei Li, Jian Dong, Xiaogang Zhou, Taolin Fang, Hong Lin, and Yiqun Ma. "Three-level Anterior Cervical Discectomy and Fusion with Self-locking Stand-alone Polyetheretherketone Cages." *Journal of Clinical Neuroscience* 18.11 (2011): 1505-509. Print.

[11] "Spinal Disorders: Isthmic Spondylolisthesis." *University of Virginia Health System*. N.p., 2012. Web. Oct. 2012. <http://www.uvaspine.com/isthmic-spondylolisthesis.php>.

[12] White, Augustus A., Dr. Med. Sc., Rollin M. Johnson, Manohar M. Panjabi, Dr. Tech., and Wayne O. Southwick. "Biomechanical Analysis of Clinical Stability in the Cervical Spine." *Clinical Orthopaedics and Related Research* 109 (1975): 85-96. Print.

[13] Pooni, JS, DWL Hukins, PF Harris, RC Hilton, and KE Davies. "Comparison of the Structure of Human Intervertebral Discs in the Cervical, Thoracic and Lumbar Regions of the Spine." *Surgical and Radiologic Anatomy* 8.3 (1986): 175-82. Print.

[14] White, Augustus A., and Manohar M. Panjabi. *Clinical Biomechanics of the Spine*. Philadelphia: Lippincott, 1990. Print.

[15] Panjabi, Manohar M., Joanne Duranceau, Vijay Goel, Thomas Oxland, and Koichiro Takata. "Cervical Human Vertebrae Quantitative Three-Dimensional Anatomy of the Middle and Lower Regions." *Spine* 16.8 (1991): 861-69. Print.

[16] *Moroney, Sean P., Albert B. Schultz, James A.A. Miller, and Gunnar B.J. Andersson.* "Load-displacement Properties of Lower Cervical Spine Motion Segments." *Journal of Biomechanics* 21.9 (1988): 769-79. Print.

[17] Panjabi, Manohar M., Donald J. Summers, Richard R. Pelker, Tapio Videman, Gary E. Friedlaender, and Wayne O. Southwick. "Three-Dimensional Load-Displacement Curves Due to Forces on the Cervical Spine." *Journal of Orthopaedic Research* 4 (1986): 152-61. Print.

[18] Rapoff, Andrew. "MER/BIO Soft Tissue Mechanics: Spine Biomechanics." Reading. Union College, Schenectady. Sept. 2012. Web. <http://cnx.org/content/m27924/latest/36-Reading%20-%20Rapoff.pdf>.

[19] "Sciatica." *Riverside*. Mayo Clinic, 2013. Web. 10 June 2013.

[20] "Engineering in Rubber." *Harboro*. The Harboro Rubber Co Ltd., 2009. Web. 24 Jan. 2013.

Appendix A: Spring System Analysis

At first, a system where springs provided the shear resistive force for the two-level spinal unit. It was found that systems of two and four springs per level would yield the stiffnesses closest to the results from Moroney et. al. It is necessary to have two different designs to test both anterior and posterior implant systems. The posterior fixture design is shown in Fig. __ while the anterior fixture design is displayed in Fig. __. Note that the posterior fixture design was created first and then the anterior fixture, but the size of the four springs in parallel per level system was too large, so the design was abandoned (which explains the simple nature of the designs).

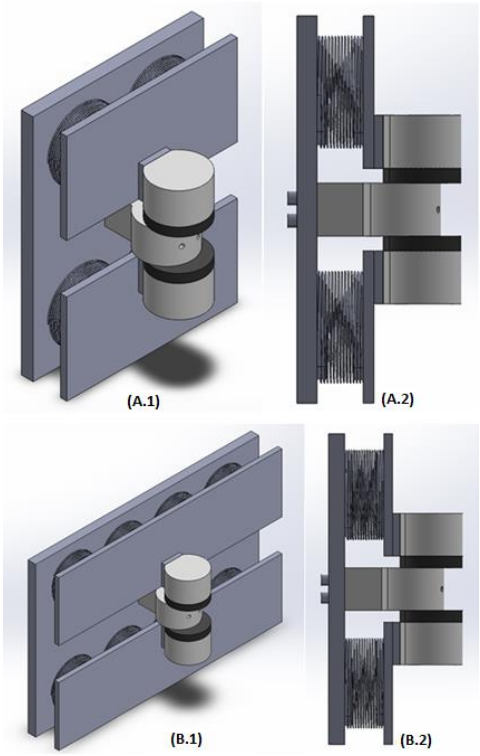

Fig. 39: Posterior Test Fixture Design (Parallel Spring Configuration) - The tan pieces represent the Delrin vertebrae, the large gray plates are steel plates, and the black pieces are the Teflon discs needed for the intervertebral disc space. The springs are in contact with the two front plates and back plate. The superior and inferior vertebrae will be fixed in position with upper and lower mounts. Parts (A.1) and (A.2) are the isometric and side views, respectively, of the 2-spring parallel system, while parts (B.1) and (B.2) are the isometric and side views, respectively, of the 4-spring parallel system. The number associated with the parallel spring system refers to the number of springs which are acting on either the superior or inferior vertebrae.

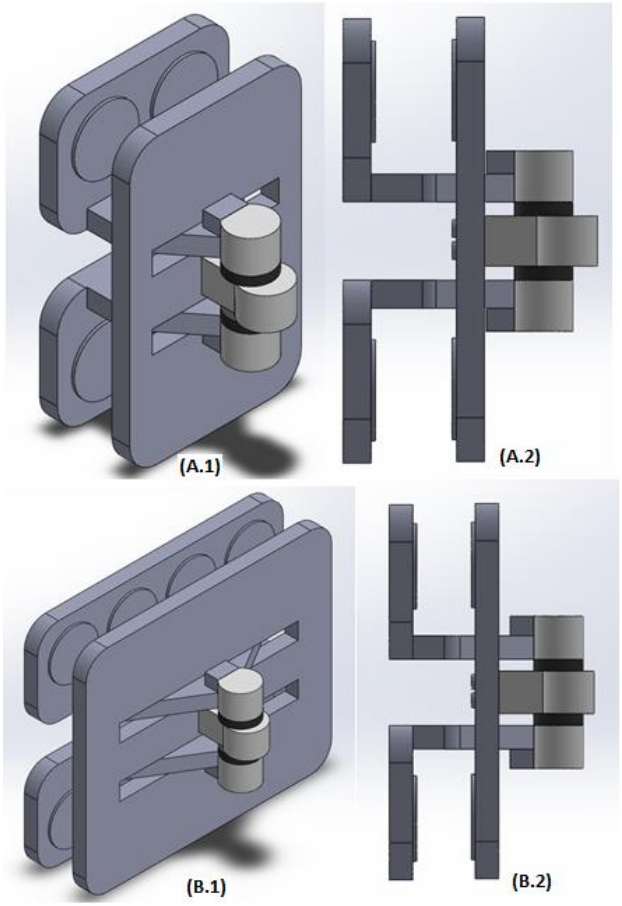

Fig. 40: Anterior Test Fixture Design (Parallel Spring Configurations) - The tan pieces represent the Delrin vertebrae, the large gray plates are steel plates, and the black pieces are the Teflon discs needed for the intervertebral disc space. The springs are in contact with the front plate and two back plates. The superior and inferior vertebrae will be fixed in position with upper and lower mounts. Parts (A.1) and (A.2) are the isometric and side views, respectively, of the 2-spring parallel system, while parts (B.1) and (B.2) are the isometric and side views, respectively, of the 4-spring parallel system. The number associated with the parallel spring system refers to the number of springs which are acting on either the superior or inferior vertebrae.

It is worth noting that the scale of this project is small and the overall height of the system should be no larger than 20-30 cm. As a result, normal springs cannot be used to provide the necessary stiffness in the small area which is being worked with; thus, high-load compression springs will be implemented into the design of the test fixture. These particular springs do not follow the traditional helical spring design, but rather use

a wave-like design, which allows them to handle larger loads in lesser space. The specifications for available high-load compression springs are shown in Table IV. For complete spring dimensions, see Appendix: High Load Compression Spring Specifications).

Table I: Potential High-Load Compression Springs for 2-Spring Parallel System – Included are the dimensions of the springs and their specifications.

Spring Number	Spring Length (mm)	Outer Diameter (mm)	Wire Thickness (mm)	Compressed Length (mm)	Change in Length (mm)	Max Load (N)	Max Mass (kg)	Stiffness (N/mm)
1a	4.572	15.240	0.305	2.591	1.981	88.964	9.069	44.832
2a	6.096	15.240	0.305	3.429	2.667	88.964	9.069	33.274
3a	6.350	24.384	0.381	3.327	3.023	111.205	11.336	36.777
4a	7.620	15.240	0.305	4.445	3.175	88.964	9.069	28.020
5a	8.458	24.384	0.381	4.420	4.039	111.205	11.336	27.495
6a	8.458	18.288	0.330	5.461	2.997	97.860	9.976	32.574
7a	10.592	18.288	0.330	7.391	3.200	97.860	9.976	30.647
8a	10.592	24.384	0.381	5.766	4.826	111.205	11.336	23.117

As is evident in Table IV, there are no high-load compression springs which fall within the desired stiffness range of 40-90N/mm; thus, the springs must be placed in parallel. In doing so, the stiffness and maximum load which can be withstood by the springs is multiplied by the number of springs which are positioned in parallel (assuming that they all have the same spring specifications). Due to the small scale which this experimental setup necessitates, it is not very practical to place a large number of springs in parallel. The springs require a large amount of space relative to the MSU—which is based off of the cervical vertebral dimensions in Table II—deeming larger scale test mechanisms difficult to work with. Table V depicts the theoretical results of placing the springs from Table IV in parallel; meaning that each spring is in parallel with another spring of the same specifications.

Table II: Theoretical Analysis of 2-Spring Parallel Systems – These are the maximum loads and effective stiffnesses when two springs from Table III of the same spring number are placed in parallel with each other.

Spring Number	Max Load (N)	Max Mass (kg)	Stiffness (N/mm)
1a	177.928	18.137	89.665
2a	177.928	18.137	66.548
3a	222.410	22.672	73.553
4a	177.928	18.137	56.041
5a	222.410	22.672	54.990
6a	195.721	19.951	65.147
7a	195.721	19.951	61.294
8a	222.410	22.672	46.233

With two springs placed in parallel on both the superior and inferior vertebrae, the overall four-spring system accurately models the presence of shear resistance from the intervertebral discs on the superior and inferior sides of the middle vertebrae. Though this system would result in the desired stiffness, only springs 5 and 8 would have displacements that would model spondylolisthesis accurately, as their max displacements are greater than 4 mm. Even so, these are the maximum displacements of the springs and in order to achieve them, there may not be linear displacement relationships as the spring approaches maximum compression. Therefore, it is necessary to consider alternate spring systems, whereby more than two springs are resisting the motion of both the superior and inferior vertebrae. It is necessary to use high-load compression springs that can undergo greater compression and have lesser stiffnesses in order to achieve this. More springs were analyzed based on theoretical dimensions given and the results are summarized in Table VI.

Table III: Potential High-Load Compression Springs for 4-Spring Parallel System – Included are the dimensions of the springs and their specifications.

Spring Number	Spring Length (mm)	Outer Diameter (mm)	Wire Thickness (mm)	Compressed Length (mm)	Change in Length (mm)	Max Load (N)	Max Mass (kg)	Stiffness (N/mm)
1b	6.350	24.384	0.305	2.210	4.140	80.068	8.162	19.264
2b	7.620	12.192	0.203	2.718	4.902	44.482	4.534	9.457
3b	7.620	15.240	0.229	2.159	5.461	26.689	2.721	4.904
4b	7.620	12.192	0.305	3.454	4.166	66.723	6.802	15.937
5b	8.458	24.384	0.305	2.870	5.588	80.068	8.162	14.360
6b	8.458	24.384	0.254	2.743	5.715	53.378	5.441	9.282
7b	10.592	24.384	0.305	3.759	6.833	80.068	8.162	11.733
8b	10.592	24.384	0.254	3.683	6.909	53.378	5.441	7.706

The high-load compression springs analyzed in Table VI have significantly lesser stiffnesses than those analyzed in Table IV, but are able to undergo more compressive displacement. With this larger room for displacement, the lower individual spring stiffness can be increased by placing more than two springs in parallel with each other. Table VII consists of the max load and stiffness data if four of the springs were placed in parallel. However, as seen in part (B) of Fig. 3, the test mechanism starts to become quite bulky. The springs in parallel achieve stiffnesses which are within the range of 40-90 N/mm or are very close; the stiffnesses which are below 40 N/mm are kept because those parallel spring systems achieve the greatest compressive displacement.

Table IV: Theoretical Analysis of 4-Spring Parallel Systems – These are the maximum loads and effective stiffnesses when four springs from Table V of the same spring number are placed in parallel with each other.

Spring Number	Max Load (N)	Max Mass (kg)	Stiffness (N/mm)
1b	320.270	32.647	77.056
2b	177.928	18.137	37.827
3b	106.757	10.882	19.614
4b	266.892	27.206	63.746
5b	320.270	32.647	57.442
6b	213.514	21.765	37.127
7b	320.270	32.647	46.934
8b	213.514	21.765	30.822

As these calculations show, the stiffnesses for the two and four spring per level systems are within the range desired; however, the stiffnesses are better for the four spring per level system, which is ultimately much too bulky compared to the size of the Delrin vertebrae.

Appendix B: Technical Drawings

Overall Bill of Materials		
Item No.	**Part Name**	**Quantity**
1	Back Plate	2
2	Flat Head No. 8-32 1.5" Machine Screw	6
3	Flat Head No. 8-32 1.25" Machine Screw	6
4	Flat Head No. 8-32 1" Machine Screw	6
5	No. 8-32 Machine Screw Nut	12
6	Connector Plate	3
7	Polyurethane Rod Segment	N/A
8	Anterior Standard Three Point Bending Front Plate	1
9	Posterior Standard Three Point Bending Front Plate	1
10	Anterior Terminal Three Point Bending Front Plate	1
11	Extension Block	3
12	¼-20 Machine Screw Nut	8
13	No. 8-32 0.75" Machine Screw	6
14	Tightening Plate Base	8
15	Tightening Plate Stabilizing Rod	8
16	Tightening Plate ¼-20 1" Rod	8
17	Delrin Vertebra (Parallel Holes)	6
18	Delrin Vertebra (Angled Side Holes)	6
19	Teflon Disc	8
20	No. 8 0.75" Wood Screw	6
21	No. 8 1.25" Wood Screw	6

Note:

- Use this Bill of Materials for total quantities of parts needed
- All Machine and Wood Screws are Phillips Head
- Item Numbers do not coincide with those from the Solidworks Assembly Bill of Materials because there were two separate fixture assemblies which resulted in different item numbers. However, the Part Names do match with the Solidworks Assembly Bill of Materials

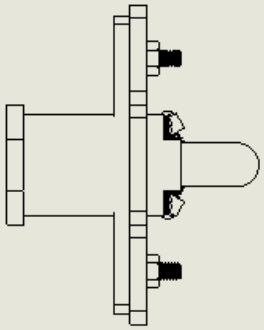

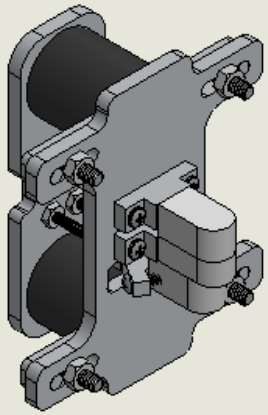

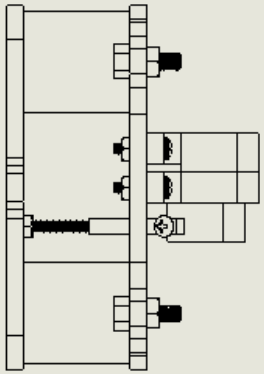

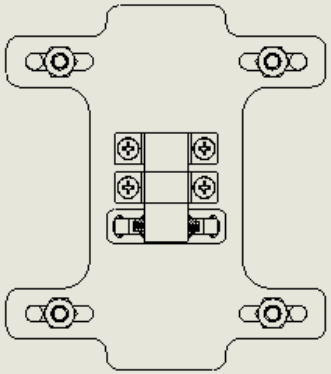

Senior Project: Tyler Heck Project Advisor: Prof. Glenn Sanders	Part Name: Anterior Terminal Three Point Bending Fixture	Material: Scale:

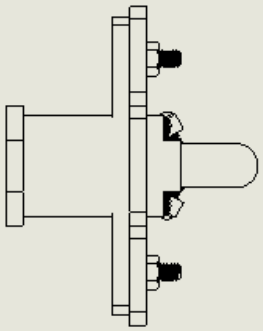

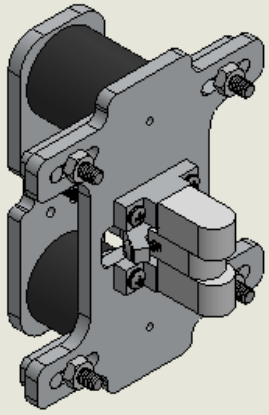

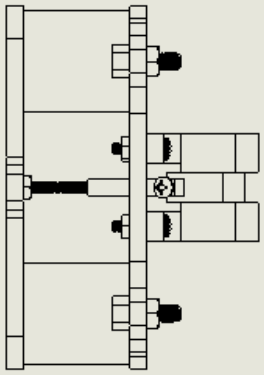

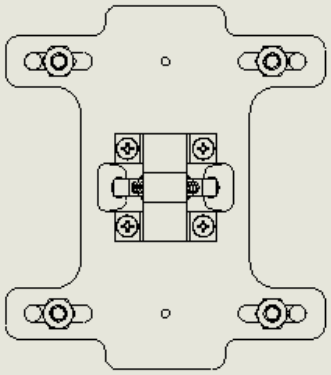

Senior Project: Tyler Heck Project Advisor: Prof. Glenn Sanders	Part Name: Anterior Standard Three Point Bending Fixture	Material: Scale:

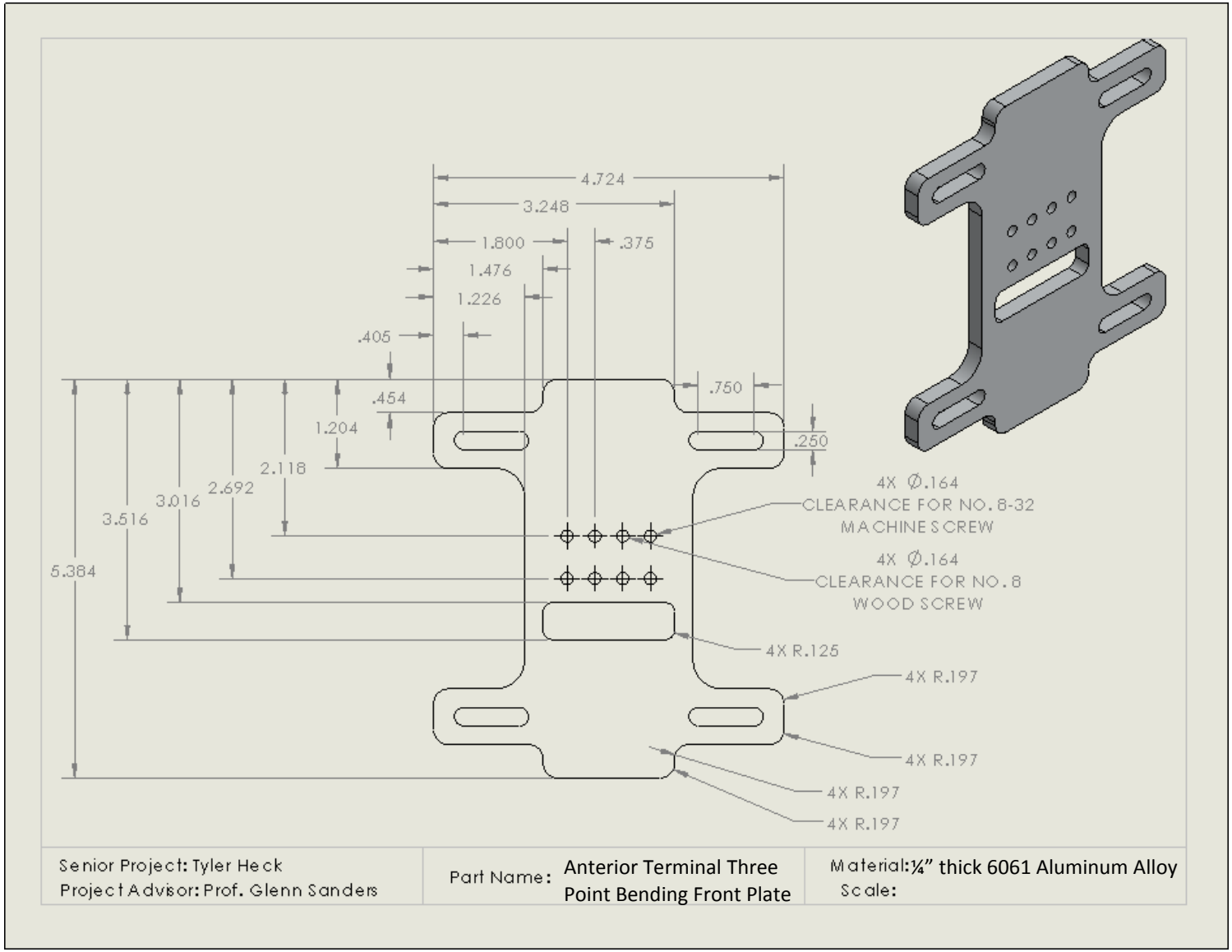
4.724
3.248
1.800
.375
1.476
1.226
.405
.454
1.204
2.118
2.692
3.016
3.516
5.384
.750
.250
4X Ø.164
CLEARANCE FOR NO. 8-32
MACHINE SCREW
4X Ø.164
CLEARANCE FOR NO. 8
WOOD SCREW
4X R.125
4X R.197
4X R.197
4X R.197
4X R.197
Senior Project: Tyler Heck
Project Advisor: Prof. Glenn Sanders
Part Name: Anterior Terminal Three Point Bending Front Plate
Material: ¼" thick 6061 Aluminum Alloy
Scale:

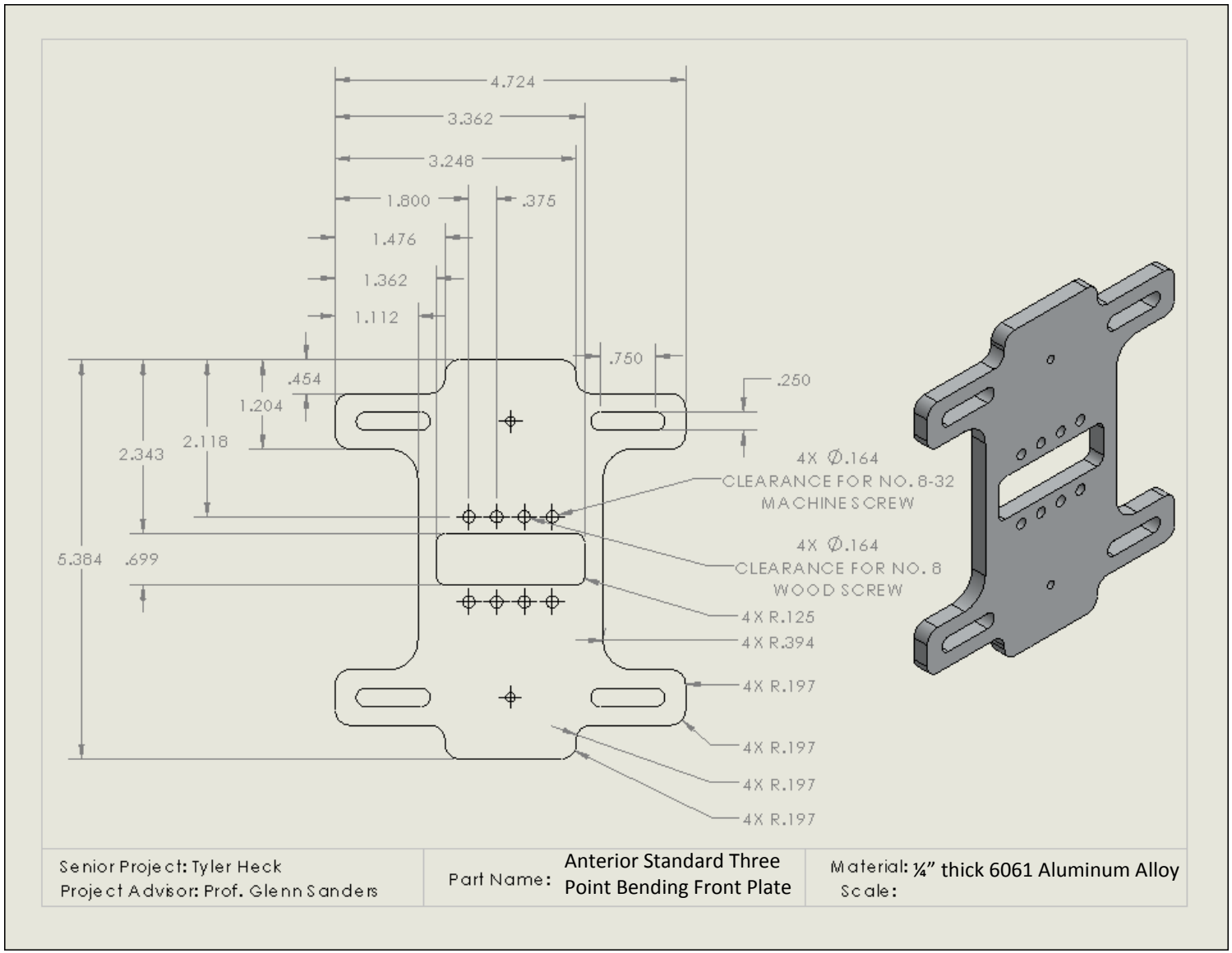
4.724
3.362
3.248
1.800
.375
1.476
1.362
1.112
.750
.250
.454
1.204
2.343
2.118
5.384
.699
4X Ø.164
CLEARANCE FOR NO. 8-32
MACHINE SCREW
4X Ø.164
CLEARANCE FOR NO. 8
WOOD SCREW
4X R.125
4X R.394
4X R.197
4X R.197
4X R.197
4X R.197
Senior Project: Tyler Heck
Project Advisor: Prof. Glenn Sanders
Part Name:
Anterior Standard Three Point Bending Front Plate
Material: ¼" thick 6061 Aluminum Alloy
Scale:

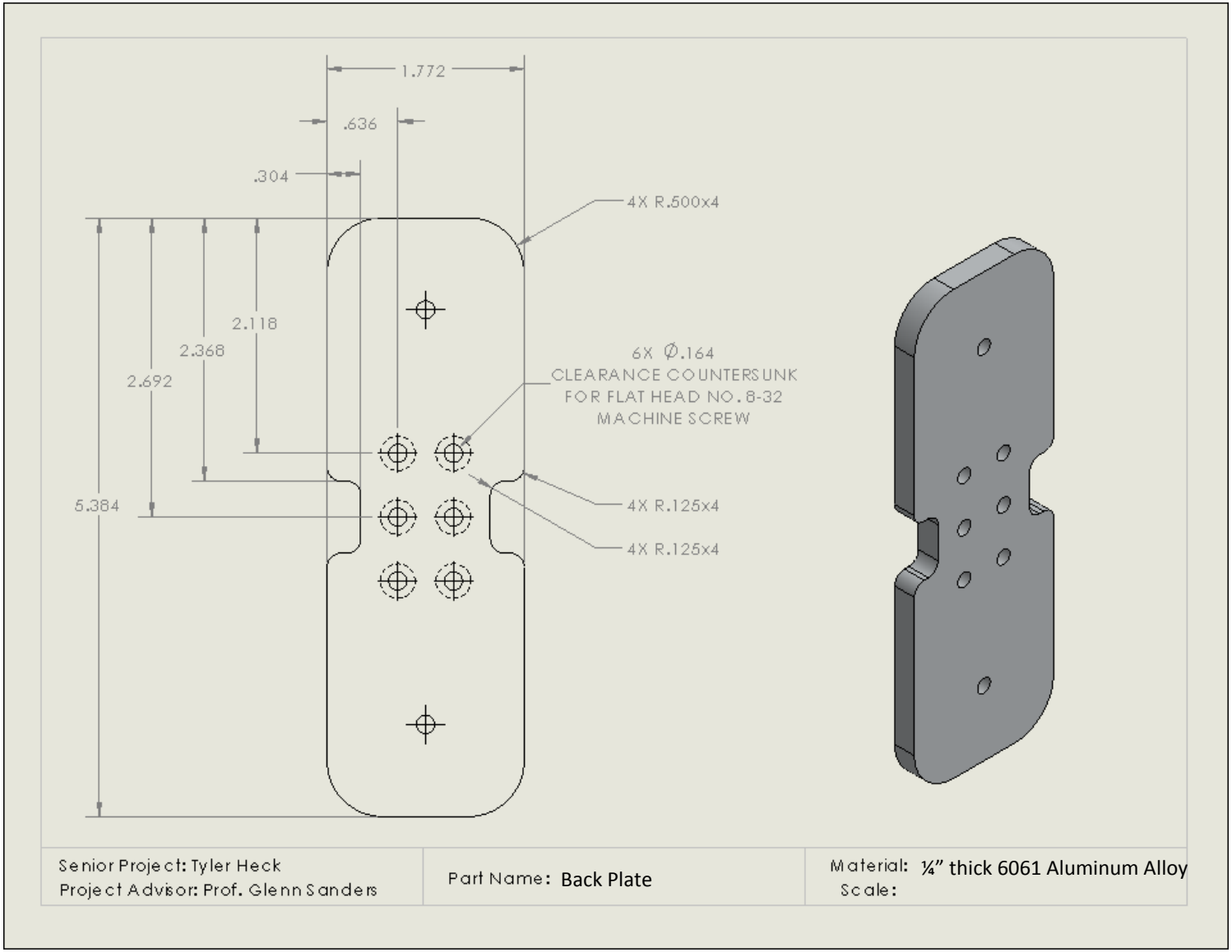
1.772
.636
.304
4X R.500x4
2.118
2.368
2.692
6X Ø.164
CLEARANCE COUNTERSUNK
FOR FLAT HEAD NO. 8-32
MACHINE SCREW
5.384
4X R.125x4
4X R.125x4
Senior Project: Tyler Heck
Project Advisor: Prof. Glenn Sanders
Part Name: Back Plate
Material: ¼" thick 6061 Aluminum Alloy
Scale:

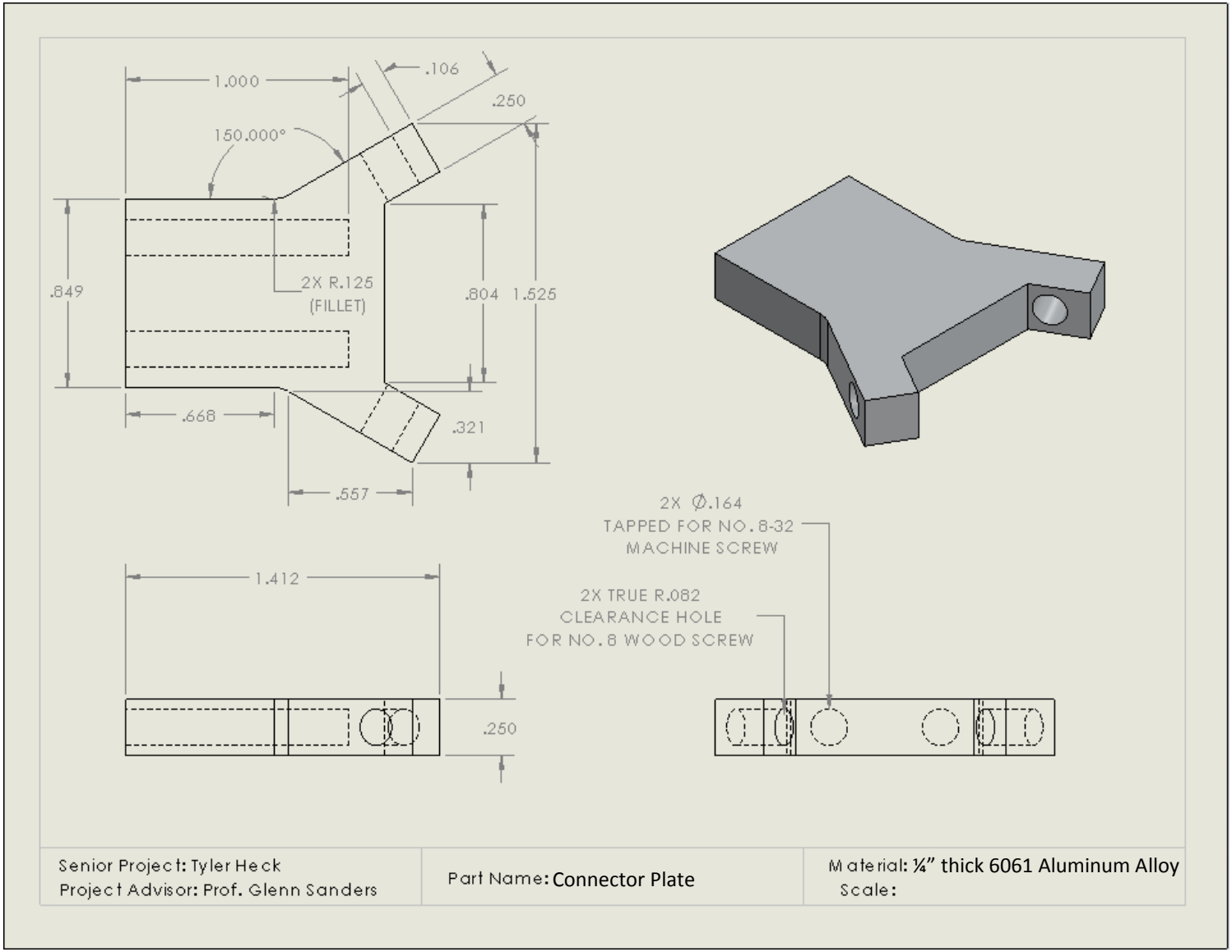
1.000
.106
.250
150.000°
.849
2X R.125
(FILLET)
.804
1.525
.668
.321
.557
2X Ø.164
TAPPED FOR NO. 8-32
MACHINE SCREW
2X TRUE R.082
CLEARANCE HOLE
FOR NO. 8 WOOD SCREW
1.412
.250
Senior Project: Tyler Heck
Project Advisor: Prof. Glenn Sanders
Part Name: Connector Plate
Material: ¼" thick 6061 Aluminum Alloy
Scale:

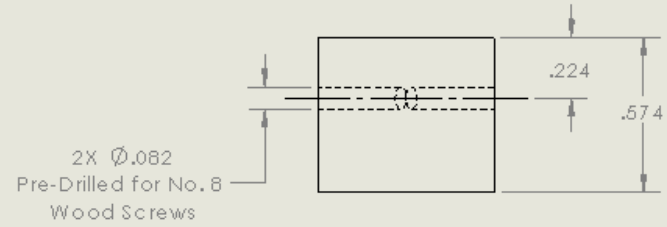

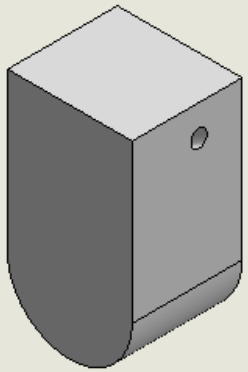

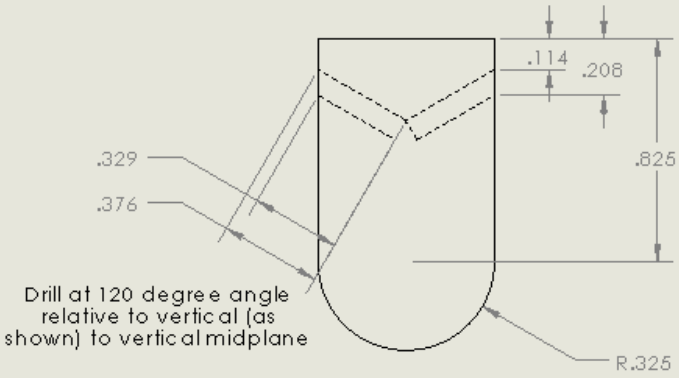

Senior Project: Tyler Heck Project Advisor: Prof. Glenn Sanders	Part Name: Delrin Vertebra Angled Side Holes (Extension)	Material: Delrin Plastic Scale:

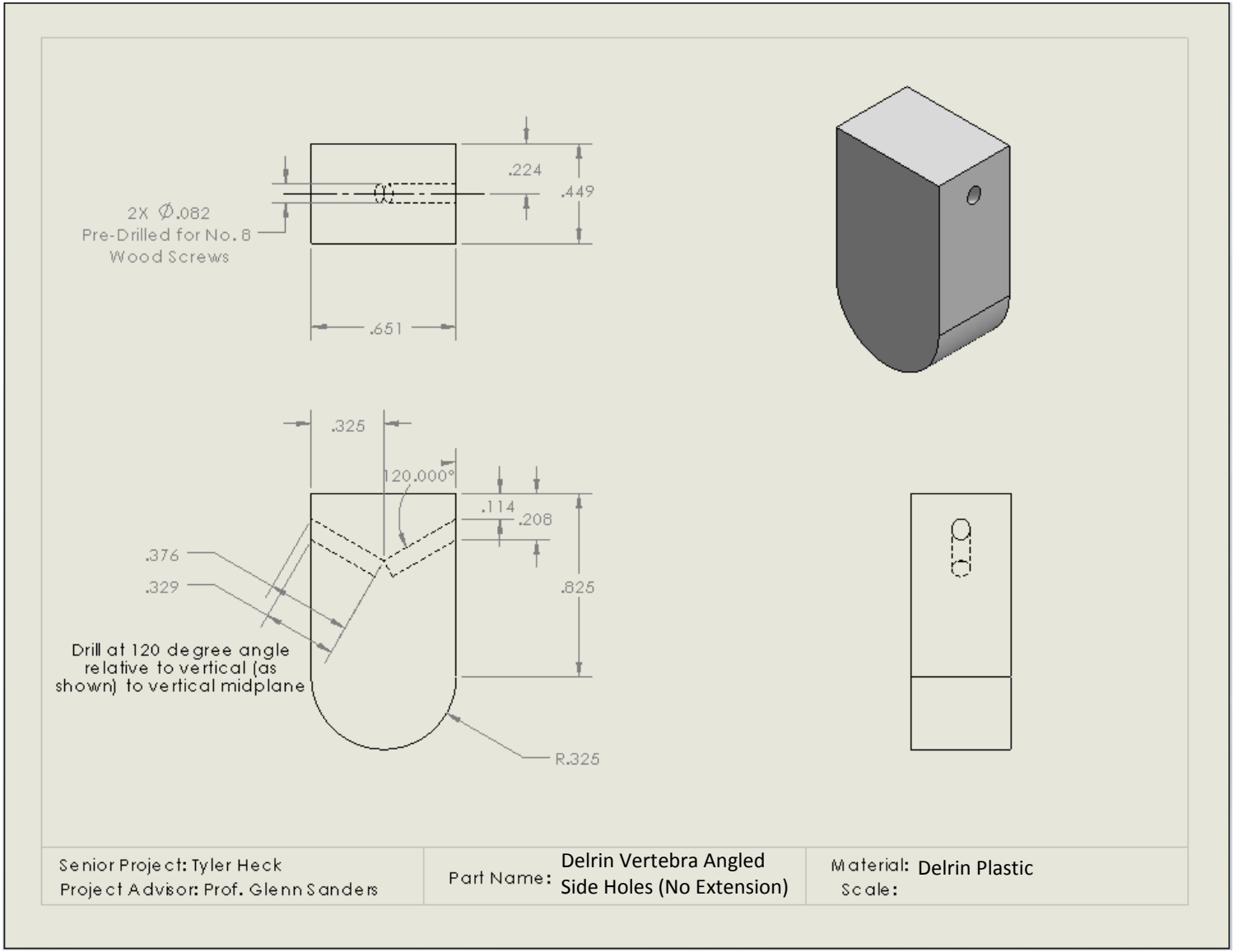
2X Ø.082
Pre-Drilled for No. 8
Wood Screws
.224
.449
.651
.325
120.000°
.114
.208
.376
.329
.825
Drill at 120 degree angle
relative to vertical (as
shown) to vertical midplane
R.325
Senior Project: Tyler Heck
Project Advisor: Prof. Glenn Sanders
Part Name: Delrin Vertebra Angled
Side Holes (No Extension)
Material: Delrin Plastic
Scale:

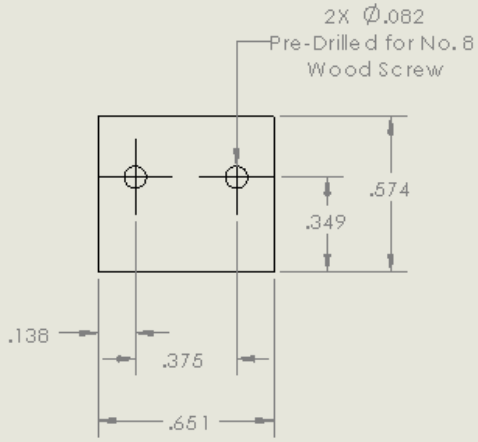

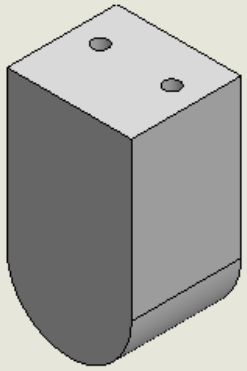

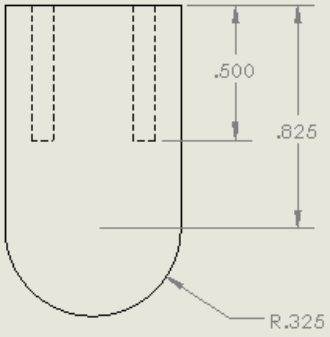

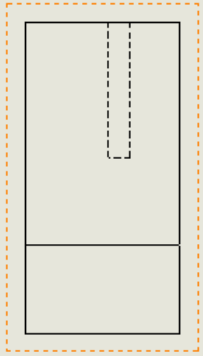

Senior Project: Tyler Heck Project Advisor: Prof. Glenn Sanders	Part Name: Delrin Vertebra Parallel Holes (Extension)	Material: Delrin Plastic Scale:

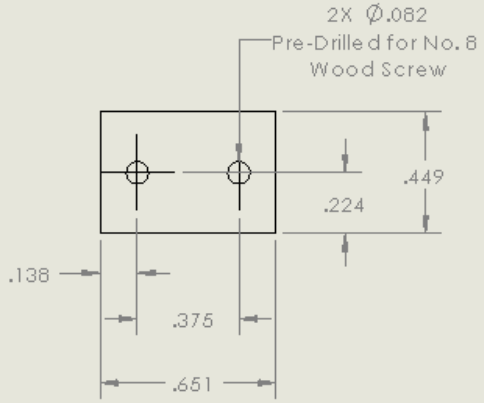

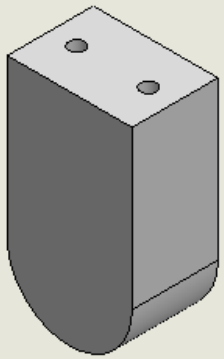

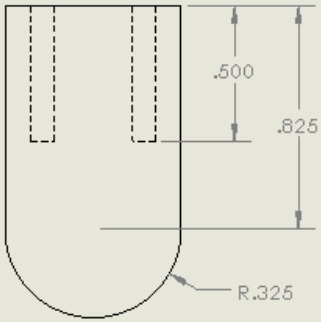

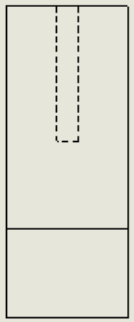

Senior Project: Tyler Heck Project Advisor: Prof. Glenn Sanders	Part Name: Delrin Vertebra Parallel Holes (No Extension)	Material: Delrin Plastic Scale:

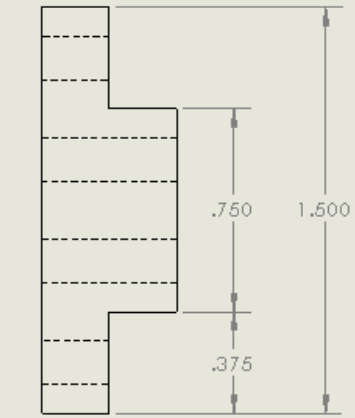

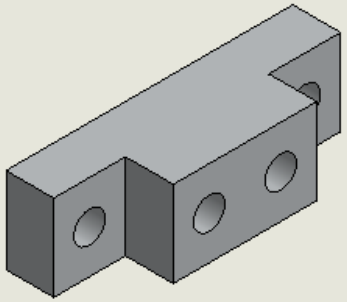

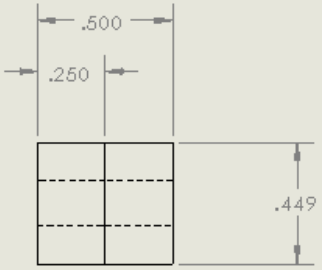

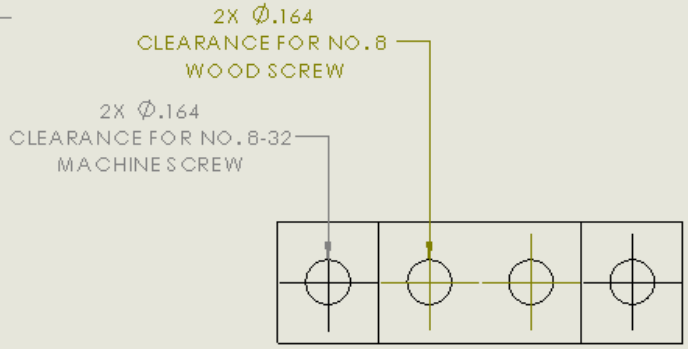

Senior Project: Tyler Heck Project Advisor: Prof. Glenn Sanders	Part Name: Extension Block	Material: Made from ½" thick 6061 Aluminum Alloy Scale:

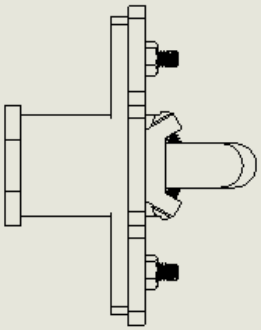

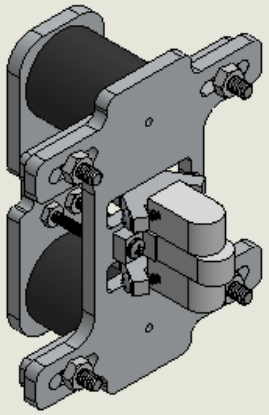

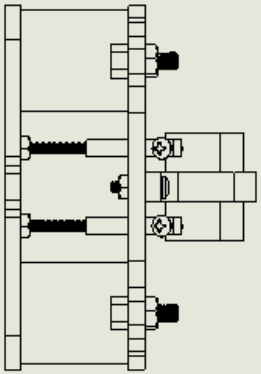

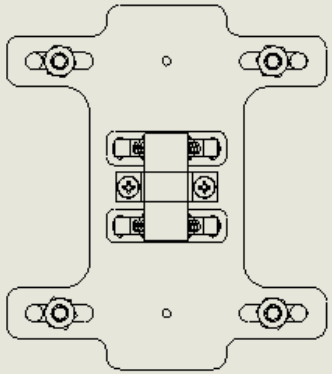

Senior Project: Tyler Heck Project Advisor: Prof. Glenn Sanders	Part Name: Posterior Standard Three Point Bending Fixture	Material: Scale:

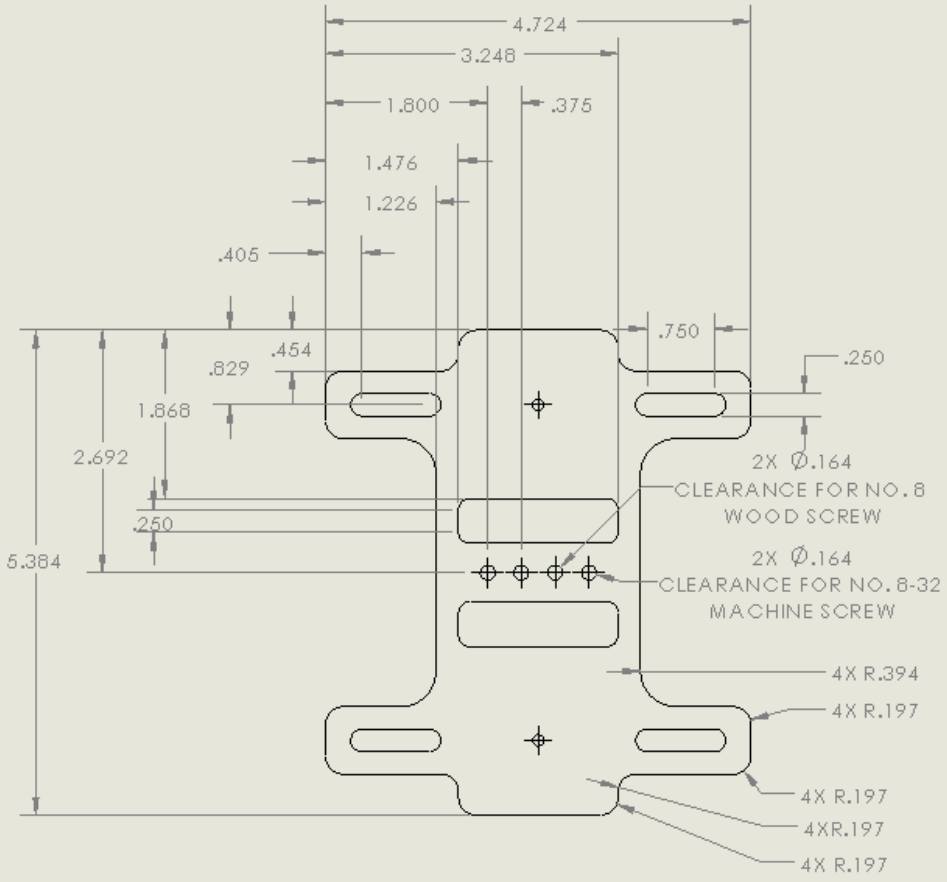

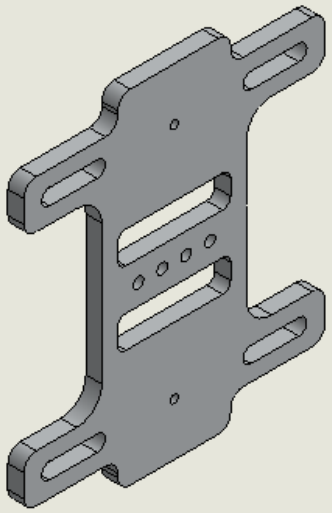

Senior Project: Tyler Heck Project Advisor: Prof. Glenn Sanders	Part Name: Posterior Standard Three Point Bending Front Plate	Material: ¼" thick 6061 Aluminum Alloy Scale:

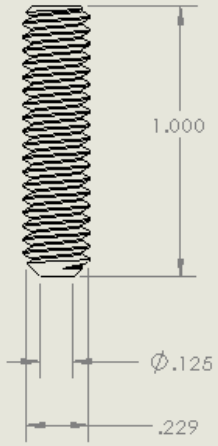

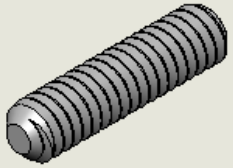

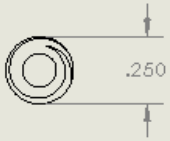

Senior Project: Tyler Heck Project Advisor: Prof. Glenn Sanders	Part Name: Altered Bolt	Material: Made from ¼”-20 1 in long machine screw

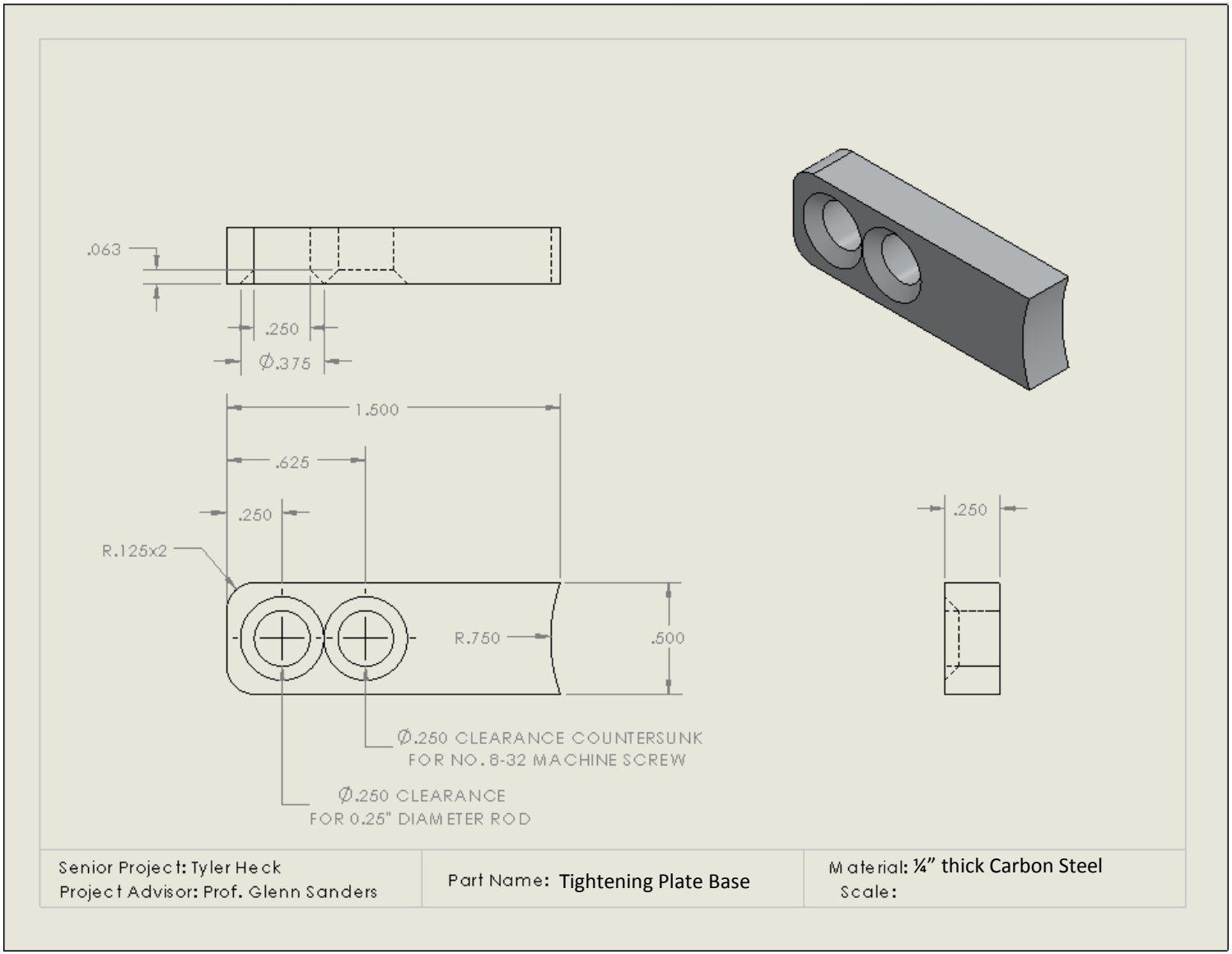
.063
.250
Ø.375
1.500
.625
.250
R.125x2
R.750
.500
.250
Ø.250 CLEARANCE COUNTERSUNK
FOR NO. 8-32 MACHINE SCREW
Ø.250 CLEARANCE
FOR 0.25" DIAMETER ROD
Senior Project: Tyler Heck
Project Advisor: Prof. Glenn Sanders
Part Name: Tightening Plate Base
Material: ¼" thick Carbon Steel
Scale:

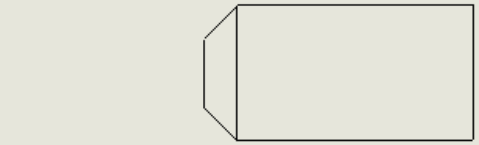

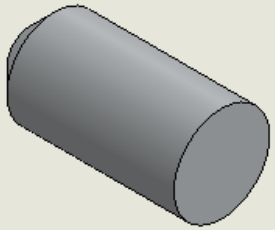

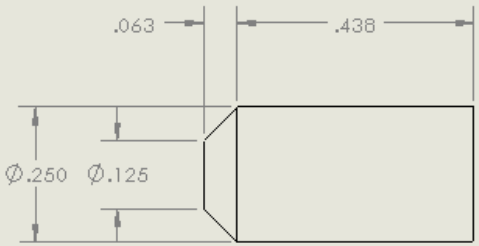

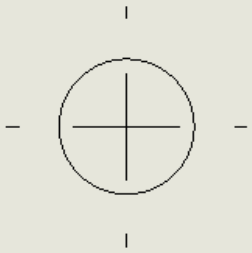

Senior Project: Tyler Heck Project Advisor: Prof. Glenn Sanders	Part Name: Stabilizing Rod	Material: Made from Carbon Steel Rod

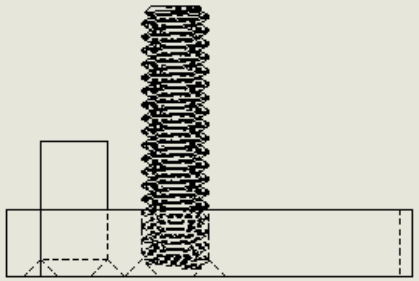

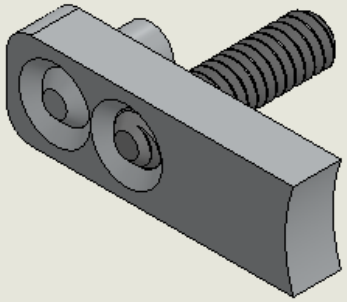

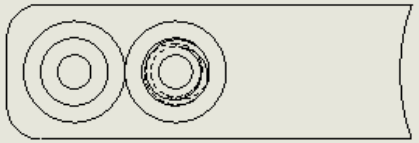

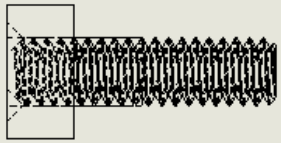

Senior Project: Tyler Heck Project Advisor: Prof. Glenn Sanders	Part Name: Tightening Plate Assembly	Material: All Carbon Steel, welding required

Appendix C: Delrin Vertebrae Size Calculations

Vertebral Body - Delrin Model Calculations for Closest Approximation									
Cervical Vertebra	**EPDu**	**EPWu**	**EPDl**	**EPWl**	**VBHp**	**EPAu**	**EPAl**	**Average End Plate Area (mm^2)**	**Radius from Average End Plate Area (mm)**
C2	-	-	15.6	17.5	-	-	194.4	194.4	7.866
C3	15	15.8	15.6	17.2	11.6	169.4	190.7	180.05	7.570
C4	15.3	17.2	15.9	17	11.4	183	199.2	191.1	7.799
C5	15.2	17.5	17.9	19.4	11.4	182.9	246.2	214.55	8.264
C6	16.4	18.5	18.5	22	10.9	221.2	289.9	255.55	9.019
C7	18.1	21.8	16.8	23.4	12.8	278.3	280.3	279.3	9.429

The upper and lower end plate areas were averaged together to get an average end plate area. Then, that was used to find a radius for the cylindrical vertebral bodies used in the test fixture to approximate the actual vertebral body.

Appendix D: Additional Finite Element Analysis

Back Plate:

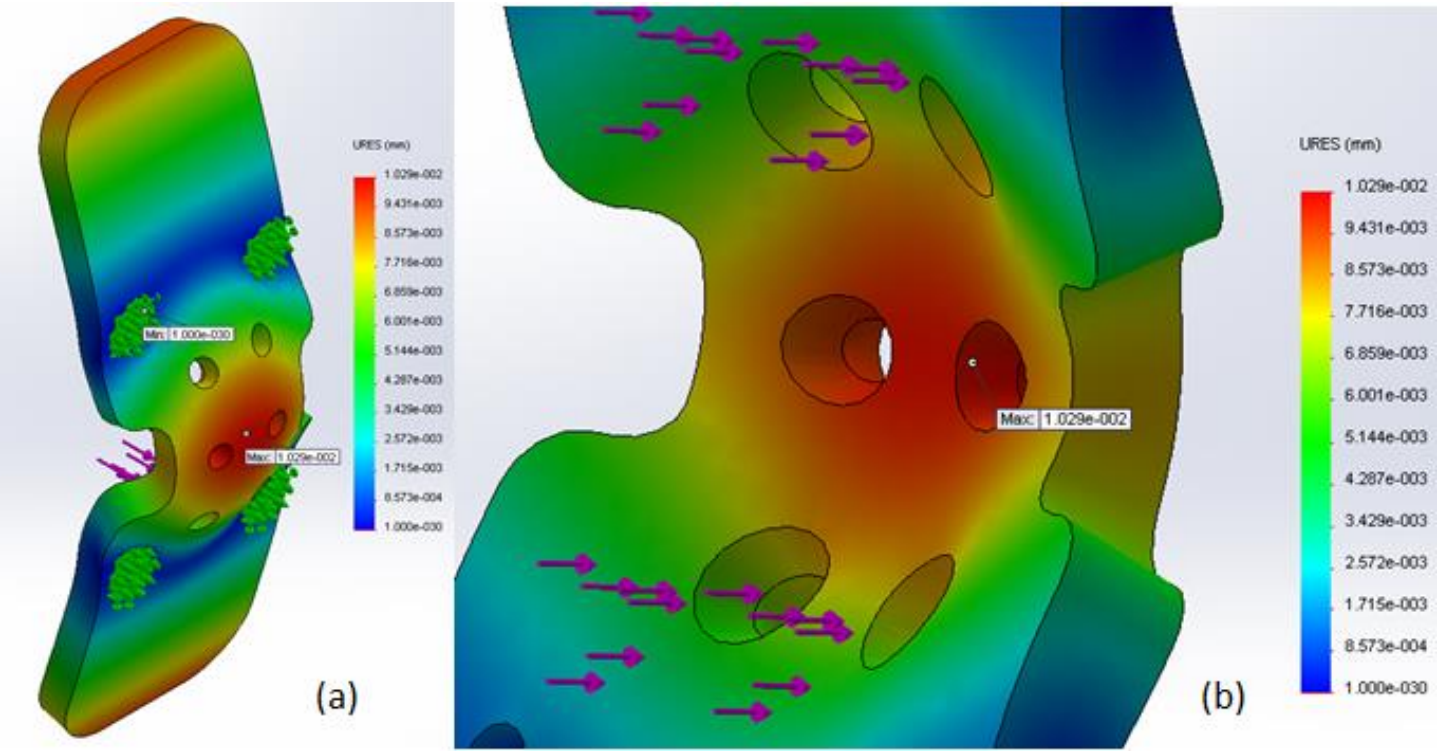

Fig 41: Anterior Fixture Aluminum Back Plate Resultant Displacement Results – For a total force magnitude of 500 N, the maximum displacement of a point in the model is 1.029 x 10^{-2} mm. Note: the deformation scale for this analysis is 1329.21.

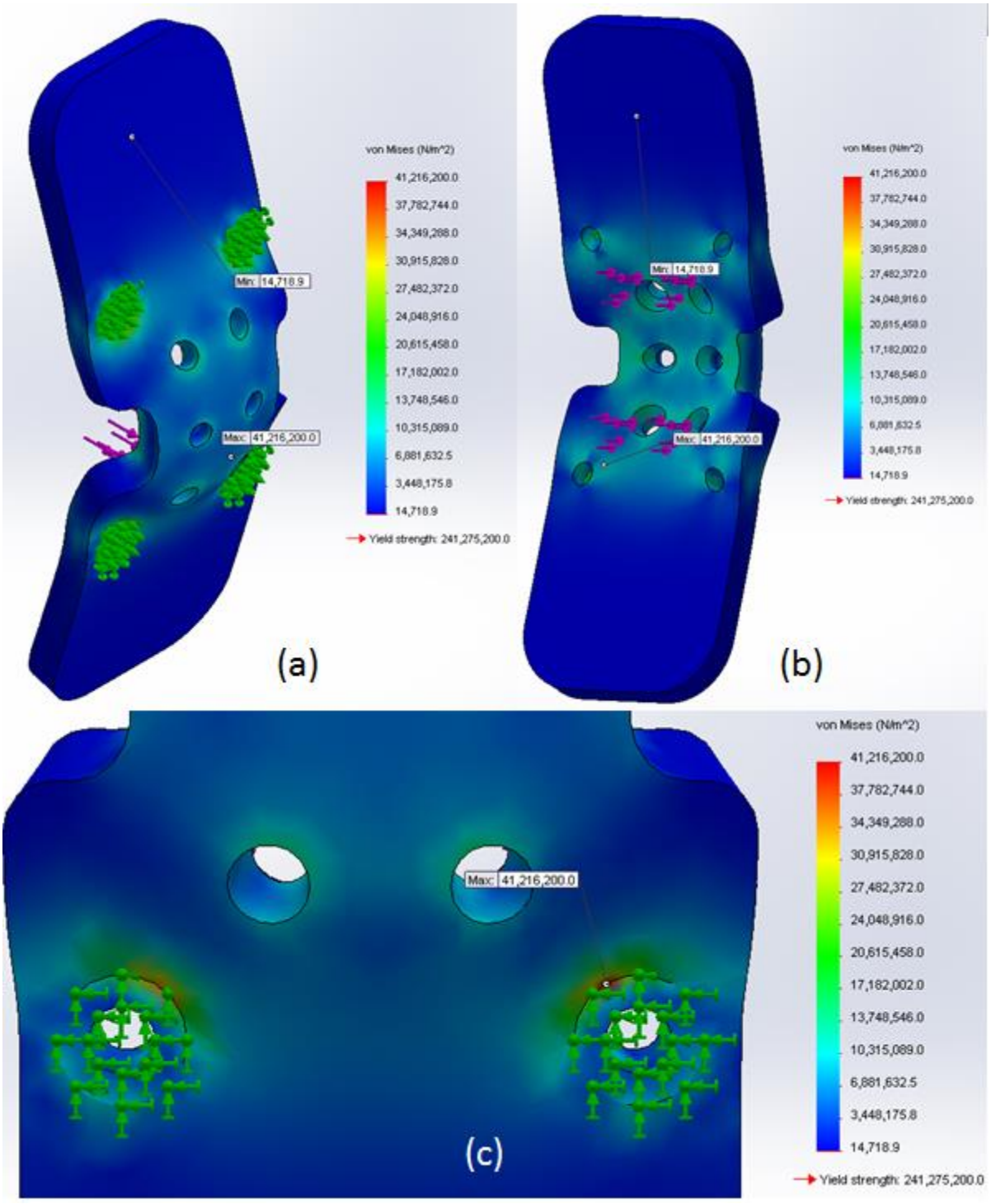

Fig. 42: Anterior Fixture Steel Back Plate Von Mises Stress Results – For a total force magnitude of 1000 N, the maximum Von Mises stress achieved in the model is 41.2 MPa, which is less than the yield stress of 241.3 MPa. Note: the deformation scale for this analysis is 3536.43.

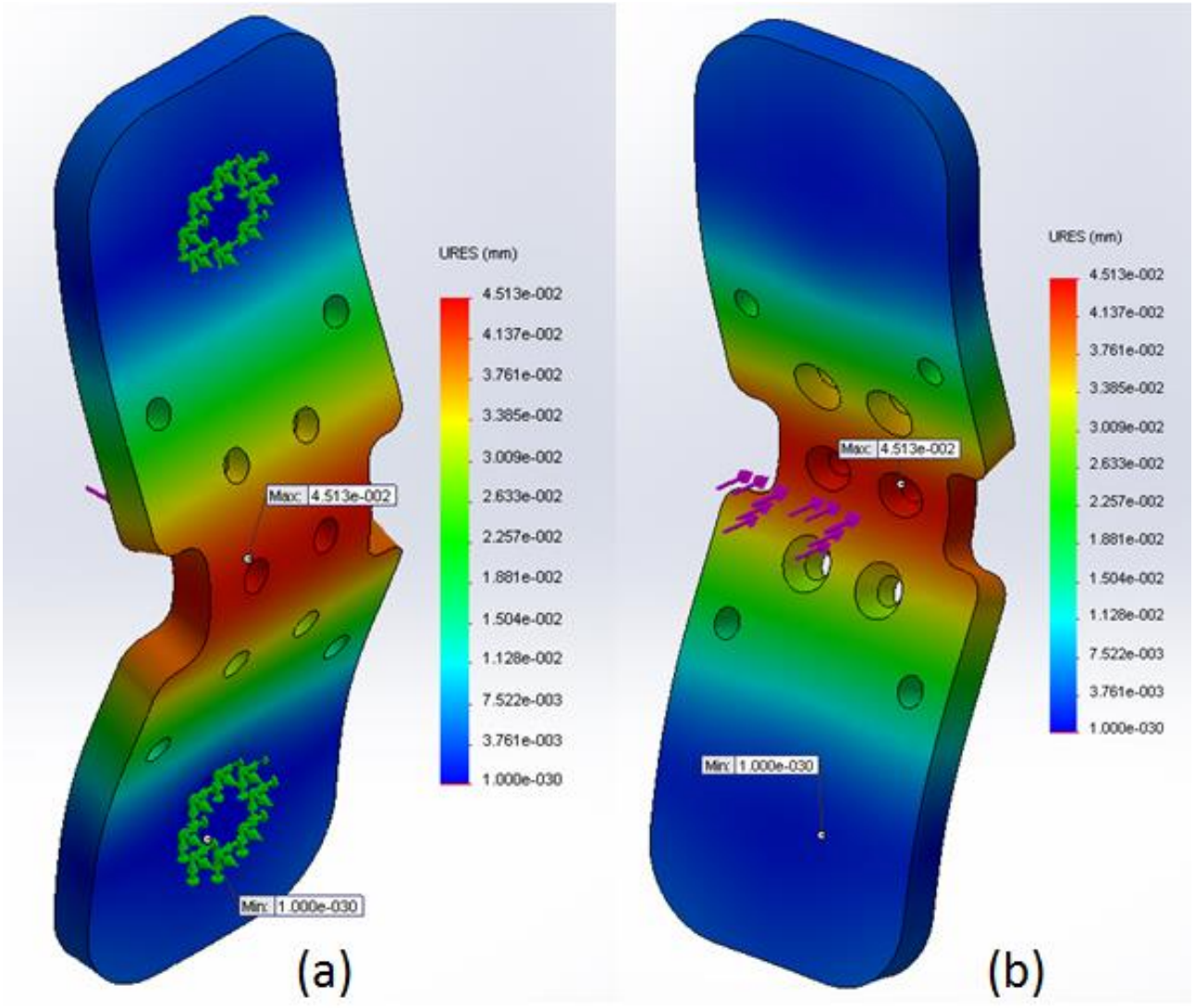

Fig 43: Posterior Fixture Aluminum Back Plate Resultant Displacement Results – For a total force magnitude of 500 N, the maximum displacement of a point in the model is 5.513 x 10^{-2} mm. Note: the deformation scale for this analysis is 302.992

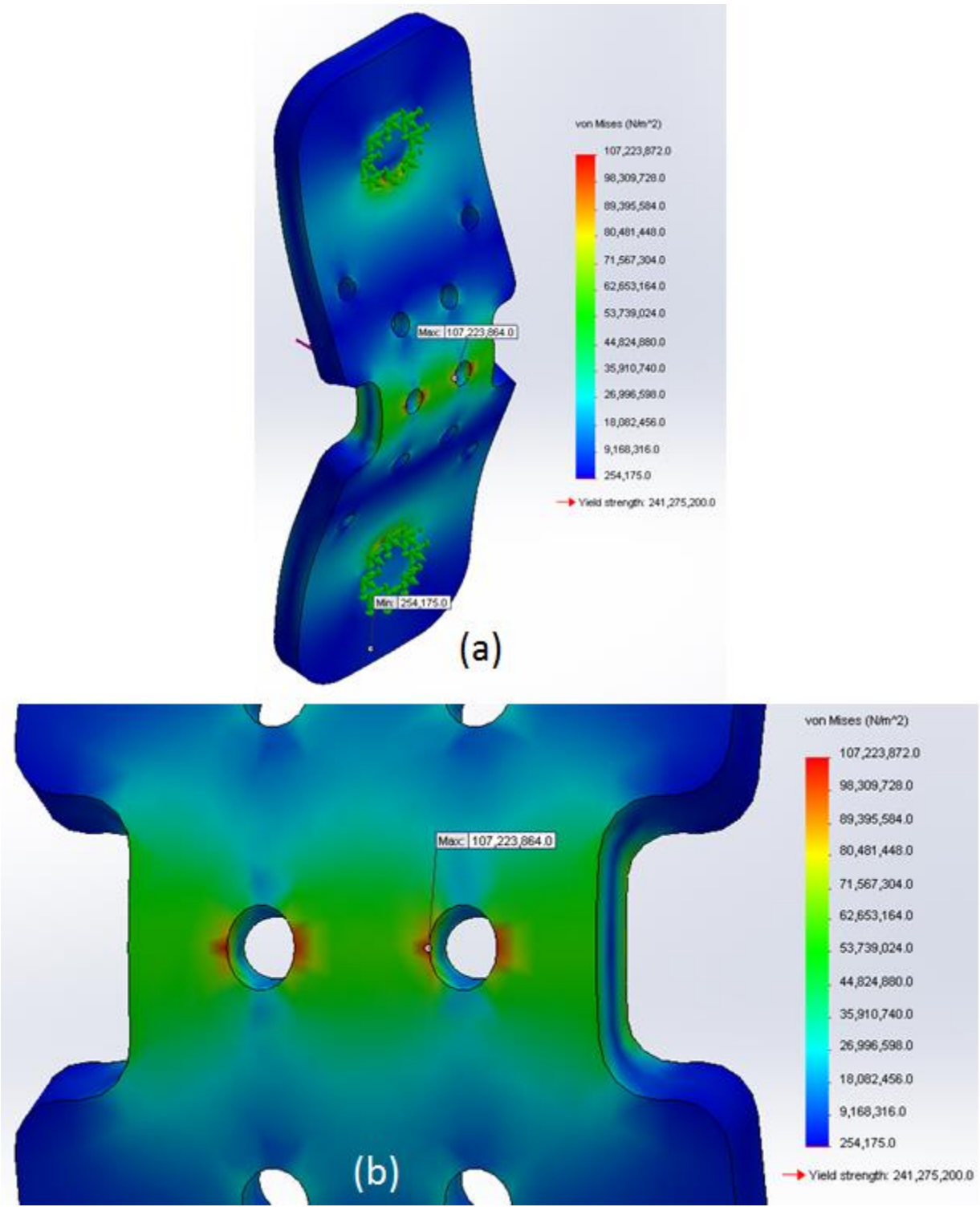

Figure 44: Posterior Steel Back Plate Von Mises Stress Results – For a total force magnitude of 1000 N, the maximum Von Mises stress achieved in the model is 107.2 MPa, which is less than the yield stress of 241.3 MPa. Note: the deformation scale for this analysis is 406.351.

Anterior Fixture Front Plate:

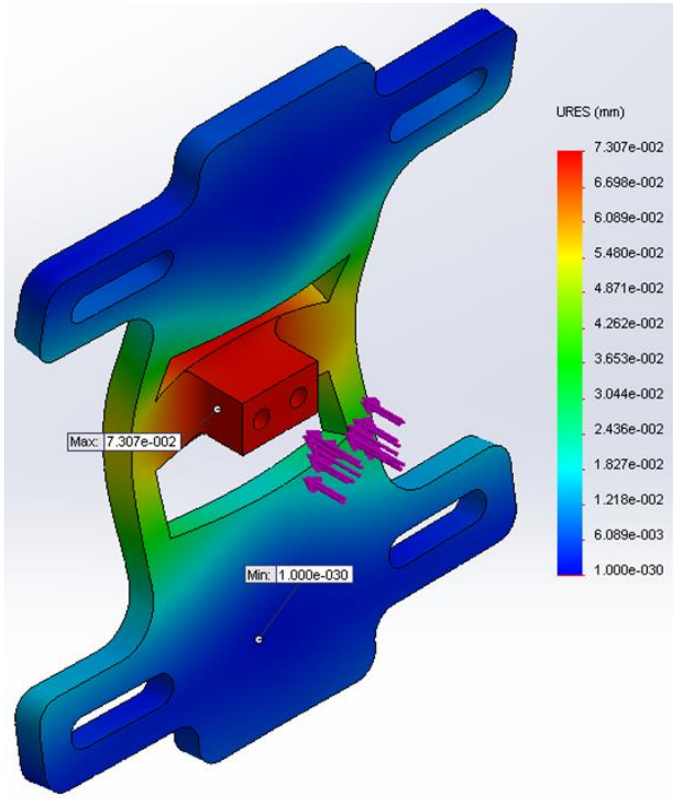

Fig. 5: Anterior Fixture Aluminum Front Plate Resultant Displacement Results – For a total force magnitude of 500 N, the maximum displacement of a point in the model is 7.307 x 10^{-2} mm. Note: the deformation scale for this analysis is 187.157.

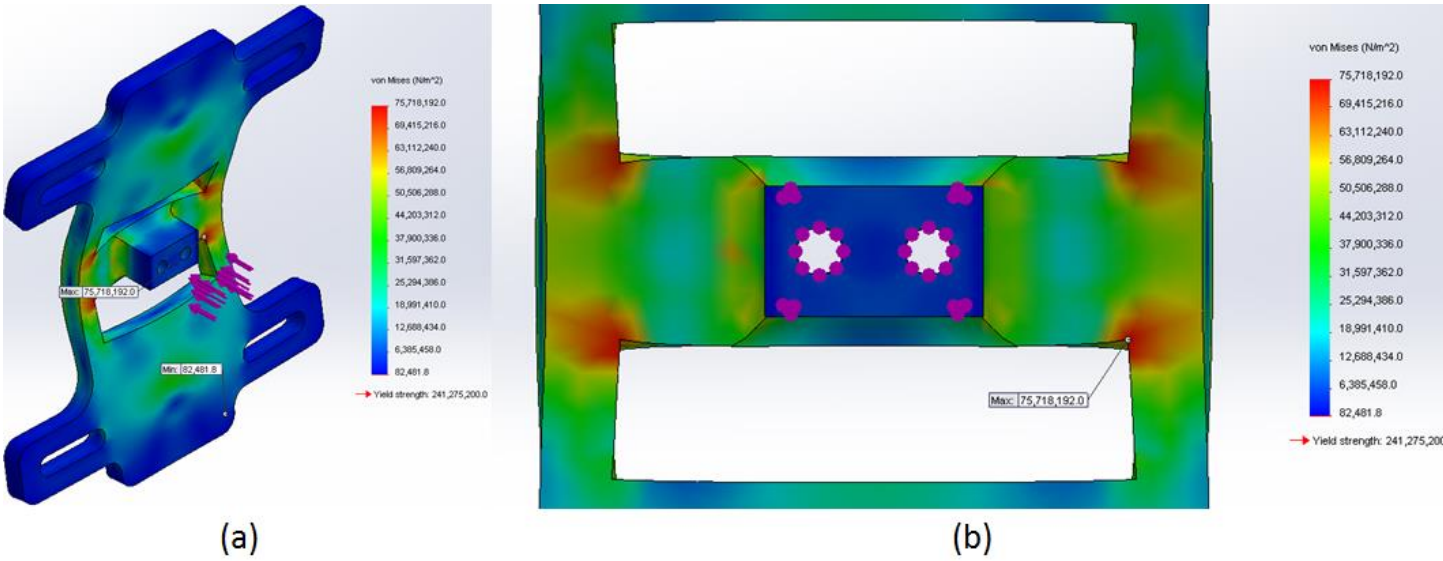

Fig. 6: Anterior Fixture Steel Front Plate Von Mises Stress Results – For a total force magnitude of 1000 N, the maximum Von Mises stress achieved in the model is 75.7 MPa, which is less than the yield stress of 241.3 MPa. Note: the deformation scale for this analysis is 255.685.

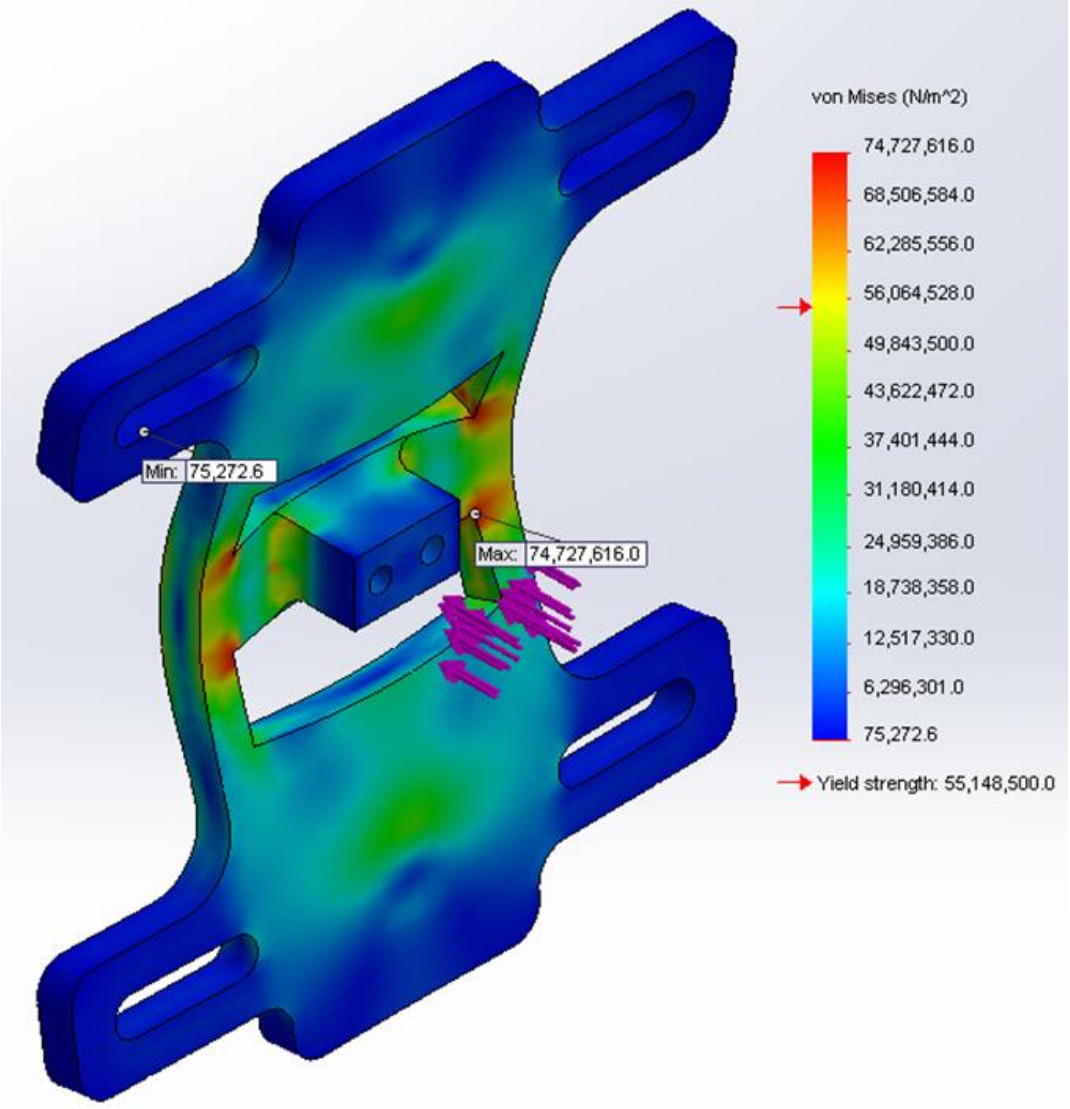

Fig. 45: Anterior Fixture Aluminum Front Plate Von Mises Stress Results – For a total force magnitude of 1000 N, the maximum Von Mises stress achieved in the model is 74.7 MPa, which is greater than the yield stress of 55.1 MPa. As a result, the front plate in this model yields. Note: the deformation scale for this analysis is 187.157.

Posterior Fixture Front Plate:

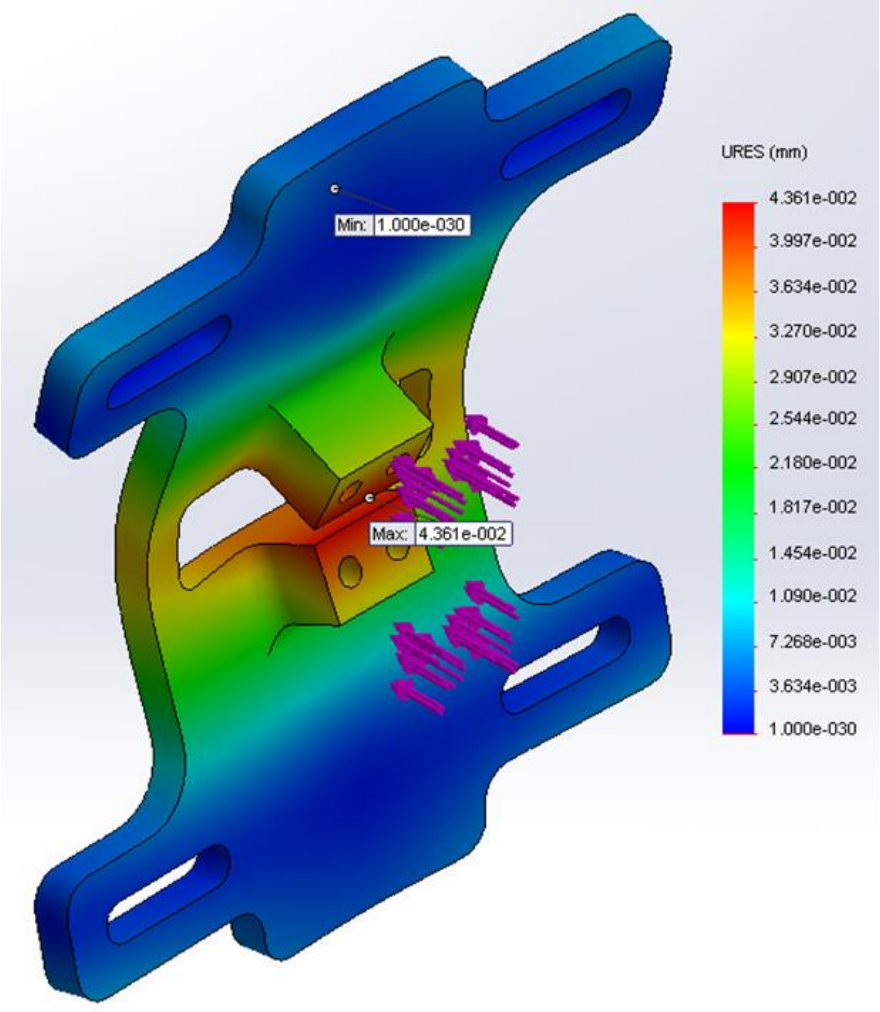

Fig. 8: Anterior Fixture Aluminum Front Plate Resultant Displacement Results – For a total force magnitude of 500 N, the maximum displacement of a point in the model is 4.361 x 10^{-2} mm. Note: the deformation scale for this analysis is 358.267.

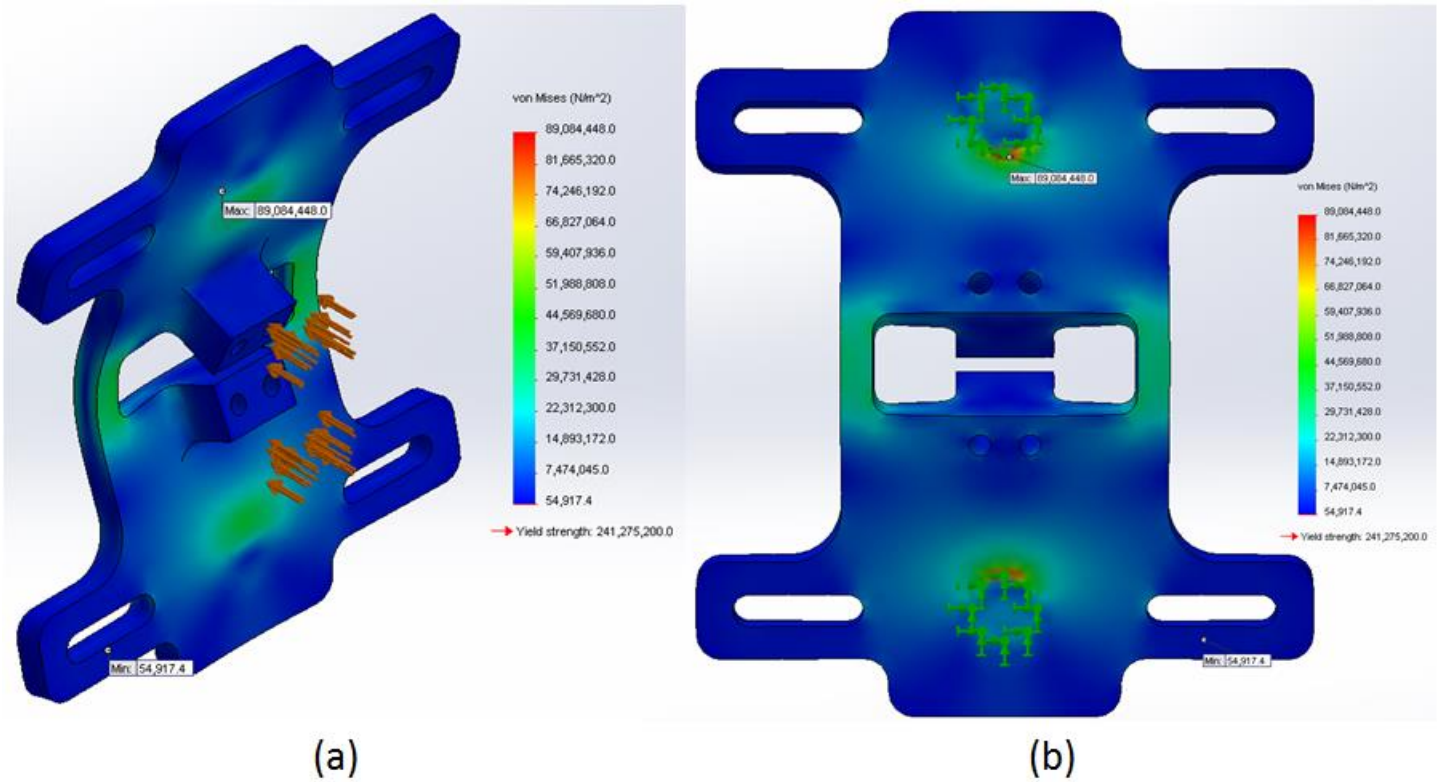

Fig. 9: Posterior Fixture Steel Front Plate Von Mises Stress Results – For a total force magnitude of 1000 N, the maximum Von Mises stress achieved in the model is 89.1 MPa, which is less than the yield stress of 241.3 MPa. Note: the deformation scale for this analysis is 483.463.

Connection Plate:

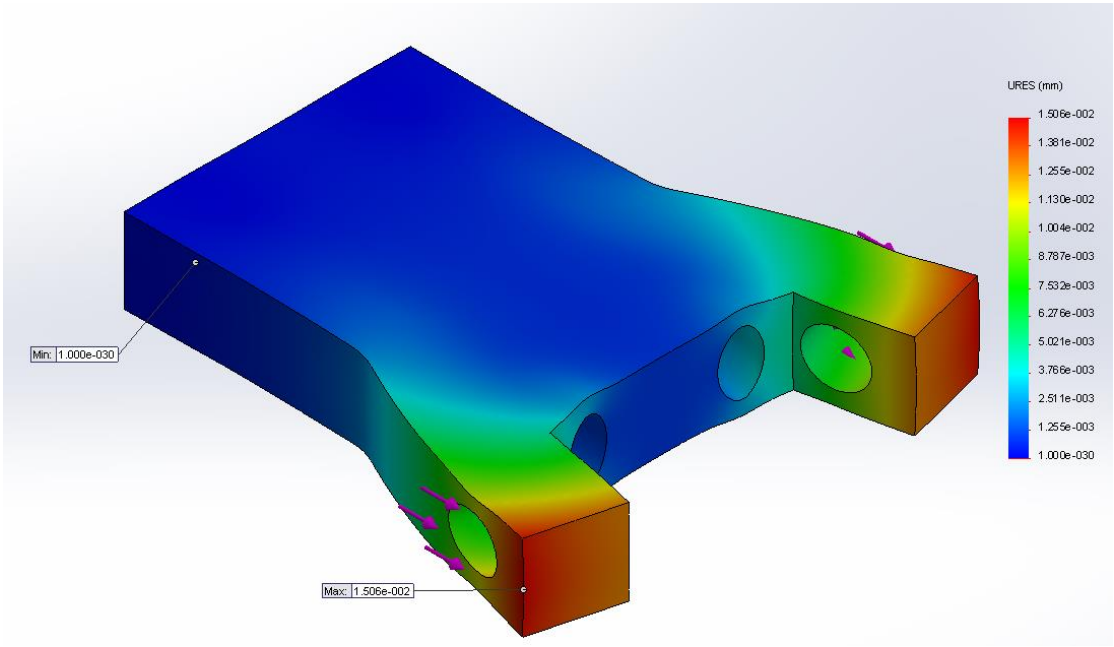

Fig. 460: Connection Plate Resultant Displacement Results – For a total force magnitude of 1000 N, the maximum displacement of a point in the model is 1.506 x 10^{-2} mm. Note: the deformation scale for this analysis is 295.018.

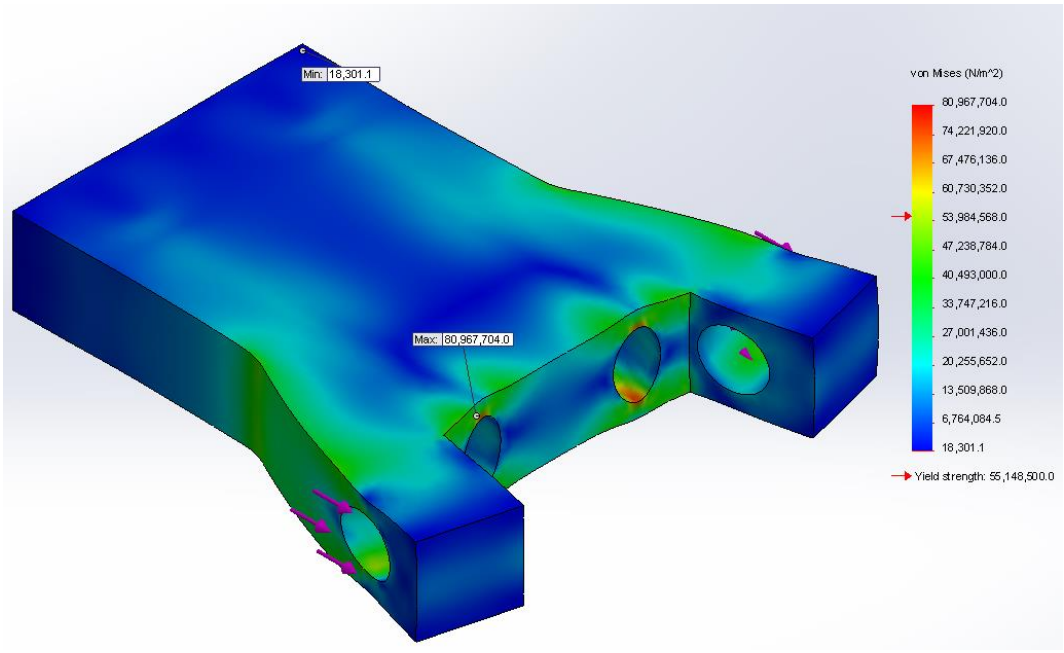

Fig. 47: Connection Plate Von Mises Stress Results – For a total force magnitude of 500 N, the maximum Von Mises stress achieved in the model is 81.0 MPa, which is greater than the yield stress of 55.1 MPa. Thus, yielding occurs, and aluminum cannot be used for the connection plate, as in the posterior model, it is possible that a force near 500 N could be experienced in the plate. Note: the deformation scale for this analysis is 214.542.

Delrin Vertebra:

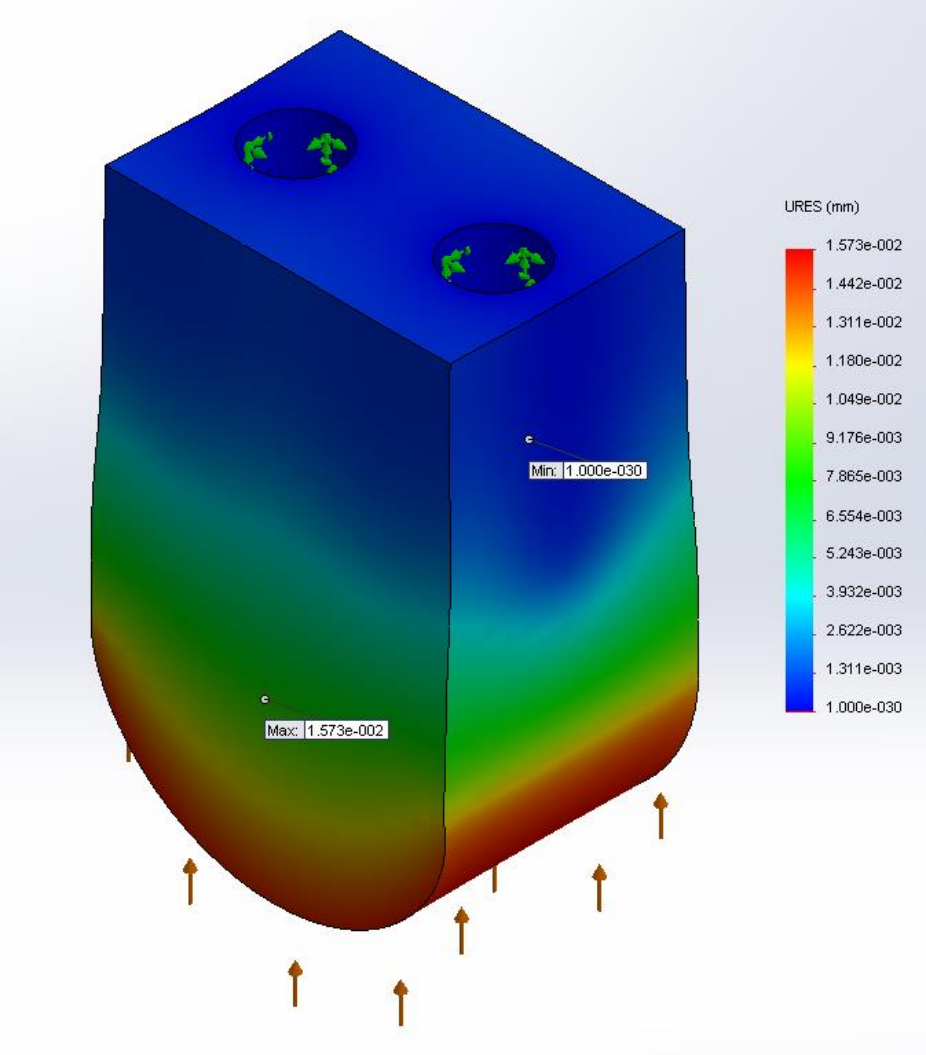

Fig. 48: Delrin Vertebra (Fixed on Back) Resultant Displacement Results – For a total force magnitude of 1000 N, the maximum displacement of a point in the model is 1.573 x 10^{-2} mm. Note: the deformation scale for this analysis is 187.586.

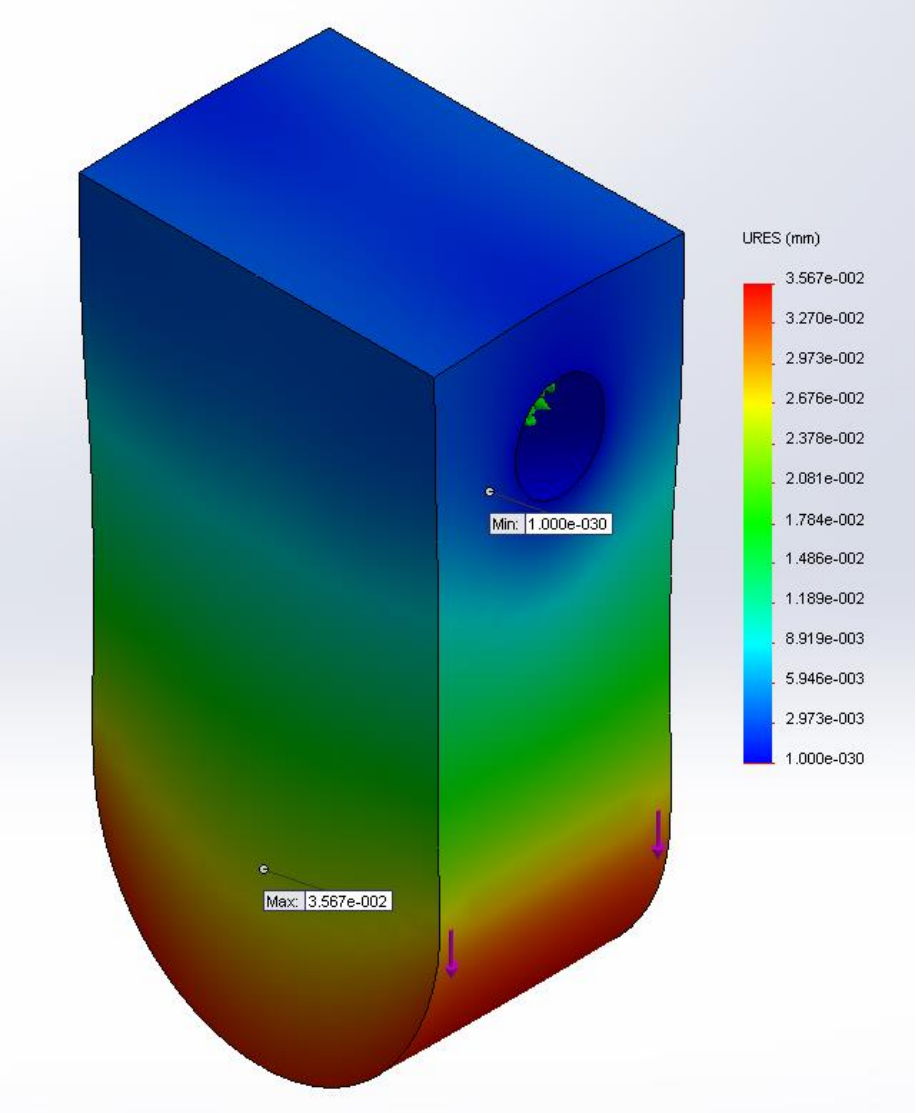

Fig. 49: Delrin Vertebra (Fixed on Sides) Resultant Displacement Results – For a total force magnitude of 1000 N, the maximum displacement of a point in the model is 3.567 x 10^{-2} mm. Note: the deformation scale for this analysis is 82.4928.

Appendix E: Preliminary Rubber Rod Calculations

Color Code: Red = Cannot Use, Green = Possible to Use, Orange = Most Feasible

For E = 1 MPa, Depth = 20 mm

Diameter (in)	Diameter (mm)	Area (mm^2)	Depth (mm)	Depth (in)	Force (N)	Stress	Strain	Delta_L	L_Final
									-
0.125	3.175	7.917	20	0.78740157	125	15788201.931	15.788	315.764	295.764
0.25	6.35	31.669	20	0.78740157	125	3947050.483	3.947	78.941	-58.941
0.375	9.525	71.256	20	0.78740157	125	1754244.659	1.754	35.085	-15.085
0.5	12.7	126.677	20	0.78740157	125	986762.621	0.987	19.735	0.265
0.625	15.875	197.933	20	0.78740157	125	631528.077	0.632	12.631	7.369
0.75	19.05	285.023	20	0.78740157	125	438561.165	0.439	8.771	11.229
0.875	22.225	387.948	20	0.78740157	125	322208.203	0.322	6.444	13.556
1	25.4	506.707	20	0.78740157	125	246690.655	0.247	4.934	15.066
1.125	28.575	641.302	20	0.78740157	125	194916.073	0.195	3.898	16.102
1.25	31.75	791.730	20	0.78740157	125	157882.019	0.158	3.158	16.842
1.375	34.925	957.9938277	20	0.78740157	125	130481.0077	0.13048	2.60962	17.39038
1.5	38.1	1140.091828	20	0.78740157	125	109640.2912	0.10964	2.192806	17.80719
1.625	41.275	1338.024437	20	0.78740157	125	93421.3132	0.09342	1.868426	18.13157
1.75	44.45	1551.792	20	0.78740157	125	80552.051	0.081	1.611	18.389
1.875	47.625	1781.393	20	0.78740157	125	70169.786	0.070	1.403	18.597
2	50.8	2026.830	20	0.78740157	125	61672.664	0.062	1.233	18.767
2.125	53.975	2288.101	20	0.78740157	125	54630.457	0.055	1.093	18.907
2.25	57.15	2565.207	20	0.78740157	125	48729.018	0.049	0.975	19.025
2.375	60.325	2858.147	20	0.78740157	125	43734.631	0.044	0.875	19.125
2.5	63.5	3166.922	20	0.78740157	125	39470.505	0.039	0.789	19.211
2.625	66.675	3491.531	20	0.78740157	125	35800.911	0.036	0.716	19.284
2.75	69.85	3831.975	20	0.78740157	125	32620.252	0.033	0.652	19.348
2.875	73.025	4188.254	20	0.78740157	125	29845.372	0.030	0.597	19.403
3	76.2	4560.367	20	0.78740157	125	27410.073	0.027	0.548	19.452
3.5	88.9	6207.167	20	0.78740157	125	20138.013	0.020	0.403	19.597
4	101.6	8107.320	20	0.78740157	125	15418.166	0.015	0.308	19.692

For E = 1 MPa, Depth = 30 mm

Diameter (in)	Diameter (mm)	Area (mm^2)	Depth (mm)	Depth (in)	Force (N)	Stress	Strain	Delta_L	L_Final
0.125	3.175	7.917	30	1.18110236	125	15788201.931	15.788	473.646	-443.646
0.25	6.35	31.669	30	1.18110236	125	3947050.483	3.947	118.412	-88.412
0.375	9.525	71.256	30	1.18110236	125	1754244.659	1.754	52.627	-22.627
0.5	12.7	126.677	30	1.18110236	125	986762.621	0.987	29.603	0.397
0.625	15.875	197.933	30	1.18110236	125	631528.077	0.632	18.946	11.054
0.75	19.05	285.023	30	1.18110236	125	438561.165	0.439	13.157	16.843
0.875	22.225	387.948	30	1.18110236	125	322208.203	0.322	9.666	20.334
1	25.4	506.707	30	1.18110236	125	246690.655	0.247	7.401	22.599
1.125	28.575	641.302	30	1.18110236	125	194916.073	0.195	5.847	24.153
1.25	31.75	791.730	30	1.18110236	125	157882.019	0.158	4.736	25.264
1.375	34.925	957.994	30	1.18110236	125	130481.008	0.130	3.914	26.086
1.5	38.1	1140.092	30	1.18110236	125	109640.291	0.110	3.289	26.711
1.625	41.275	1338.02444	30	1.18110236	125	93421.3132	0.093421313	2.802639396	27.1973606
1.75	44.45	1551.79165	30	1.18110236	125	80552.05067	0.080552051	2.41656152	27.58343848
1.875	47.625	1781.39348	30	1.18110236	125	70169.78636	0.070169786	2.105093591	27.89490641
2	50.8	2026.82992	30	1.18110236	125	61672.66379	0.061672664	1.850179914	28.14982009
2.125	53.975	2288.10096	30	1.18110236	125	54630.45651	0.054630457	1.638913695	28.3610863
2.25	57.15	2565.207	30	1.18110236	125	48729.018	0.049	1.462	28.538
2.375	60.325	2858.147	30	1.18110236	125	43734.631	0.044	1.312	28.688
2.5	63.5	3166.922	30	1.18110236	125	39470.505	0.039	1.184	28.816
2.625	66.675	3491.531	30	1.18110236	125	35800.911	0.036	1.074	28.926
2.75	69.85	3831.975	30	1.18110236	125	32620.252	0.033	0.979	29.021
2.875	73.025	4188.254	30	1.18110236	125	29845.372	0.030	0.895	29.105
3	76.2	4560.367	30	1.18110236	125	27410.073	0.027	0.822	29.178
3.5	88.9	6207.167	30	1.18110236	125	20138.013	0.020	0.604	29.396
4	101.6	8107.320	30	1.18110236	125	15418.166	0.015	0.463	29.537

For E = 1 MPa, Depth = 40 mm

Diameter (in)	Diameter (mm)	Area (mm^2)	Depth (mm)	Depth (in)	Force (N)	Stress	Strain	Delta_L	L_Final
0.125	3.175	7.917	40	1.57480315	125	15788201.931	15.788	631.528	-591.528
0.25	6.35	31.669	40	1.57480315	125	3947050.483	3.947	157.882	-117.882
0.375	9.525	71.256	40	1.57480315	125	1754244.659	1.754	70.170	-30.170
0.5	12.7	126.677	40	1.57480315	125	986762.621	0.987	39.471	0.529
0.625	15.875	197.933	40	1.57480315	125	631528.077	0.632	25.261	14.739
0.75	19.05	285.023	40	1.57480315	125	438561.165	0.439	17.542	22.458
0.875	22.225	387.948	40	1.57480315	125	322208.203	0.322	12.888	27.112
1	25.4	506.707	40	1.57480315	125	246690.655	0.247	9.868	30.132
1.125	28.575	641.302	40	1.57480315	125	194916.073	0.195	7.797	32.203
1.25	31.75	791.730	40	1.57480315	125	157882.019	0.158	6.315	33.685
1.375	34.925	957.994	40	1.57480315	125	130481.008	0.130	5.219	34.781
1.5	38.1	1140.092	40	1.57480315	125	109640.291	0.110	4.386	35.614
1.625	41.275	1338.024	40	1.57480315	125	93421.313	0.093	3.737	36.263
1.75	44.45	1551.792	40	1.57480315	125	80552.051	0.081	3.222	36.778
1.875	47.625	1781.393481	40	1.57480315	125	70169.78636	0.07017	2.806791	37.19321
2	50.8	2026.829916	40	1.57480315	125	61672.66379	0.061673	2.466907	37.53309
2.125	53.975	2288.10096	40	1.57480315	125	54630.45651	0.05463	2.185218	37.81478
2.25	57.15	2565.206613	40	1.57480315	125	48729.01831	0.048729	1.949161	38.05084
2.375	60.325	2858.146874	40	1.57480315	125	43734.63139	0.043735	1.749385	38.25061
2.5	63.5	3166.921744	40	1.57480315	125	39470.50483	0.039471	1.57882	38.42118
2.625	66.675	3491.531223	40	1.57480315	125	35800.91141	0.035801	1.432036	38.56796
2.75	69.85	3831.975311	40	1.57480315	125	32620.25192	0.03262	1.30481	38.69519
2.875	73.025	4188.254007	40	1.57480315	125	29845.37227	0.029845	1.193815	38.80619
3	76.2	4560.367312	40	1.57480315	125	27410.0728	0.02741	1.096403	38.9036
3.5	88.9	6207.166619	40	1.57480315	125	20138.01267	0.020138	0.805521	39.19448
4	101.6	8107.319666	40	1.57480315	125	15418.16595	0.015418	0.616727	39.38327

For E = 5 MPa, Depth = 20 mm

Diameter (in)	Diameter (mm)	Area (mm^2)	Depth (mm)	Depth (in)	Force (N)	Stress	Strain	Delta_L	L_Final
0.125	3.175	7.917	20	0.78740157	125	15788201.931	3.158	63.153	-43.153
0.25	6.35	31.669	20	0.78740157	125	3947050.483	0.789	15.788	4.212
0.375	9.525	71.256	20	0.78740157	125	1754244.659	0.351	7.017	12.983
0.5	12.7	126.677	20	0.78740157	125	986762.621	0.197	3.947	16.053
0.625	15.875	197.932609	20	0.78740157	125	631528.0772	0.12631	2.526112	17.47389
0.75	19.05	285.022957	20	0.78740157	125	438561.1648	0.08771	1.754245	18.24576
0.875	22.225	387.948	20	0.78740157	125	322208.203	0.064	1.289	18.711
1	25.4	506.707	20	0.78740157	125	246690.655	0.049	0.987	19.013
1.125	28.575	641.302	20	0.78740157	125	194916.073	0.039	0.780	19.220
1.25	31.75	791.730	20	0.78740157	125	157882.019	0.032	0.632	19.368
1.375	34.925	957.994	20	0.78740157	125	130481.008	0.026	0.522	19.478
1.5	38.1	1140.092	20	0.78740157	125	109640.291	0.022	0.439	19.561
1.625	41.275	1338.024	20	0.78740157	125	93421.313	0.019	0.374	19.626
1.75	44.45	1551.792	20	0.78740157	125	80552.051	0.016	0.322	19.678
1.875	47.625	1781.393	20	0.78740157	125	70169.786	0.014	0.281	19.719
2	50.8	2026.830	20	0.78740157	125	61672.664	0.012	0.247	19.753
2.125	53.975	2288.101	20	0.78740157	125	54630.457	0.011	0.219	19.781
2.25	57.15	2565.207	20	0.78740157	125	48729.018	0.010	0.195	19.805
2.375	60.325	2858.147	20	0.78740157	125	43734.631	0.009	0.175	19.825
2.5	63.5	3166.922	20	0.78740157	125	39470.505	0.008	0.158	19.842
2.625	66.675	3491.531	20	0.78740157	125	35800.911	0.007	0.143	19.857
2.75	69.85	3831.975	20	0.78740157	125	32620.252	0.007	0.130	19.870
2.875	73.025	4188.254	20	0.78740157	125	29845.372	0.006	0.119	19.881
3	76.2	4560.367	20	0.78740157	125	27410.073	0.005	0.110	19.890
3.5	88.9	6207.167	20	0.78740157	125	20138.013	0.004	0.081	19.919
4	101.6	8107.320	20	0.78740157	125	15418.166	0.003	0.062	19.938

For E = 5 MPa, Depth = 30 mm

Diameter (in)	Diameter (mm)	Area (mm^2)	Depth (mm)	Depth (in)	Force (N)	Stress	Strain	Delta_L	L_Final
0.125	3.175	7.917	30	1.18110236	125	15788201.931	3.158	94.729	-64.729
0.25	6.35	31.669	30	1.18110236	125	3947050.483	0.789	23.682	6.318
0.375	9.525	71.256	30	1.18110236	125	1754244.659	0.351	10.525	19.475
0.5	12.7	126.677	30	1.18110236	125	986762.621	0.197	5.921	24.079
0.625	15.875	197.933	30	1.18110236	125	631528.077	0.126	3.789	26.211
0.75	19.05	285.022957	30	1.18110236	125	438561.1648	0.087712233	2.631366989	27.36863301
0.875	22.225	387.947914	30	1.18110236	125	322208.2027	0.064441641	1.933249216	28.06675078
1	25.4	506.707	30	1.18110236	125	246690.655	0.049	1.480	28.520
1.125	28.575	641.302	30	1.18110236	125	194916.073	0.039	1.169	28.831
1.25	31.75	791.730	30	1.18110236	125	157882.019	0.032	0.947	29.053
1.375	34.925	957.994	30	1.18110236	125	130481.008	0.026	0.783	29.217
1.5	38.1	1140.092	30	1.18110236	125	109640.291	0.022	0.658	29.342
1.625	41.275	1338.024	30	1.18110236	125	93421.313	0.019	0.561	29.439
1.75	44.45	1551.792	30	1.18110236	125	80552.051	0.016	0.483	29.517
1.875	47.625	1781.393	30	1.18110236	125	70169.786	0.014	0.421	29.579
2	50.8	2026.830	30	1.18110236	125	61672.664	0.012	0.370	29.630
2.125	53.975	2288.101	30	1.18110236	125	54630.457	0.011	0.328	29.672
2.25	57.15	2565.207	30	1.18110236	125	48729.018	0.010	0.292	29.708
2.375	60.325	2858.147	30	1.18110236	125	43734.631	0.009	0.262	29.738
2.5	63.5	3166.922	30	1.18110236	125	39470.505	0.008	0.237	29.763
2.625	66.675	3491.531	30	1.18110236	125	35800.911	0.007	0.215	29.785
2.75	69.85	3831.975	30	1.18110236	125	32620.252	0.007	0.196	29.804
2.875	73.025	4188.254	30	1.18110236	125	29845.372	0.006	0.179	29.821
3	76.2	4560.367	30	1.18110236	125	27410.073	0.005	0.164	29.836
3.5	88.9	6207.167	30	1.18110236	125	20138.013	0.004	0.121	29.879
4	101.6	8107.320	30	1.18110236	125	15418.166	0.003	0.093	29.907

For E = 5 MPa, Depth = 40 mm

Diameter (in)	Diameter (mm)	Area (mm^2)	Depth (mm)	Depth (in)	Force (N)	Stress	Strain	Delta_L	L_Final
0.125	3.175	7.917304361	40	1.57480315	125	15788201.93	3.15764	126.3056	-86.3056
0.25	6.35	31.66921744	40	1.57480315	125	3947050.483	0.78941	31.5764	8.423596
0.375	9.525	71.25573925	40	1.57480315	125	1754244.659	0.350849	14.03396	25.96604
0.5	12.7	126.6768698	40	1.57480315	125	986762.6207	0.197353	7.894101	32.1059
0.625	15.875	197.932609	40	1.57480315	125	631528.0772	0.126306	5.052225	34.94778
0.75	19.05	285.022957	40	1.57480315	125	438561.1648	0.087712	3.508489	36.49151
0.875	22.225	387.9479137	40	1.57480315	125	322208.2027	0.064442	2.577666	37.42233
1	25.4	506.7074791	40	1.57480315	125	246690.6552	0.049338	1.973525	38.02647
1.125	28.575	641.3016532	40	1.57480315	125	194916.0732	0.038983	1.559329	38.44067
1.25	31.75	791.7304361	40	1.57480315	125	157882.0193	0.031576	1.263056	38.73694
1.375	34.925	957.9938277	40	1.57480315	125	130481.0077	0.026096	1.043848	38.95615
1.5	38.1	1140.091828	40	1.57480315	125	109640.2912	0.021928	0.877122	39.12288
1.625	41.275	1338.024437	40	1.57480315	125	93421.3132	0.018684	0.747371	39.25263
1.75	44.45	1551.791655	40	1.57480315	125	80552.05067	0.01611	0.644416	39.35558
1.875	47.625	1781.393481	40	1.57480315	125	70169.78636	0.014034	0.561358	39.43864
2	50.8	2026.829916	40	1.57480315	125	61672.66379	0.012335	0.493381	39.50662
2.125	53.975	2288.10096	40	1.57480315	125	54630.45651	0.010926	0.437044	39.56296
2.25	57.15	2565.206613	40	1.57480315	125	48729.01831	0.009746	0.389832	39.61017
2.375	60.325	2858.146874	40	1.57480315	125	43734.63139	0.008747	0.349877	39.65012
2.5	63.5	3166.921744	40	1.57480315	125	39470.50483	0.007894	0.315764	39.68424
2.625	66.675	3491.531223	40	1.57480315	125	35800.91141	0.00716	0.286407	39.71359
2.75	69.85	3831.975311	40	1.57480315	125	32620.25192	0.006524	0.260962	39.73904
2.875	73.025	4188.254007	40	1.57480315	125	29845.37227	0.005969	0.238763	39.76124
3	76.2	4560.367312	40	1.57480315	125	27410.0728	0.005482	0.219281	39.78072
3.5	88.9	6207.166619	40	1.57480315	125	20138.01267	0.004028	0.161104	39.8389
4	101.6	8107.319666	40	1.57480315	125	15418.16595	0.003084	0.123345	39.87665

For E = 10 MPa, Depth = 20 mm

Diameter (in)	Diameter (mm)	Area (mm^2)	Depth (mm)	Depth (in)	Force (N)	Stress	Strain	Delta_L	L_Final
0.125	3.175	7.917	20	0.78740157	125	15788201.931	1.579	31.576	-11.576
0.25	6.35	31.669	20	0.78740157	125	3947050.483	0.395	7.894	12.106
0.375	9.525	71.256	20	0.78740157	125	1754244.659	0.175	3.508	16.492
0.5	12.7	126.6768698	20	0.78740157	125	986762.6207	0.09868	1.973525	18.02647
0.625	15.875	197.933	20	0.78740157	125	631528.077	0.063	1.263	18.737
0.75	19.05	285.023	20	0.78740157	125	438561.165	0.044	0.877	19.123
0.875	22.225	387.948	20	0.78740157	125	322208.203	0.032	0.644	19.356
1	25.4	506.707	20	0.78740157	125	246690.655	0.025	0.493	19.507
1.125	28.575	641.302	20	0.78740157	125	194916.073	0.019	0.390	19.610
1.25	31.75	791.730	20	0.78740157	125	157882.019	0.016	0.316	19.684
1.375	34.925	957.994	20	0.78740157	125	130481.008	0.013	0.261	19.739
1.5	38.1	1140.092	20	0.78740157	125	109640.291	0.011	0.219	19.781
1.625	41.275	1338.024	20	0.78740157	125	93421.313	0.009	0.187	19.813
1.75	44.45	1551.792	20	0.78740157	125	80552.051	0.008	0.161	19.839
1.875	47.625	1781.393	20	0.78740157	125	70169.786	0.007	0.140	19.860
2	50.8	2026.830	20	0.78740157	125	61672.664	0.006	0.123	19.877
2.125	53.975	2288.101	20	0.78740157	125	54630.457	0.005	0.109	19.891
2.25	57.15	2565.207	20	0.78740157	125	48729.018	0.005	0.097	19.903
2.375	60.325	2858.147	20	0.78740157	125	43734.631	0.004	0.087	19.913
2.5	63.5	3166.922	20	0.78740157	125	39470.505	0.004	0.079	19.921
2.625	66.675	3491.531	20	0.78740157	125	35800.911	0.004	0.072	19.928
2.75	69.85	3831.975	20	0.78740157	125	32620.252	0.003	0.065	19.935
2.875	73.025	4188.254	20	0.78740157	125	29845.372	0.003	0.060	19.940
3	76.2	4560.367	20	0.78740157	125	27410.073	0.003	0.055	19.945
3.5	88.9	6207.167	20	0.78740157	125	20138.013	0.002	0.040	19.960
4	101.6	8107.320	20	0.78740157	125	15418.166	0.002	0.031	19.969

For E = 10 MPa, Depth = 30 mm

Diameter (in)	Diameter (mm)	Area (mm^2)	Depth (mm)	Depth (in)	Force (N)	Stress	Strain	Delta_L	L_Final
0.125	3.175	7.917	30	1.18110236	125	15788201.931	1.579	47.365	-17.365
0.25	6.35	31.669	30	1.18110236	125	3947050.483	0.395	11.841	18.159
0.375	9.525	71.256	30	1.18110236	125	1754244.659	0.175	5.263	24.737
0.5	12.7	126.677	30	1.18110236	125	986762.621	0.099	2.960	27.040
0.625	15.875	197.932609	30	1.18110236	125	631528.0772	0.063152808	1.894584232	28.10541577
0.75	19.05	285.023	30	1.18110236	125	438561.165	0.044	1.316	28.684
0.875	22.225	387.948	30	1.18110236	125	322208.203	0.032	0.967	29.033
1	25.4	506.707	30	1.18110236	125	246690.655	0.025	0.740	29.260
1.125	28.575	641.302	30	1.18110236	125	194916.073	0.019	0.585	29.415
1.25	31.75	791.730	30	1.18110236	125	157882.019	0.016	0.474	29.526
1.375	34.925	957.994	30	1.18110236	125	130481.008	0.013	0.391	29.609
1.5	38.1	1140.092	30	1.18110236	125	109640.291	0.011	0.329	29.671
1.625	41.275	1338.024	30	1.18110236	125	93421.313	0.009	0.280	29.720
1.75	44.45	1551.792	30	1.18110236	125	80552.051	0.008	0.242	29.758
1.875	47.625	1781.393	30	1.18110236	125	70169.786	0.007	0.211	29.789
2	50.8	2026.830	30	1.18110236	125	61672.664	0.006	0.185	29.815
2.125	53.975	2288.101	30	1.18110236	125	54630.457	0.005	0.164	29.836
2.25	57.15	2565.207	30	1.18110236	125	48729.018	0.005	0.146	29.854
2.375	60.325	2858.147	30	1.18110236	125	43734.631	0.004	0.131	29.869
2.5	63.5	3166.922	30	1.18110236	125	39470.505	0.004	0.118	29.882
2.625	66.675	3491.531	30	1.18110236	125	35800.911	0.004	0.107	29.893
2.75	69.85	3831.975	30	1.18110236	125	32620.252	0.003	0.098	29.902
2.875	73.025	4188.254	30	1.18110236	125	29845.372	0.003	0.090	29.910
3	76.2	4560.367	30	1.18110236	125	27410.073	0.003	0.082	29.918
3.5	88.9	6207.167	30	1.18110236	125	20138.013	0.002	0.060	29.940
4	101.6	8107.320	30	1.18110236	125	15418.166	0.002	0.046	29.954

For E = 10 MPa, Depth = 40 mm

Diameter (in)	Diameter (mm)	Area (mm^2)	Depth (mm)	Depth (in)	Force (N)	Stress	Strain	Delta_L	L_Final
0.125	3.175	7.917	40	1.57480315	125	15788201.931	1.579	63.153	-23.153
0.25	6.35	31.669	40	1.57480315	125	3947050.483	0.395	15.788	24.212
0.375	9.525	71.256	40	1.57480315	125	1754244.659	0.175	7.017	32.983
0.5	12.7	126.677	40	1.57480315	125	986762.621	0.099	3.947	36.053
0.625	15.875	197.932609	40	1.57480315	125	631528.0772	0.063153	2.526112	37.47389
0.75	19.05	285.022957	40	1.57480315	125	438561.1648	0.043856	1.754245	38.24576
0.875	22.225	387.948	40	1.57480315	125	322208.203	0.032	1.289	38.711
1	25.4	506.707	40	1.57480315	125	246690.655	0.025	0.987	39.013
1.125	28.575	641.302	40	1.57480315	125	194916.073	0.019	0.780	39.220
1.25	31.75	791.730	40	1.57480315	125	157882.019	0.016	0.632	39.368
1.375	34.925	957.994	40	1.57480315	125	130481.008	0.013	0.522	39.478
1.5	38.1	1140.092	40	1.57480315	125	109640.291	0.011	0.439	39.561
1.625	41.275	1338.024	40	1.57480315	125	93421.313	0.009	0.374	39.626
1.75	44.45	1551.792	40	1.57480315	125	80552.051	0.008	0.322	39.678
1.875	47.625	1781.393	40	1.57480315	125	70169.786	0.007	0.281	39.719
2	50.8	2026.830	40	1.57480315	125	61672.664	0.006	0.247	39.753
2.125	53.975	2288.101	40	1.57480315	125	54630.457	0.005	0.219	39.781
2.25	57.15	2565.207	40	1.57480315	125	48729.018	0.005	0.195	39.805
2.375	60.325	2858.147	40	1.57480315	125	43734.631	0.004	0.175	39.825
2.5	63.5	3166.922	40	1.57480315	125	39470.505	0.004	0.158	39.842
2.625	66.675	3491.531	40	1.57480315	125	35800.911	0.004	0.143	39.857
2.75	69.85	3831.975	40	1.57480315	125	32620.252	0.003	0.130	39.870
2.875	73.025	4188.254	40	1.57480315	125	29845.372	0.003	0.119	39.881
3	76.2	4560.367	40	1.57480315	125	27410.073	0.003	0.110	39.890
3.5	88.9	6207.167	40	1.57480315	125	20138.013	0.002	0.081	39.919
4	101.6	8107.320	40	1.57480315	125	15418.166	0.002	0.062	39.938

Appendix F: Polyurethane Rod Segment Testing

A = Largest diameter rod (~1.5 in)
B = Middle diameter rod (~0.75 in)
C = Smallest diameter rod (~0.625 in)
1 = Longest Segment (~40 mm)
2 = Middle Length Segment (~30 mm)
3 = Shortest Segment (~20 mm)

Polyurethane Rod Testing					Date: 2 Mar 13					
	Height (mm)	**Height (in)**	**Diameter (mm)**	**Diameter (in)**	**Load Cell (lb)**	**Specimen Number**	**Preload (N)**	**Max Load (N)**	**Max X-Head (mm)**	**Prediction of Load for 5 mm displacement**
A1	38.9	1.53	38.0	1.50	50	4	1	195	4.48	217.63
	39.0	1.54	37.8	1.49	50					
	38.8	1.53	37.9	1.49	50					
Average	38.9	1.53	37.9	1.49						
A2	28.6	1.13	37.8	1.49	50	9	1	195	3.36	290.18
	28.5	1.12	37.7	1.48	50					
	28.7	1.13	37.6	1.48	50					
Average	28.6	1.13	37.7	1.48						
A3	18.5	0.73	37.5	1.48	50	2	1	195	2.43	401.23
	18.4	0.72	37.7	1.48	50					
	18.6	0.73	37.6	1.48	50					
Average	18.5	0.73	37.6	1.48						